

**Interplay between  
vascular endothelial growth factor-A  
and extracellular matrix in angiogenesis:  
molecular and cellular mechanisms**

Inaugural-Dissertation  
zur  
Erlangung des Doktorgrades  
der Mathematisch-Naturwissenschaftlichen Fakultät  
der Universität zu Köln

vorgelegt von  
Stephanie Traub  
aus Göppingen

Mai 2011

Berichterstatter

Univ. Prof. Dr. Matthias Hammerschmidt  
Univ. Prof. Dr. Mats Paulsson

Tag der mündlichen Prüfung: 17. Mai 2011



# Table of Contents

<b>Summary</b>	<b>1</b>
<b>Zusammenfassung</b>	<b>3</b>
<b>1 Introduction</b>	<b>5</b>
<b>1.1 Structure and function of the skin</b>	<b>5</b>
<b>1.2 Wound healing</b>	<b>6</b>
1.2.1 Inflammation	7
1.2.2 Tissue formation	8
1.2.3 Tissue remodelling	9
<b>1.3 The medical need of pro-angiogenic therapies</b>	<b>9</b>
1.3.1 Non-healing wounds as targets for pro-angiogenic therapy	10
1.3.2 Pro-angiogenic therapies as pre-requisite for tissue engineering	11
1.3.3 Basic principles for the use of growth factors in tissue engineering	11
<b>1.4 The vascular endothelial growth factor</b>	<b>11</b>
1.4.1 Discovery and effect on endothelial cells	11
1.4.2 Molecular properties and regulation of expression	12
1.4.3 VEGF-A receptors and signaling	13
1.4.4 VEGF-A co-receptors	16
1.4.5 Crosstalk between VEGFR-2 and integrins in angiogenesis	18
1.4.6 Role of VEGF-A during wound healing	20
<b>1.5 Cellular and molecular mechanisms of angiogenesis</b>	<b>21</b>
1.5.1 Induction of angiogenesis and the role of VEGF-A	21
1.5.2 Vascular guidance by tip cells and the role of tip cell selection	22
1.5.3 The role of VEGF-A binding to the extracellular matrix in tip cell guidance	23
1.5.4 Maturation of the vascular network	23
<b>1.6 Strategies aiming at the optimization of VEGF-A induced angiogenesis in tissue engineering</b>	<b>24</b>
1.6.1 Stabilization of the VEGF-A <sub>165</sub> heparin-binding site in the proteolytic environment of the chronic wound	24
1.6.2 Targeted delivery of VEGF-A for pro-angiogenic therapies	25
1.6.3 Amplification of VEGF-A <sub>165</sub> induced signals	27
<b>2 Hypothesis</b>	<b>30</b>
<b>3 Results</b>	<b>31</b>
<b>3.1 Design of VEGF-A based fusion proteins for the co-stimulation of VEGFR-2 and integrin <math>\alpha v \beta 3</math></b>	<b>31</b>
3.1.1 Domain organization of engineered VEGF-A proteins	31
3.1.2 Design of the linker interconnecting FNIII10 and VEGFmut in the bi-functional constructs	31
<b>3.2 Production and identification of the recombinant fusion proteins</b>	<b>32</b>
3.2.1 Expression of GST-tagged proteins in <i>E. coli</i>	32
3.2.1.1 Purification of FNIII10 and TG-FNIII10	32
3.2.1.2 Purification of TG-PL-FLV and VEGFmut as GST-fusion proteins	33
3.2.2 Purification of VEGFmut-containing proteins from bacterial inclusion bodies	35
3.2.2.1 Purification of VEGFmut by heparin affinity chromatography	35
3.2.2.2 Purification of the engineered VEGF-proteins	37
3.2.3 Protein expression in eucaryotic cells	38

## Table of contents

---

3.2.4	Confirmation of the identity of recombinant proteins produced	39
3.2.5	Determination of protein concentrations	40
3.2.6	Endotoxin test	42
<b>3.3</b>	<b>Functional characterization of recombinant proteins</b>	<b>43</b>
3.3.1	Covalent incorporation of engineered VEGF-proteins into fibrin matrices	43
3.3.1.1	Retention of proteins produced in <i>E. coli</i> equipped with a TG-sequence in fibrin gels	43
3.3.1.2	Release of proteins produced in HEK293-EBNA cells from fibrin gels	45
3.3.2	HUVEC attachment to TG-FNIII10 is partially dependent on integrin $\alpha v \beta 3$	46
3.3.3	FLV and FNIII10 promote cell attachment and spreading of HUVECs	47
3.3.4	Recombinant VEGF-proteins produced in <i>E. coli</i> promote VEGFR-2 phosphorylation	49
3.3.5	VEGFR-2 phosphorylation is induced by VEGF-proteins produced in eucaryotic cells	49
3.3.5.1	The activity of bi-functional proteins is reduced as compared to VEGFmut-proteins as determined by western blot	49
3.3.5.2	The overall VEGFR-2 phosphorylation detected by ELISA reproduces phosphorylation on tyrosine 1175	50
3.3.6	VEGFmut and FLV bind to VEGFR-2 with high affinities: Surface plasmon resonance binding studies	52
<b>3.4</b>	<b><i>In vivo</i> characterization of engineered VEGF proteins applied to wounds in fibrin matrices</b>	<b>54</b>
3.4.1	Cellular invasion of fibrin gels and induction of angiogenesis in day 10 and day 15 wounds	55
3.4.2	TG-VEGFmut and TG-FLV induce a prominent angiogenic response, but differ in their potency to recruit pericytes	57
<b>4</b>	<b>Discussion</b>	<b>62</b>
<b>4.1</b>	<b>Covalent binding of VEGF-A<sub>165</sub> to fibrin matrices is superior to soluble VEGF-A<sub>165</sub> to induce sustained angiogenesis during wound repair</b>	<b>62</b>
<b>4.2</b>	<b>FNIII10 fusion to VEGF-A<sub>165</sub> promotes enhanced cell attachment and spreading <i>in vitro</i> compared to FNIII10 and VEGF-A<sub>165</sub> alone</b>	<b>65</b>
<b>4.3</b>	<b>Covalent binding of FLV to fibrin is not superior to covalently fibrin-bound VEGF-A<sub>165</sub> in the induction of wound angiogenesis</b>	<b>68</b>
<b>4.4</b>	<b>Recombinant fusion proteins composed of various protein domains raise the possibility of synergistic signaling and novel biological functions</b>	<b>70</b>
<b>5</b>	<b>Perspectives</b>	<b>74</b>
<b>6</b>	<b>Materials and methods</b>	<b>76</b>
<b>6.1</b>	<b>Chemicals</b>	<b>76</b>
<b>6.2</b>	<b>Special equipment</b>	<b>76</b>
<b>6.3</b>	<b>Bacterial cell culture</b>	<b>76</b>
6.3.1	<i>Escherichia coli</i> ( <i>E. coli</i> ) strains	76
6.3.2	General culture conditions	77
6.3.3	Generation of chemical competent bacteria using calcium chloride (Cohen et al. 1972)	78
6.3.4	Transformation of chemical competent bacteria	78
6.3.5	Generation of bacterial frozen stocks	78
<b>6.4</b>	<b>Culture of eucaryotic cells</b>	<b>78</b>
6.4.1	Eucaryotic cells	78
6.4.2	General culture conditions	79
6.4.2.1	Culture of HEK 293 EBNA cells	79
6.4.2.2	Culture of HUVECs	79

---

<b>6.5</b>	<b>General protein biochemical methods</b>	<b>79</b>
6.5.1	Determination of protein concentration	79
6.5.1.1	Determination of protein concentration by spectrometry	79
6.5.1.2	Determination of protein concentration by the BCA assay	80
6.5.1.3	Determination of protein concentration by VEGF specific ELISA	80
6.5.2	Sodium dodecylsulfate polyacrylamide gel electrophoresis (SDS-PAGE)	80
6.5.3	Protein detection on SDS-PAGE gels	82
6.5.4	Immunoblotting of proteins	82
6.5.4.1	Western blot transfer	82
6.5.4.2	Immunodetection of proteins	83
<b>6.6</b>	<b>Cloning and cloning strategy</b>	<b>84</b>
6.6.1	DNA and amino acid sequences of protein domains used and cloning into the bacterial expression vector pGEX-4T-1	84
6.6.2	Protein expression vectors used for cloning	86
6.6.3	Polymerase chain reaction (PCR)	88
6.6.4	DNA agarose gel electrophoresis	88
6.6.5	DNA restriction digest and 5' dephosphorylation of the vector	89
6.6.6	DNA ligation	89
6.6.7	Subcloning	90
<b>6.7</b>	<b>Recombinant protein expression in bacteria</b>	<b>90</b>
6.7.1	Expression and purification of GST-tagged proteins	91
6.7.2	Thrombin processing of GST-VEGFmut and GST-TG-PL-FLV	92
6.7.3	Purification of recombinant proteins from bacterial inclusion bodies	92
6.7.4	Endotoxin test	93
<b>6.8</b>	<b>Expression of recombinant proteins in HEK293-EBNA cells</b>	<b>93</b>
<b>6.9</b>	<b>Functional characterization of recombinant proteins</b>	<b>94</b>
6.9.1	Cell attachment to TG-FNIII10 in presence and absence of integrin-specific inhibitors	94
6.9.2	Cell spreading assay	95
6.9.3	Investigation of VEGFR-2 activation and downstream signaling by western blot	96
6.9.4	Determination of VEGFR-2 phosphorylation by ELISA	96
6.9.5	Surface plasmon resonance (SPR) biosensor binding studies	97
<b>6.10</b>	<b>Fibrin gel formulation</b>	<b>98</b>
6.10.1	Protein stock preparation	98
6.10.2	Functionalization of fibrin matrices: incorporation and release of VEGF proteins	99
<b>6.11</b>	<b>Wounding of db/db mice</b>	<b>99</b>
6.11.1	Tissue harvest	100
6.11.2	Staining for CD31 and desmin	101
6.11.2.1	Quantification of wound angiogenesis on CD31 and desmin stained sections	101
6.11.2.2	Statistical analysis of CD31 and desmin stained section	101
<b>7</b>	<b>References</b>	<b>102</b>
	<b>Abbreviations</b>	<b>115</b>
	<b>Danksagungen</b>	<b>118</b>
	<b>Erklärung</b>	<b>120</b>
	<b>Curriculum Vitae</b>	<b>121</b>

## Summary

The induction of angiogenesis by stimulation of physiological vessel growth using pro-angiogenic growth factors is currently under intense investigation in medical research. It is well accepted, that angiogenesis is a rate-limiting step in skin regeneration, as it ensures supply of novel tissue with nutrients and oxygen. Chronic wounds are characterized by a lack of angiogenesis and thus represent a major target for the induction of angiogenesis by therapeutic means. For the delivery of VEGF-A<sub>165</sub> to chronic wounds and the induction of effective angiogenesis, in general it is proposed that first, the stabilization of the growth factor against protease activities, and second, the tight control of its release are beneficial.

The aim of this study was to optimize wound angiogenesis in non-healing wounds in response to recombinant VEGF-A<sub>165</sub> by improving bioavailability and potency of the growth factor.

To stabilize the growth factor in the chronic wound environment, recently a mutated form of VEGF-A<sub>165</sub> (VEGFmut) resistant to plasmin cleavage was generated in our group. This mutant was used in this study for the analysis of protein delivery. For this purpose, a hybrid protein composed of VEGFmut and a factor XIIIa transglutaminase substrate sequence (TG) was generated. This sequence allows covalent incorporation of the recombinant protein into fibrin matrix. Furthermore, a second strategy to increase the angiogenic response was investigated which aimed at the stimulation of synergistic signaling downstream of VEGFR-2 and integrin  $\alpha\beta3$ . To this end, bi-functional proteins consisting of the fibronectin type III domain 10 (FNIII10) and VEGFmut denoted as FLV were generated for the concomitant activation of both receptors.

The recombinant proteins were expressed in *E. coli*. FNIII10 and TG-FNIII10 were purified as GST-fusion proteins, whereas VEGF-containing constructs were produced in bacterial inclusion bodies, refolded, dimerized, and purified by heparin affinity chromatography. However, purification of the bi-functional proteins was challenging, as they tended to precipitate and dimerization was ineffective. To overcome these problems, in a subsequent approach, FNIII10, TG-FNIII10, VEGFmut, TG-VEGFmut, FLV and TG-FLV were expressed in eucaryotic cells (HEK293-EBNA) and purified by a C-terminal poly-histidine tag.

The biological activity of these proteins was confirmed in various *in vitro* assays. First, HUVECs were shown to attach to TG-FNIII10 in a concentration dependent manner, and this attachment was reduced by integrin  $\alpha\beta3$  function-blocking antibodies. Second, recombinant proteins fused to a TG sequence were covalently incorporated into fibrin gels by the activity of factor XIIIa,

and were retained by up to 90 % after two days of washing, whereas their soluble counterparts were released in a burst release during the first 8 hours. Third, the biological activity of the VEGF-variants was shown *in vitro* by their ability to induce VEGFR-2 phosphorylation in HUVECs by western blot analysis and ELISA. Intriguingly, the bi-functional protein FLV failed to induce detectable synergistic signaling on the receptor level when it was added to HUVECs. In contrast, when HUVECs were seeded on microscopy slides coated with the recombinant proteins, FLV promoted attachment and spreading to a higher degree than FNIII10 or VEGFmut alone. Together, these findings indicate that the immobilized proteins show different potential in the induction of cellular responses.

The potency of these proteins to induce angiogenesis was also assessed *in vivo* using wound healing as a model. Fibrin gels containing 0.468  $\mu\text{M}$  (corresponding to 20  $\mu\text{g/mL}$  effective VEGF-concentration) of either VEGFmut, TG-VEGFmut, TG-FLV or no recombinant protein were applied to full-thickness punch biopsy wounds created on the back of db/db mice, which are used as a model of impaired wound healing. When compared to fibrin treatment only, wound closure was accelerated upon treatment with various VEGF-proteins. More important, both TG-VEGF and TG-FLV proved to be significantly more potent in inducing blood vessel growth into the wound area, when compared to soluble VEGFmut. Differences between the two TG-isoforms were observed in the maturity of neovessels as indicated by the recruitment of pericytes: pericyte recruitment was more efficient in fibrin/TG-VEGF treated wounds than in fibrin/TG-FLV treated wounds at day 10.

Collectively, the findings of this study support a critical role for the interplay between VEGF-A and extracellular matrix during wound angiogenesis, and suggest that protein engineering provides a novel molecular approach to use these interactions for therapeutic angiogenesis.



## Zusammenfassung

Im klinischen Alltag sind chronische Wundheilungsstörungen ein häufiges Krankheitsbild, dem eine Fehlregulation der Angiogenese in Folge eines proteasereichen Mikromilieus zugrunde liegt. Die Stimulation der Angiogenese durch therapeutische Maßnahmen stellt daher eine vielversprechende Behandlungsoption dar.

Ziel dieser Arbeit war es, die durch VEGF-A<sub>165</sub> stimulierte Angiogenese in chronischen Wunden zu optimieren. In dieser Arbeit wurde die Fragestellung bearbeitet, ob die Stabilisierung von VEGF-A gegen in der Wunde angereicherte Proteasen, sowie die räumlich und zeitlich kontrollierte Verfügbarkeit des Wachstumsfaktors der Wundheilung förderlich sind.

Eine Mutation im VEGF-A<sub>165</sub> Protein (VEGFmut) verhindert den Abbau durch Plasmin in chronischen Wunden, wie unsere Arbeitsgruppe bereits in früheren Untersuchungen zeigen konnte. Die Verfügbarkeit von VEGFmut kann über die kovalente Bindung an Fibrin kontrolliert werden. Zu diesem Zweck wurde ein Fusionsprotein generiert, welches VEGFmut an die Substratsequenz für Faktor XIIIa koppelt (TG-VEGFmut). Um die Angiogenese darüber hinaus zu verstärken, wurde ein weiteres bifunktionales Fusionsprotein hergestellt, welches VEGFmut über einen Linker mit der Fibronectin Typ III Domäne 10 (FNIII10) verbindet und somit simultan an den VEGF-Rezeptor 2 und das Integrin  $\alpha\beta 3$  binden soll. Dieses Fusionsprotein FNIII10-Linker-VEGFmut (FLV) soll einen synergistischen Effekt in Folge der Kostimulation von VEGF-Rezeptor 2 und Integrin  $\alpha\beta 3$  erzielen.

Die rekombinanten Proteine wurden zunächst in *E. coli* exprimiert. FNIII10 und TG-FNIII10 wurden als GST-Fusionsproteine aufgereinigt, während die VEGFmut-basierten Proteine aus bakteriellen Inklusionskörperchen gewonnen und über ihre Heparinaffinität aufgereinigt wurden. Insbesondere für die bifunktionalen Proteine erwies sich die Aufreinigung als schwierig, da Präzipitatbildung und unvollständige Dimierisierung beobachtet wurden. Aus diesem Grund wurden FNIII10, TG-FNIII10, VEGFmut, TG-VEGFmut, FLV und TG-FLV in einem zweiten Ansatz in eukaryotischen Zellen (HEK293-EBNA) exprimiert.

Die biologische Aktivität der aufgereinigten Proteine wurde in unterschiedlichen *in vitro* und *in vivo* Experimenten untersucht. *In vitro* Versuche an primären Endothelzellen aus der Nabelschnurvene (HUVECs) zeigten, dass TG-FNIII10 die Zelladhäsion konzentrationsabhängig fördert. Die Zelladhäsion konnte teilweise durch funktionsblockierende Antikörper gegen Integrin  $\alpha\beta 3$  gehemmt werden. Desweiteren wurden VEGFmut und FLV über die Faktor XIIIa Substratsequenz kovalent im Fibrinnetz gebunden und wurden auch nach zweitägigem Waschen

im Gel zurückgehalten. Demgegenüber wurden die löslichen Proteine VEGFmut und FLV innerhalb von 8 Stunden vollständig aus dem Fibringel herausgewaschen. Ferner führte die Stimulation mit den rekombinanten VEGF-Proteinen in HUVECs zur Phosphorylierung von VEGFR-2, wie mittels Western Blot Untersuchungen und ELISA nachgewiesen wurde. Interessanterweise war die Phosphorylierung des Rezeptors nach Stimulation mit löslichem FLV im Vergleich zu VEGFmut reduziert, obwohl beide Proteine VEGFR-2 mit hoher Affinität binden, wie Oberflächenplasmon-Resonanzmessungen zeigten. Im Gegensatz dazu förderte auf Objektträgern immobilisiertes FLV die Zelladhäsion und -ausbreitung stärker als FNIII10 oder VEGFmut alleine. Diese Ergebnisse deuten darauf hin, dass insbesondere die bifunktionalen Proteine in gebundener Form ein anderes Signalisierungspotential haben als in löslicher Form.

*In vivo* Untersuchungen der rekombinanten Proteine in einem Model für gestörte Wundheilung an diabetischen Mäusen zeigten eine beschleunigte Wundheilung, wenn die Wunden mit Fibringelen, die 0.468  $\mu\text{M}$  (entsprechend 20  $\mu\text{g/ml}$  effektiver VEGF-Konzentration) VEGFmut, TG-VEGFmut oder TG-FLV enthielten, behandelt wurden. Wunden, die mit den kovalent an Fibrin gebundenen Proteinen TG-VEGFmut und TG-FLV behandelt wurden, zeigten an Tag 10 nach Wundsetzung eine deutlich erhöhte Angiogenese gegenüber Wunden, die mit löslichem VEGFmut in Fibrin oder nur mit Fibringel behandelt wurden. Darüberhinaus unterschieden sich zu diesem Zeitpunkt die Blutgefäße der mit TG-VEGFmut oder TG-FLV behandelten Wunden hinsichtlich ihrer Reife; die Rekrutierung von Perizyten in den mit TG-VEGFmut behandelten Wunden war deutlich weiter fortgeschritten.

Zusammenfassend deuten die Ergebnisse dieser Arbeit auf eine entscheidende Rolle für das Zusammenspiel von VEGF-A und der extrazellulären Matrix während der Wundangiogenese hin. Diese Ergebnisse könnten ferner als Grundlage neuer Ansätze für die Steuerung der Angiogenese auf molekularer Ebene und deren therapeutische Nutzung dienen.

# 1 Introduction

## 1.1 Structure and function of the skin

The skin is the outer barrier of the body, separating the “inside” from the “foreign outside” and hence has important protective functions. In humans, the skin is the body’s largest organ, measuring between 1.5 and 2 m<sup>2</sup> in area and 2-3 mm in thickness, with a weight of about 9 kg. Being a physical barrier, the skin protects the body passively from pathogens, but also hosts compounds of the humoral, cellular and complement immune response. Further, the skin plays a major role in homeostasis: it is semi-permeable, and protects the body from loss of water and nutrients. This organ is also an important storage compartment for water and lipids, and the place of vitamin D synthesis. Due to its high degree of vascularization, the skin regulates the body’s temperature by controlled vascular dilation or constriction. Importantly, the skin is also highly innervated and thus enables sensory perceptions of temperature, pressure, touch, vibration and pain (McGrath et al. 2008).

This important organ is divided into two layers (Figure 1), namely the highly cellular epidermis and the underlying dermis consisting of connective tissue, that are separated from each other by the basal lamina. In the epidermis, up to 95 % of all cells found are keratinocytes. Besides sensory Merkel cells, melanocytes, and Langerhans cells, a subset of dendritic cells, are present whereas vasculature is absent (McGrath et al. 2008). The epidermis regenerates continuously, which is accomplished by a permanent turnover of keratinocytes (Koster 2009). During its developmental program, the keratinocyte moves from the basement membrane towards the body’s surface, thereby forming defined layers according to its differentiation state that characterize the epidermis as a stratified epithelium (Figure 1 A). These layers are named *stratum basale*, *spinosum*, *granulosum* and *corneum* (McGrath et al. 2008). In the *stratum basale*, as well as in the bulge region of hair follicles, clusters of epidermal stem cells are located, which constantly replenish the pool of developing keratinocytes via a pool of transiently amplifying daughter cells. Subsequent keratinocyte differentiation comprises a state of increased synthetic activity and ultimately results in the loss of cytoplasmic organelles and the formation of a cornified envelope consisting of various crosslinked proteins (Proksch et al. 2008; Smack et al. 1994). At the body’s surface, the cornified, dead cells are continuously shed off and replaced by underlying cells. This process, named keratinization, contributes to the protection against UV-damage, water loss and environmental damage (McGrath et al. 2008).

The dermis predominantly consists of connective tissue and is a cushion that protects the body from mechanical injury. The connective tissue of the dermis is mainly formed of proteoglycan macromolecules, which attract and retain water due to their negative charge. Collagen is another major component that accounts for approximately 75 % of the dermis' dry weight and gives tensile strength to the skin. Networks formed by elastic fibers interconnect with the collagen fibers and confer elasticity to the tissue (McGrath et al. 2008). Fibroblasts are the major cell type found in the dermis, and synthesize the extracellular matrix components described. Furthermore, the dermis contains melanocytes as well as cells of the immune system such as lymphocytes, macrophages and mast cells. It is also the location of sensual preception, as it is highly innervated by sensory as well as by peripheral and motor nerve endings. The dermis hosts the appendages of the skin, namely hair follicles, sebaceous glands, apocrine and eccrine sweat glands and also carries many blood and lymphatic vessels (McGrath et al. 2008).

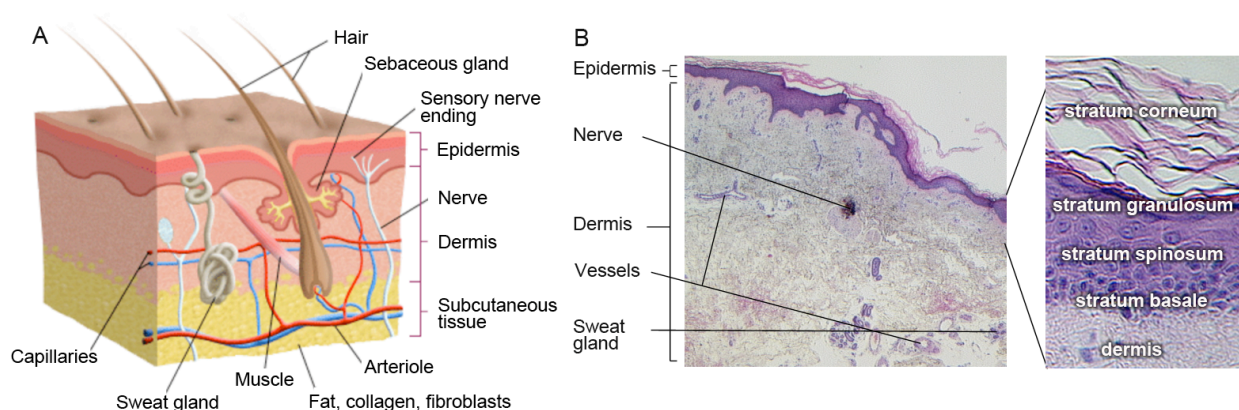


**Figure 1: Anatomy of the skin.** (A) Schematic representation of organization and composition of the skin (Rush University Medical Center). (B) Histological sections of the skin.

## 1.2 Wound healing

As skin functions described above are essential for health and survival of organisms, skin repair after injury is a critical process that aims at the quick re-establishment of tissue integrity. It is a highly organized process involving many different cell types, cytokines and proteins of the extracellular matrix. Commonly, the healing process is divided into three overlapping phases, namely inflammation, tissue formation and tissue remodeling.

### **1.2.1 Inflammation**

The formation of a blood clot consisting of platelets and extravasated plasma proteins is the first step during tissue regeneration, and is part of the inflammatory response. Damage of the vessel wall or exposure of subendothelial structures to the blood flow result in the activation of pro-enzymes of the coagulation cascade in the plasma, ultimately leading to the proteolytic activation of thrombin and fibrin polymerization. Thrombin in addition activates the transglutaminase factor XIIIa, which crosslinks fibrin fibers covalently, and platelets, that bind to fibrin via platelet integrin  $\alpha$ IIb $\beta$ 3 (Du and Ginsberg 1997; Laurens et al. 2006).

Besides stopping bleeding and thereby reestablishing homeostasis, the clot fills the disrupted tissue and provides a provisional matrix meeting all prerequisites for cell invasion, proliferation and differentiation required for tissue regeneration (Shaw and Martin 2009). This provisional matrix is an excellent substrate for cell migration. Fibrin itself has been shown to promote migration of several cell types such as keratinocytes, fibroblasts and endothelial cells (Geer et al. 2002; Gorodetsky et al. 1998), and this ability to promote cell migration is additionally potentiated by binding of other plasma derived proteins to the provisional matrix such as fibronectin and vitronectin (Clark 2003; Makogonenko et al. 2002; Preissner and Jenne 1991). The fibrin clot also serves as a reservoir of growth factors. An important source of chemoattractants are the platelets entrapped in the clot, as they release vascular endothelial growth factor-A (VEGF-A), platelet-derived growth factor-B (PDGF-B), transforming growth factor- $\beta$  (TGF- $\beta$ ), hepatocyte growth factor (HGF), among others (Anitua et al. 2004). Cytokines sequestered in the clot either bind directly to fibrin, as it is known for the basic fibroblast growth factor (bFGF), VEGF-A, PDGF, and TGF- $\beta$  (Clark 2003; Sahni and Francis 2000; Sahni et al. 1998), or interact with fibrin indirectly via heparin or fibronectin (Makogonenko et al. 2002; Odrljin et al. 1996; Raut and Gaffney 1996). Storage of a variety of different growth factors such as bFGF, heparin-binding epidermal growth factor (HB-EGF), PDGF, or VEGF in the clot can be accomplished by this means (Clark 2003; Martino and Hubbell 2010).

Neutrophils from the blood immobilized in the clot are the first immune cells present at the wound site. They become activated and release chemokines and cytokines which in turn results in the activation of tissue-resident immune cells and, together with factors of the complement system and fibrinopeptides, promote the recruitment of additional neutrophils from the bloodstream to the wound site within several hours (Cumberbatch et al. 2000; Jameson et al. 2004; Noli and Miolo 2001; Shaw and Martin 2009). Also mast cells in the tissue contribute to

the recruitment of neutrophils from the blood flow by the exocytosis of vasoactive mediators and cytokines within several hours after injury (Eming et al. 2007c; Trautmann et al. 2000; Weller et al. 2006). Neutrophils phagocytose pathogens, tissue, and cell debris in the wound, and are also an important source of pro-inflammatory cytokines that serve to activate local keratinocytes and fibroblasts (Hubner et al. 1996).

Monocytes arrive at the wound side slightly later than neutrophils, at around day one post-injury. They become recruited from the circulation by factors released in the wound and differentiate into macrophages when invading the tissue (Eming et al. 2007c). Macrophages phagocytose damaged extracellular matrix components and cells as well as dead neutrophils. Furthermore, they play an essential role in antigen presentation and in the synthesis of growth factors, which in turn promote the recruitment of tissue resident cells to the clot and their proliferation and the synthesis of a novel extracellular matrix. VEGF-A, bFGF, PDGF, TGF- $\beta$  and TGF- $\alpha$  are among the cytokines secreted (DiPietro and Polverini 1993; Eming et al. 2007c).

### **1.2.2 Tissue formation**

The fibrin clot only serves as a temporary wound closure and becomes replaced by granulation tissue, which is characterized by a granular appearance due to the formation of a microvascular network and by high cell density. As a general principle, cells at the wound edges become activated by factors released in the wound, proliferate, and invade the wound to substitute the fibrin clot by novel tissue. This activation requires that cells change their integrin-expression profile and start to synthesize proteases to proteolytically invade the provisional matrix.

Fibroblasts at the wound edges begin to proliferate as an early response to injury, and invade the provisional matrix around day 3 or 4 post-injury (Fernandez et al. 2008; Hinz et al. 2007; Rajkumar et al. 2006; Shaw and Martin 2009). In the fibrin clot, fibroblasts deposit an early new matrix consisting of collagen, and re-arrange it by bundling collagen fibers and adjusting these collagen bundles (Hinz et al. 2007). Furthermore, a subset of fibroblasts differentiates into highly contractile myofibroblasts characterized by the expression of  $\alpha$ -smooth-muscle actin ( $\alpha$ -SMA). Both fibroblasts and myofibroblasts contract to draw the wound edges closer together (Hinz et al. 2007).

Only several hours after injury, both basal and suprabasal keratinocytes from the wound edges and hair follicles start to migrate collectively over and through the provisional matrix towards the middle of the wound (Martin 1997; Matoltsy and Viziám 1970; Nguyen et al. 2000). By the expression of matrix-metalloproteases (MMPs) and plasmin activators, migrating keratinocytes

carve a path between scab and viable tissue (Grondahl-Hansen et al. 1988; Pilcher et al. 1999; Shaw and Martin 2009). Keratinocytes next to the wound edges proliferate strongly to replace cells lost during injury, which is reflected by the formation of a thick, hyperproliferative epithelium (Garlick and Taichman 1994; Martin 1997). Once the wound area has been covered by a layer of keratinocytes, their migration stops due to contact inhibition. A new basal lamina is synthesized, to which both keratinocytes and fibroblasts contribute (Werner et al. 2007), followed by reestablishment of the stratified epithelium starting at the wound margins (Gipson et al. 1988).

Simultaneously, capillaries from the surrounding tissue become activated by pro-angiogenic mediators released in the wound, and sprout into the provisional matrix (Tonnesen et al. 2000) in order to supply the granulation tissue with oxygen and nutrients, and to remove metabolic end products. Angiogenesis is an essential process during normal wound repair and requires tight temporal and spatial coordination of the interaction between various cell types, cytokines and the extracellular matrix (Eming et al. 2007a). During wound healing, the induction of an appropriate angiogenic response is crucial for successful skin regeneration, and this work aims at the optimal induction of wound angiogenesis. The molecular regulation of angiogenesis will be discussed more in detail in section 1.5.

### **1.2.3 Tissue remodelling**

During the last and longest phase of wound healing, the cell-rich granulation tissue gets transformed into a matrix-rich scar tissue. To that end, myofibroblasts and many fibroblasts undergo apoptosis, and the vascular network matures by the recruitment of pericytes and reorganization by pruning. Further, collagen is reorganized, and collagen III, the predominant collagen-isoform in the provisional matrix, is substituted by collagen I. Collagen gets crosslinked, and elastic fibers are deposited, which increases strength and elasticity of the scar (Braiman-Wiksman et al. 2007).

## **1.3 The medical need of pro-angiogenic therapies**

For many medical applications, the modulation of the angiogenic response is a major target in research. While angiogenesis can occur in various pathologic settings such as tumor growth or retinal angiopathy, the induction of a functional vasculature is desirable in various diseases resulting from malperfusion of tissues, such as myocardial or leg ischemia and wound healing

impairments. Therapeutic angiogenesis aims at the induction of a functional vasculature by stimulation of tissue resident cells by biochemical means (Zisch et al. 2003).

### **1.3.1 Non-healing wounds as targets for pro-angiogenic therapy**

The normal progression through the stages of wound healing is orchestrated and tightly controlled by a multitude of mediators, coordinating the behavior of various cell types as described in earlier sections. However, some wounds fail to progress through these normal stages of wound healing and become chronic. Such non-healing wounds are rather frequent with 3-4 % of people older than 60 years of age affected in western societies (Tredget and Ding 2009). As many of the causes are age related, due to the demographic development of these societies, an increase of cases is to be expected in future years (Clark et al. 2007). Chronic wounds severely reduce the overall quality of life of the concerned patients, as they are care intensive, often cause chronic pain and longstanding unfitness for work, impair normal ambulating and lead to social isolation (Eming et al. 2007b; Menke et al. 2007). Furthermore, infections and malignant transformations are severe problems, often requiring amputation as ultimate mean of treatment (Chraibi et al. 2004). As of today, there is no efficient treatment for chronic wounds, thus therapy and care cause important costs to the health care system (Walmsley, 2002).

Wound healing impairments may have several causes, but the primary one is tissue ischemia secondary to venous insufficiency, diabetes or pressure (Nwomeh et al. 1998b). The resulting hypoxia leads to cell death in tissues and the recruitment of macrophages, which in turn secrete neutrophil chemoattractants and pro-inflammatory substances (Eming et al. 2007c). Neutrophils release extensive amounts of MMPs and neutrophil-derived elastase (Nwomeh et al. 1998a) whereas, during normal wound healing, protease expression is tightly regulated in time and space and coordinated with the expression of their inhibitors. These proteases together with neutrophil-derived reactive oxygen species damage resident cells, components of the extracellular matrix, and tissue growth factors, which prevents tissue formation and contributes to an amplification of the inflammatory response (Menke et al. 2007). Thus, chronic wounds are characterized by an inflammatory response that is sustained, uncontrolled and self-amplifying, and represent a major target for pro-angiogenic therapies, as these aim at treating the underlying, primary cause of disease.



### **1.3.2 Pro-angiogenic therapies as pre-requisite for tissue engineering**

Not only during tissue regeneration, but also for tissue engineering approaches, the induction of capillary growth is of importance, as oxygen diffusion into tissues is spatially limited. For this reason, the controlled induction of functional angiogenesis is under investigation for the amelioration of organ or grafted tissue take after transplantation, and also crucial for the *in vitro* generation of organ substitutes (Zisch et al. 2003).

### **1.3.3 Basic principles for the use of growth factors in tissue engineering**

Major tissue engineering approaches for the stimulation of angiogenesis consist in the delivery of growth factors either as protein or expression vector to the site of hypoxia. For the induction of a functional vasculature, a sustained presence of the growth factor within the tissue at a low dose is required, as the side effects of excessive local doses of pro-angiogenic growth factors counteract physiological vessel growth. VEGF-A is recognized to regulate all steps required to induce angiogenesis as described in the following section, and hence has been a major molecule of interest in the development of pro-angiogenic drugs (Zisch et al. 2003). However, exposure of tissues to extensive local doses of this growth factor resulted in the formation of instable, abnormal, highly tortuous and leaky vessels as well as haemangioma (Horowitz et al. 1997; Ozawa et al. 2004; Yancopoulos et al. 2000; Zisch et al. 2003).

## **1.4 The vascular endothelial growth factor**

### **1.4.1 Discovery and effect on endothelial cells**

The vascular endothelial growth factor-A (VEGF-A) is the master regulator of angiogenesis and was discovered twice independently for its most striking characteristic properties. First, in 1983, a tumor-secreted protein was described capable to increase vascular leakage in the skin very potently, and therefore named vascular permeability factor (VPF, Senger et al. 1983). Second, in 1989, two groups described a heparin-binding protein secreted by pituitary follicular cells, acting as an endothelial cell specific mitogen, hence termed vascular endothelial growth factor (VEGF, Ferrara and Henzel 1989; Gospodarowicz et al. 1989). When the cDNA of both proteins was

cloned in the same year, it turned out that VEGF and VPF were identical (Ferrara 2004; Keck et al. 1989; Leung et al. 1989).

Since its discovery, VEGF-A has been a major target in research and is well characterized as the main growth factor controlling all steps during angiogenesis. VEGF-A induces proliferation and migration in endothelial cells, and is an important survival factor counteracting apoptosis. VEGF-A signaling leads to the expression of proteases to allow for basal membrane degradation and alters the expression of integrins to mediate cell attachment to provisional matrices. Furthermore, VEGF-A induces tube formation by endothelial cells and favors vasodilatation (Bates and Curry 1996; Bates and Jones 2003; Connolly et al. 1989; Conolly 1989; Ferrara and Henzel 1989; Koolwijk et al. 1996; Ku et al. 1993; Senger et al. 1983).

#### **1.4.2 Molecular properties and regulation of expression**

VEGF-A belongs to the VEGF family of growth factors that in mammals currently comprises five members named VEGF-A through D and placental growth factor (PlGF). Related proteins are also found in parapoxvirus (VEGF-E) and snake venom (VEGF-F). Members of this family are secreted homodimeric glycoproteins and share a homology domain, composed of eight spatially highly conserved cysteine residues organized in a cysteine knot motif (reviewed in Ferrara 2004). Out of these, six cysteines stabilize the monomers by the formation of intramolecular disulfide bonds, and the monomers are linked to each other by two additional disulfide bonds in an anti-parallel fashion (Wiesmann et al. 1997).

VEGF-A is the most abundant and best investigated family member. The growth factor is encoded by a single gene comprising 8 exons, and differential splicing gives rise to isoforms of different molecular weight. To date, at least 13 isoforms have been described, and they are commonly denoted by their amino acid length following signal peptide removal. Out of these, VEGF-A<sub>121</sub>, 145, 148, 162, 165, 183, 189, and 206 promote angiogenesis. Splicing at a distal site gives rise to the so-called VEGF-A<sub>xxx</sub>b isoforms, VEGF-A<sub>121b</sub>, 145b, 165b, 183b and 189b, which are thought to have anti-angiogenic properties (Woolard et al. 2004). VEGF-A<sub>121</sub>, 165, 189 and 206 are the isoforms predominantly expressed by VEGF-A-expressing cells (Houck et al. 1991). VEGF-A isoforms differ in their biological activity, and in their affinity to the extracellular matrix, which is due to the presence or absence of sequences required for the binding to co-receptors and heparan sulfate proteoglycans. In the VEGF-A-gene, exons 6 and 7 encode for two independent heparin-binding domains. VEGF-A<sub>121</sub>, which is encoded by exons 1-5 and 8, is a freely diffusible protein. In contrast, VEGF-A<sub>165</sub> additionally comprises exon 7

and shows moderate heparin affinity, and therefore, about 50-70% of secreted VEGF-A<sub>165</sub> remains extracellular matrix-associated (Ferrara and Henzel 1989; Gospodarowicz et al. 1989). VEGF-A<sub>189</sub> and VEGF-A<sub>206</sub> are completely sequestered in the extracellular matrix as they bind to heparin very strongly due to amino acids encoded by exons 6 and 7 (Houck et al. 1992).

As the overall effect of angiogenesis on a tissue under physiological as well as under pathological conditions is the increase of oxygen and nutrients supply (Bates and Jones 2003), it is not surprising that one of the major regulators of VEGF-A expression is the availability of oxygen. Under hypoxia, VEGF-A-transcription is initiated by the hypoxia-inducible factor-1 (HIF-1), a hetero-dimeric protein formed from HIF-1 $\alpha$  and HIF-1 $\beta$  (Mole et al. 2002). Under normoxia, HIF- $\alpha$  is ubiquitinated, targeted for the proteasome and quickly degraded (Ivan et al. 2001). By contrast, under hypoxic conditions, HIF-1 $\alpha$  is stabilized and translocates into the nucleus, where it forms an active transcription factor complex with HIF-1 $\beta$  and other co-factors (Ivan et al. 2001). This complex induces transcription of genes downstream of hypoxia-response elements, such as VEGF-A (Kietzmann et al. 1999). Under hypoxia, both the transcription and the translation rate of VEGF-A are increased, and VEGF-A-mRNA is protected from degradation (Akiri et al. 1998; Bates and Jones 2003; Levy et al. 1997). Additionally, several growth factors, including EGF, TGF- $\alpha$  and - $\beta$ , keratinocyte growth factor (KGF), insulin-like growth factor-1, FGF and PDGF, as well as the pro-inflammatory cytokines interleukin-1 $\alpha$  and -6, hormones, oncogenes, and tumor suppressor genes upregulate the transcription of VEGF-A (Deroanne et al. 1997; Finkenzeller et al. 1997; Goad et al. 1996; Li et al. 1995; Neufeld et al. 1999; Ryuto et al. 1996).

### **1.4.3 VEGF-A receptors and signaling**

VEGF-A binds to VEGF receptor (VEGFR)-1 and -2, which are members of the receptor tyrosine kinase superfamily. The extracellular domain of VEGFRs folds into seven immunoglobulin-like domains. A single transmembrane domain is followed by a juxta-membrane domain, a split tyrosin kinase domain and a C-terminal, intracellular tail (de Vries et al. 1992; Shibuya et al. 1990). Ligand binding leads to receptor homo- or hetero-dimerization and activation of the kinase domain (Figure 2).

The role of signaling mediated by VEGFR-1 has been under debate for a long time (Ferrara 2004). VEGF-A binds to VEGFR-1 with a much higher affinity than to VEGFR-2 (Joukov et al. 1997; Waltenberger et al. 1994), but VEGFR-1 autophosphorylation is barely detectable in response to VEGF-A (de Vries et al. 1992). Nevertheless, this receptor is crucial during embryonic development, as the knock-out of VEGFR-1 is embryonic lethal, due to endothelial overgrowth and to the formation of an unorganized vasculature (Fong et al. 1999). In these mice, VEGFR-2 phosphorylation is increased. However, mice expressing a VEGFR-1 in which the kinase domain was deleted are healthy (Hiratsuka et al. 1998). These observations led to the idea that VEGFR-1 might act as a negative regulator of VEGFR-2 by exerting a decoy function by trapping VEGF-A, thereby weakening VEGF-A-mediated signaling (Fong et al. 1999). In a recent publication, the understanding of VEGFR-1's role in VEGF-A signaling was extended. Expressing a chimeric receptor consisting of the extracellular domain of the epidermal growth factor receptor fused to the intracellular domain of VEGFR-1, confirmed that VEGFR-1 is indeed a negative regulator of VEGFR-2 signaling, but that this effect is regulated by VEGFR-1 downstream signaling and not only by ligand trapping (Zeng et al. 2001). Also, macrophage and monocyte migration towards VEGF-A is dependent of VEGFR-1 (Barleon et al. 1996).

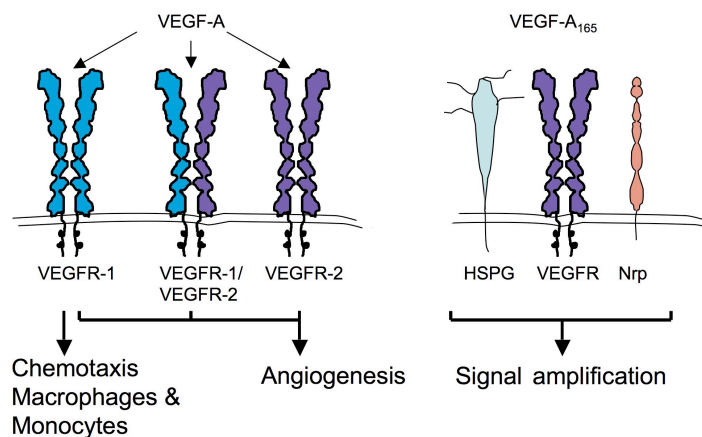


**Figure 2: Schematic representation of VEGF-A receptors and VEGF-A<sub>165</sub> co-receptors (Lohela et al. 2009; Olsson et al. 2006).**

VEGF-A exerts its striking effects on endothelial cell biology via VEGFR-2 mediated signaling, and major downstream signaling pathways are summarized in Figure 3 (reviewed in Lamalice et al. 2007 and Zachary 2005).

The major downstream target of VEGFR-2 is phospholipase C  $\gamma$  (PLC $\gamma$ ). PLC $\gamma$  is recruited to the plasma membrane upon VEGF-A stimulation and binds to phospho-tyrosine 1175 of VEGFR-2 via its C-terminal src homology 2 (SH2) domain (Takahashi et al. 1999; Takahashi et al. 2001). PLC $\gamma$  catalyzes the generation of diacylglycerol and inositol-1, 4, 5-trisphosphate from phosphatidylinositol-4, 5-bisphosphate, and signaling leads to activation of the Raf-MEK-MAPK pathway (Takahashi et al. 1999) downstream of the calcium dependent protein kinase C (PKC) and the protein kinase D (Wong and Jin 2005). Thereby, VEGFR-2 signaling mediates the major signal towards proliferation in endothelial cells.

Another major downstream pathway of VEGFR-2 is the PI3K – Akt/protein kinase B (PKB) pathway promoting endothelial cell survival. Upon VEGF-A stimulation, the adapter protein Shb is recruited to phosphorylated tyrosine 1175 of VEGFR-2 and becomes tyrosine phosphorylated in a Src-dependent manner (Holmqvist et al. 2004). Subsequent activation of PI3K and generation of phosphorylated inositolphospholipids at the plasma membrane allows the recruitment and activation of the serine-threonine kinase Akt/PKB. Akt in turn phosphorylates and thereby inhibits the death-promoting protein Bad (Datta et al. 1997).

VEGF-A is a strong chemoattractant for endothelial cells, and chemotactic migration is induced by VEGFR-2. In general, cell migration is based on modifications of the cell's cytoskeleton. Particularly, the formation of membrane protrusions such as filopodia and lamellipodia, and the formation of contractile stress fibers underlie this process. Regulation of the actin cytoskeleton downstream of VEGFR-2 can be accomplished by the recruitment of the SH2 domain containing adapter protein Nck to the autophosphorylation site on tyrosine 1214, and activation of the Src-kinase Fyn. Fyn activity subsequently leads to activation of p21 activated kinase (PAK-2), cell division control protein 42 (Cdc42), mitogen-activated protein kinase kinase 3 (MKK3/6), stress-activated protein kinase 2/p38 (SAPK2/p38) and mitogen-activated protein kinase activated protein kinase 2 (MAPKAP K2, Lamalice et al. 2004). Actin polymerization and the formation of stress fibers downstream of MAPKAP K2 can be induced either by phosphorylation of the actin filament capping protein heat shock protein 27 (HSP27), resulting in uncapping of the filaments (Landry and Huot 1995), or by activation of LIM kinases that phosphorylate cofilin, which in turn inhibits its actin filament destabilizing activity (Kobayashi et al. 2006). An additional pathway inducing actin nucleation downstream of Nck involves the activation of the Arp2/3 complex downstream of the neuronal Wiskott-Aldrich syndrome protein (N-WASP, Li et al. 2001).

Besides on the re-arrangement of the cytoskeleton, cell migration also depends on the formation and the turnover of focal adhesions. The focal adhesion kinase (FAK) is a key regulator for focal adhesion turnover, and its activation downstream of VEGFR-2 and integrin  $\alpha\beta3$ , a receptor for the provisional matrix constituent vitronectin with a crucial role in angiogenesis, was investigated in much detail. Upon VEGF-A stimulation, the formation of a complex consisting of VEGFR-2, HSP90 and  $\beta3$  integrin was shown to take place. Two parallel downstream signaling pathways subsequently contribute to FAK phosphorylation on tyrosines 397, 407 and 861 and on serine 732, and result in cell migration. FAK is recruited to activated integrins resulting in its autophosphorylation (Parsons 2003) and the recruitment and activation of the Src kinase Pyk-2 (Le Boeuf et al. 2006). Pyk-2 and the Rho-associated coiled-coil-forming protein kinase ROCK, which becomes activated downstream of VEGFR-2 and Rho A then mediate the full activation of FAK (Le Boeuf et al. 2004).

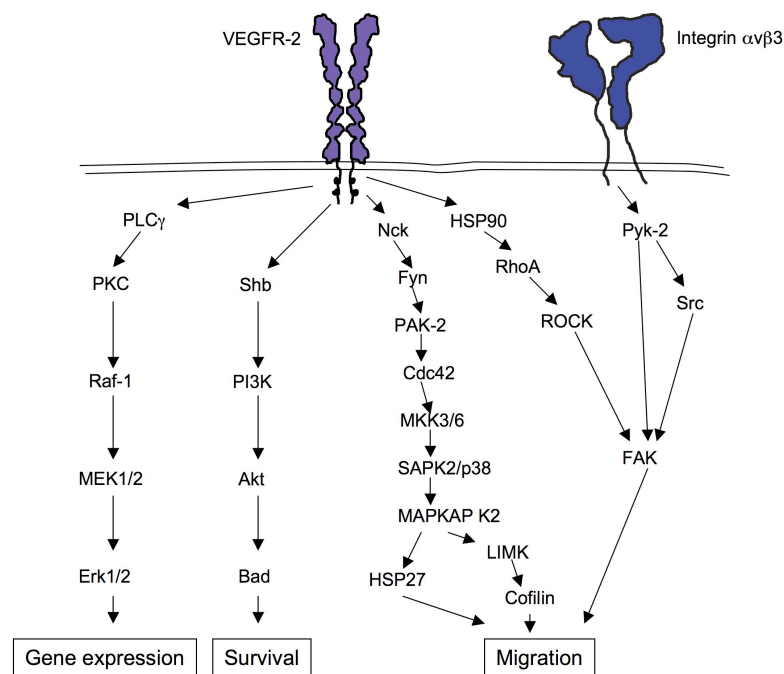


**Figure 3: Schematic summary of the downstream signaling pathways induced by VEGFR-2 (Lamallice et al. 2007; Zachary 2005).**

#### 1.4.4 VEGF-A co-receptors

Heparan sulfate and neuropilin (Nrp) are co-receptors of VEGF-A and can strongly increase the biological response of endothelial cells to the growth factor isoforms that they bind (Figure 2).

In the early studies, VEGF-A is described as a heparin-binding protein. *In vivo*, VEGF-A isoforms comprising a heparin-binding domains encoded by exons 6 and 7 interact with

heparin-like domains of heparan sulfates found as a component of proteoglycans on cell surfaces, in the extracellular matrix and in the basement membrane of most mammalian tissues (Bernfield et al. 1999). A need of heparan sulfate proteoglycans (HSPGs) for the full activation of signaling pathways induced by VEGF-A, FGF-2 and PDGF-BB has been described (Gitay-Goren et al. 1992; Rolny et al. 2002; Yayon et al. 1991).

For VEGF-A<sub>165</sub>, it is known that the C-terminal region encoded by exon 7 and corresponding to amino acids 111-165 is essential not only for the interaction with heparin, but also for its full mitogenic potency, as it was shown using plasmin-generated VEGF-A<sub>165</sub> fragments (Keyt et al. 1996). Plasmin-mediated processing of VEGF-A<sub>165</sub> gives rise to two shorter fragments, VEGF-A<sub>110</sub> and VEGF-A<sub>111-165</sub>. VEGF-A<sub>110</sub> is still able to bind to VEGFR-2 but is a less potent mitogen than VEGF-A<sub>165</sub>. Instead, its mitogenicity is comparable to that of VEGF-A<sub>121</sub> (Keyt et al. 1996). *In vitro* experiments using human umbilical vein endothelial cells (HUVECs) showed, that heparin increases VEGF-A<sub>165</sub> affinity to VEGFR-2 and also to Nrp-1, leading to increased VEGFR-2 phosphorylation and cell proliferation. The effect of VEGF-A<sub>121</sub> by contrast is not potentiated by addition of heparin, underlining the importance of the presence of a heparin-binding domain (Ashikari-Hada et al. 2005). For this potentiation, presentation of VEGF-A to VEGFR-2 by heparan sulfate on neighboring cells seems to be necessary, which mechanistically may prevent receptor downregulation by its internalization, and promote prolonged VEGFR-2 signaling (Jakobsson et al. 2006).

Nrp-1 and -2 are additional VEGF-A co-receptors. These transmembrane glycoproteins were originally discovered as adhesion proteins on neurons, where they are involved in axonal guidance as semaphorin-receptors (Schwarz and Ruhrberg 2010). Both Nrps are very similar in structure and consist of a large extracellular domain linked to a short cytoplasmic domain via a transmembrane domain. Nrp-1 binds to VEGF-A<sub>165</sub> and VEGF-A<sub>121</sub>, while Nrp-2 binds to VEGF-A<sub>165</sub> and VEGF-A<sub>145</sub> (Gluzman-Poltorak et al. 2000; Pan et al. 2007; Soker et al. 1998). In porcine aortic endothelial cells co-transfected with Nrp-1 and VEGFR-2, chemoattraction towards VEGF-A<sub>165</sub> is increased as compared to cells transfected with either receptor alone (Soker et al. 1998). The increased chemotactic response observed in co-transfected PAE cells was attributed to the formation of complexes between Nrp-1 and VEGFR-2 (Whitaker et al. 2001), and it was demonstrated that complex formation can take place between receptors of one cell or between neighboring cells, and results in enhanced VEGFR-2 signaling under certain conditions (Soker et al. 2002). Whether Nrp-1 can signal on its own is still under discussion and may be cell type specific (Wang et al. 2003).

### 1.4.5 Crosstalk between VEGFR-2 and integrins in angiogenesis

Early evidence shows that angiogenesis not only requires growth factor stimulation but is also dependent on outside-in signaling mediated by integrins. Integrins are heterodimeric transmembrane cell surface receptors for the extracellular matrix. By linking the extracellular matrix and the cell cytoskeleton, integrin outside-in signaling has a major impact on cell behavior, and integrin occupancy modulates cellular functions such as survival, cell-cycle progression, substrate adhesion, migration, and signaling via other cell surface receptors. Integrins are composed of one  $\alpha$  and one  $\beta$  subunit that are non-covalently linked to each other, and the subunit composition determines the ligand specificity of a given integrin. Angiogenesis is a process that is profoundly dependent on the extracellular matrix, and so the prominent role that integrins play during vascular remodeling is not surprising. On quiescent endothelial cells, integrins  $\alpha1\beta1$ ,  $\alpha2\beta1$ ,  $\alpha3\beta1$ ,  $\alpha5\beta1$ ,  $\alpha6\beta1$ ,  $\alpha6\beta4$  and  $\alpha v\beta5$  are expressed (Stupack and Cheresh 2002), mediating the attachment to laminins, collagens, fibronectin or vitronectin. Angiogenic stimuli alter the integrin-expression profile and result in upregulation of  $\alpha1\beta1$  and  $\alpha6\beta1$  (Lee et al. 2006; Stupack and Cheresh 2002) as well as a dramatic upregulation of  $\alpha v\beta3$  expression (Lee et al. 2006; Stupack and Cheresh 2002), thus allowing activated integrins to interact with proteins of the provisional matrix and matricryptic sites of extracellular matrix proteins that become exposed upon proteolytic processing (Stupack and Cheresh 2002).

Early evidence of the importance of integrins specifically points to an essential role of  $\alpha v\beta3$  in angiogenesis. The expression of this integrin is absent on quiescent vessels, but strongly upregulated in angiogenic vessels in the granulation tissue of human wounds and in the chick chorioallantoic membrane (CAM, Brooks et al. 1994a).  $\alpha v\beta3$  is functionally required for angiogenesis, as inhibition by either function blocking antibodies or cyclic arginine-glycine-aspartic acid (RGD)-peptides selectively induces apoptosis of activated endothelial cells (Brooks et al. 1994a; Brooks et al. 1994b). Ligation of  $\alpha v\beta3$  hence promotes an important survival signal for activated endothelial cells that involves the inhibition of p53 binding to DNA (Stromblad et al. 1996).

Importantly, integrin  $\alpha v\beta3$  also plays a critical role in the full activation of VEGFR-2 (Soldi et al. 1999) and other receptor tyrosine kinases such as PDGF-receptor  $\beta$ , insulin receptor, and TGF $\beta$  type II receptor (Scaffidi et al. 2004; Schneller et al. 1997). In endothelial cells attaching to an  $\alpha v\beta3$  ligand, VEGFR-2 signaling is markedly increased; the phosphorylation of VEGFR-2 is stronger, and cells proliferate and migrate more compared to cells stimulated with VEGF-A<sub>165</sub> on ligands specific to other integrins. Integrin  $\alpha v\beta3$  is activated by VEGF-A<sub>165</sub>-stimulation



downstream of VEGFR-2 via a signaling pathway that seems to involve PI3K and Akt (Byzova et al. 2000). Moreover, both receptors can be co-immunoprecipitated upon VEGF-A<sub>165</sub> stimulation (Hall et al. 2004; Hall and Hubbell 2004; Soldi et al. 1999). This interaction between VEGFR-2 and integrin  $\alpha\beta3$  was shown to involve the extracellular domains of the receptors, to be mediated by the integrin  $\beta3$  subunit, and to require also the  $\alpha v$  subunit (Borges et al. 2000). Mahabeleshwar and co-workers showed that the stimulation of either receptor leads to complex formation and to the mutual transactivation of the receptors resulting in increased phosphorylation of VEGFR-2 and  $\beta3$  (Mahabeleshwar et al. 2007). Furthermore, in these complexes, VEGFR-2 associates with activated  $\alpha\beta3$  integrin in angiogenic cells, both in HUVEC stimulated with VEGF-A *in vitro*, and in vessels in biopsies taken from prostate cancers *in vivo* (Mahabeleshwar et al. 2008). Research done by this group indicates that autophosphorylation of VEGFR-2 upon VEGF-A stimulation recruits cSrc to the receptor and leads to interaction of VEGFR-2 with  $\alpha\beta3$ .  $\beta3$  is subsequently phosphorylated on two cytoplasmic tyrosine residues by cSrc, which is necessary for the prolonged and full activation of VEGFR-2 (Figure 4). Furthermore, basal VEGFR-2 phosphorylation can be triggered by integrin  $\alpha\beta3$  ligation in endothelial cells even in the absence of VEGFR-2 and can start the angiogenic program in CAMs (Hall et al. 2004; Mahabeleshwar et al. 2007). The angiogenic program can also be activated by direct binding of VEGF-A<sub>165</sub> to  $\alpha\beta3$  (Hall et al. 2004; Hutchings et al. 2003).

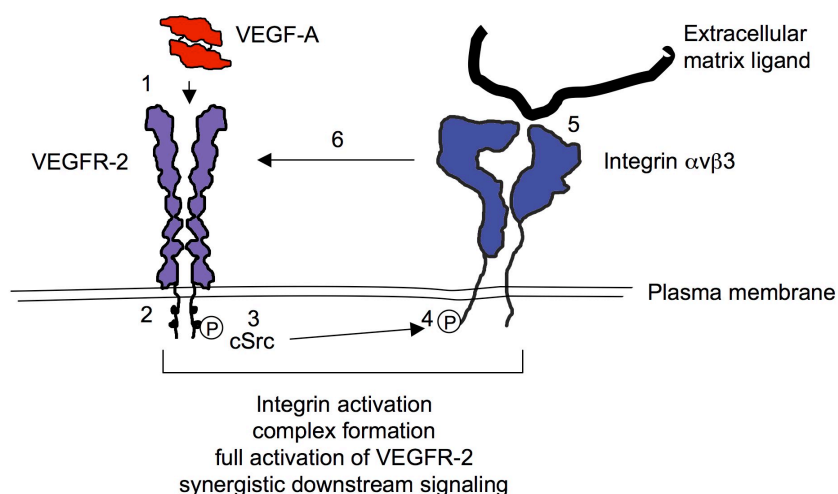


**Figure 4: Model of the molecular mechanisms of transactivation of VEGFR-2 and integrin  $\alpha\beta3$ .** VEGF-A binding to VEGFR-2 (1) results in receptor autophosphorylation (2). cSrc is recruited to phosphorylated VEGFR-2 and activated (3), and mediates the phosphorylation of  $\beta3$  (4), thereby activating integrin  $\alpha\beta3$  (5). Complex formation between the activated receptors (6) allows for their full activation and synergistic signaling (Somanath et al. 2009).

Silencing experiments, in which the expression of  $\beta$ -integrin subunits  $\beta 1$ ,  $\beta 3$  and  $\beta 5$  was downregulated, showed that the silencing of  $\beta 3$  integrin had the most profound effect on endothelial cell biology. HUVECs in which the expression of  $\beta 3$  was downregulated by siRNA were not capable of tube formation and phosphorylation of VEGFR-2 was reduced. Silencing of the other  $\beta$ -subunits resulted in less severe dysfunction in these experiments (Mahabeleshwar et al. 2008), even though also integrins  $\alpha 1\beta 1$  and  $\alpha 2\beta 1$  have been shown to be crucial for angiogenesis *in vitro* and *in vivo* (Senger et al. 1997; Senger et al. 2002).

However, the role of integrin  $\alpha v\beta 3$  as a pro-angiogenic modulator has recently been questioned. Even though the majority of mice deficient in  $\alpha v$  integrins dies *in utero*, these mice still develop a vascular system, in which angiogenic sprouting and vascular remodeling takes place. Lethality is not caused by absence of vessel growth, but by hemorrhages in the brain and the interstitium (Bader et al. 1998). Similarly, deficiency in integrin  $\beta 3$  results in mortality, which in part is due to placental defects, and to hemorrhages. Nevertheless, mice surviving birth develop a normally vascularized retina indicative of functional angiogenesis (Hodivala-Dilke et al. 1999). This may result from compensatory mechanisms, as in these mice, the expression of VEGFR-2 is upregulated and enhanced phosphorylation is observed (Reynolds et al. 2004). By contrast, knock-in mice in which the tyrosine residues on integrin  $\beta 3$  were mutated, develop normally. However, the mutated  $\beta 3$  integrin is not capable to form complexes with VEGFR-2 and signaling is reduced. Also, pathological angiogenesis in response to subcutaneously implanted tumors is abolished (Mahabeleshwar et al. 2006). Importantly, the strictly anti-angiogenic effect of RGD-mimetics was queried in a recent study, as low concentrations of these molecules currently in clinical trials for the inhibition of tumor angiogenesis were shown to promote angiogenesis (Reynolds et al. 2009). Thus, the molecular regulation of angiogenesis by integrin  $\alpha v\beta 3$  is not entirely clear.

#### **1.4.6 Role of VEGF-A during wound healing**

VEGF-A-mediated signaling and the angiogenic response induced by VEGF-A are crucial for normal wound healing. In unwounded skin, VEGF-A expression is absent, but immediately after injury, VEGF-A is released by platelets and monocytes (Bottomley et al. 1999) and exerts an important function in the recruitment of monocytes into the clot. Also other inflammatory cell types are important sources of VEGF-A. Furthermore, hypoxia in the wound area induces

VEGF-A expression in keratinocytes, fibroblasts and dermal microvessels (Connolly et al. 1989; Namiki et al. 1995; Senger et al. 1983). At the mRNA- and protein level, VEGF-A becomes upregulated in wounds at day 3 post wounding and declines around day 13. After three weeks, VEGF-A expression is absent again. The expression of VEGF-A is thus restricted both in time and space and parallels the time course and location of active wound angiogenesis (Bates and Jones 2003; Brown et al. 1992; Kishimoto et al. 2000).

The importance of VEGF-A in tissue regeneration first became evident during a study employing diabetic mice, characterized by delayed wound closure. In these mice, VEGF-A mRNA is briefly upregulated on day one post-injury, but downregulated relative to control levels from day three on, which is the time granulation tissue formation normally starts. In wild type mice by contrast, VEGF-A expression is upregulated concomitantly with granulation tissue formation (Frank et al. 1995). Furthermore, in a pig wounding model, it was shown that application of VEGF-A neutralizing antibodies inhibits wound angiogenesis and granulation tissue formation (Howdieshell et al. 2001). By contrast, both topical application of VEGF-A protein as well as transfection of the skin with a plasmid encoding for VEGF-A improved the closure of wounds in diabetic mice (Galiano et al. 2004; Roth et al. 2006).

## **1.5 Cellular and molecular mechanisms of angiogenesis**

### **1.5.1 Induction of angiogenesis and the role of VEGF-A**

Angiogenesis is the growth of new capillaries out of pre-existing ones and hence clearly distinctive from vasculogenesis, the formation of a primitive capillary plexus from precursor cells during early stages of development. Angiogenesis occurs in the adult in a very limited array of situations physiologically, among these are the female reproductive cycle and skin regeneration. Endothelial cells are among the most quiescent cell populations of the human body (Folkman 2006). Hence, angiogenesis requires activation of endothelial cells, involving a profound change in their genetic program. This re-programming allows endothelial cells to proliferate, to migrate towards angiogenic stimuli and to interact with provisional and interstitial extracellular matrices (Cheresh and Stupack 2008). During the early stages of angiogenesis, this re-programming of endothelial cells is induced by VEGF-A. Internalization of vascular endothelial cadherin leads to the loosening of cell-cell junctions between endothelial cells (Potter et al. 2005), which is a prerequisite for cells to migrate. The disruption of cell-cell contacts also increases vascular permeability, thus permitting leakage of plasma proteins from the circulation,

to form a provisional matrix permissive for migration. VEGF-A signaling furthermore stimulates the turnover of focal adhesions, the reorganization of the cytoskeleton resulting in a loss of cell polarity, and stimulates proliferation (see above). Importantly, the growth factor also triggers the expression of proteases to degrade the basal membrane, the connective tissue or the provisional matrix being invaded and of an additional set of integrins that recognize substrates found in these tissues (Cheresh and Stupack 2008).

### **1.5.2 Vascular guidance by tip cells and the role of tip cell selection**

Importantly, during the sprouting process, cells need guidance to determine their migration. In the developing mouse retina, but also *ex vivo* in rat aortic ring assays, it was demonstrated that the growing vessels are guided by a single cell that is peculiar by the dynamic extension and regression of multiple filopodia (Gerhardt et al. 2003). These cells are named tip cells and followed by a phalanx of lumen-bearing stalk cells. Due to their filopodia, tip cells are highly polar and capable of probing their environment for pro- and anti-angiogenic cues far from the cell body. Particularly, tip cells were shown to be enriched in VEGFR-2 that is prominently located to filopodia, rendering them thus capable to act as a sensor for VEGF (Gerhardt et al. 2003). The tip cell phenotype is induced by VEGF-A, as topical VEGF-A increases the number of tip cells induced, while the application of VEGF-A-neutralizing antibodies in the developing mouse retina abolishes tip cell formation and extension of filopodia (Gerhardt et al. 2003). For ordered angiogenesis to take place, it is necessary to ensure that not all VEGF-A stimulated cells become tip cells, as that is the default fate for VEGF-A-stimulated endothelial cells (Bentley et al. 2008). This is accomplished by lateral inhibition mediated by delta-like ligand 4 (Dll4) and notch signaling. It was shown that VEGF-A-stimulated cells up-regulate the notch-ligand Dll4 via the VEGFR-2/PI3K/Akt axis (Liu et al. 2003). Dll4 binds to and activates notch in neighboring cells. Notch signaling in these cells downregulates the expression of VEGFR-2 (Williams et al. 2006), hence making cells less responsive to VEGF-A, and leading to a decreased Dll4-expression. Cells with a strong notch signal therefore adapt to stalk cells (Hellstrom et al. 2007). In this way, cells that receive the stronger VEGF-A stimulus and express more Dll4 acquire the tip cell phenotype and laterally inhibit adjacent cells from doing the same (Bentley et al. 2008). For tip cell selection, but also for their guidance, VEGF-A-gradients are of crucial importance (Bentley et al. 2008).

### **1.5.3 The role of VEGF-A binding to the extracellular matrix in tip cell guidance**

For VEGF-A isoforms possessing a heparin-binding domain, VEGF-A localization within the extracellular matrix can be controlled and gradients can be established, which is not the case for diffusible VEGF-A isoforms. Disturbance of these gradients leads to vascular malformations, as demonstrated in mice selectively expressing one of the three main VEGF-A isoforms VEGF-A<sub>120</sub>, VEGF-A<sub>164</sub> and VEGF-A<sub>188</sub> (in mice, VEGF-As are one amino acid shorter than in humans, Ruhrberg et al. 2002; Stalmans et al. 2002). In the developing retina of mice that express exclusively the soluble isoform VEGF-A<sub>120</sub>, VEGF-A is no longer localized to astrocytes but distributed in a more diffuse pattern. Hence, the VEGF-A gradient is less steep in these mice. This is reflected by the extension of short filopodia not only in tip cells but also in stalk cells. The vessels are bigger as stalk cell proliferation is increased, branching is decreased and migration is impaired in mice expressing solely VEGF-A<sub>120</sub> (Gerhardt et al. 2003; Ruhrberg et al. 2002). In contrast, expression of only the tightly matrix bound isoform VEGF-A<sub>188</sub> has the opposite effect on the vascular network: vessels are very thin and hyperbranched. Mice which express only VEGF-A<sub>165</sub>, the VEGF-A isoform partially matrix bound and partially soluble, develop a normal retinal vasculature (Stalmans et al. 2002). Taken together, these results demonstrate that both tip cell migration and stalk cell proliferation are regulated by VEGF-A, but that tip cell migration is dependent on extracellular gradients, while stalk cell proliferation depends on local VEGF-A concentrations (Gerhardt et al. 2003).

### **1.5.4 Maturation of the vascular network**

Newly induced vasculature is immature and characterized by high instability, leakiness, and high dependence on VEGF-A-signaling for its survival. Vessels mature by the recruitment of pericytes, a vascular mural cell type that covers the outside of the vessel and helps to build a novel basal membrane in which it is embedded (Armulik et al. 2005; Jain 2003). It was shown that pericytes become recruited to the novel vessel by PDGF-B, which in binding to the PDGFR- $\beta$  induces the proliferation of pericytes and their migration along the nascent vessel (Hellstrom et al. 1999; Hoch and Soriano 2003). PDGF-B in turn is secreted by tip cells (Gerhardt et al. 2003) and sequestered to the growing vessel's wall by binding to HSPGs (Abramsson et al. 2007). Between the two cell types, special cell-cell contacts are established, which allow communication between the cells (Armulik et al. 2005). Both endothelial cells and

pericytes constitute to a novel basement membrane, containing laminins, fibronectin, nidogen-1 and perlecan (Stratman et al. 2009). Basement membrane synthesis is accompanied by altered integrin expression in both cell types and contributes to the regulation of the vessel's diameter. Additionally, the basement membrane is stabilized by protease inhibitors released by vascular cells: endothelial cells secrete the soluble tissue inhibitor of metalloproteinase-2 (TIMP-2) while pericytes secrete TIMP-3, which becomes sequestered in the basal membrane due to heparin-binding motifs (Saunders et al. 2006). Besides inhibiting several proteases, TIMP-3 was also shown to negatively regulate pro-angiogenic signaling induced by VEGF-A by competing with VEGF-A for VEGFR-2 (Qi et al. 2003).

Homeostasis and quiescence of the endothelium are actively maintained by angiopoietin-1/tyrosine kinase with immunoglobulin and epidermal growth factor homology domain-2 (Ang1/Tie-2) signaling, a pathway that is also essential for the maturation of the vasculature (Armulik et al. 2005; Murakami and Simons 2009). Tie-2 is an endothelium-specific receptor tyrosine kinase and becomes activated upon binding of Ang1, which is constitutively expressed by perivascular and mural cells (Davis et al. 1996; Suri et al. 1996). Downstream signaling results in vessel stabilization and resistance to VEGF-A-induced leakiness (Gavard et al. 2008).

## **1.6 Strategies aiming at the optimization of VEGF-A induced angiogenesis in tissue engineering**

### **1.6.1 Stabilization of the VEGF-A<sub>165</sub> heparin-binding site in the proteolytic environment of the chronic wound**

In our laboratory, it was shown that VEGF-A<sub>165</sub> becomes degraded in wound fluid obtained from chronic wounds because the activation of the serine-protease plasmin is enhanced in these wounds (Lauer et al. 2000). VEGF-A<sub>165</sub> processing by plasmin gives rise to VEGF-A<sub>110</sub>, which is the receptor binding domain of the molecule, and VEGF-A<sub>111-165</sub>, which contains the heparin-binding domain (Keyt et al. 1996; Lauer et al. 2000). Although VEGF-A<sub>110</sub> retains its ability to bind to both VEGFR-1 and -2, its potency is markedly decreased as it retains no affinity to VEGF-A co-receptors that interact with the heparin-binding domain (Keyt et al. 1996). Upon prolonged incubation with plasmin or chronic wound fluid, VEGF-A is completely degraded (Lauer et al. 2000). Thus, the poor stability coupled with decreased potency of the growth factor may account for the lack of granulation tissue formation observed in chronic wounds.

In order to increase the stability of VEGF-A<sub>165</sub> in non-healing skin lesions, several variants of this growth factor isoform in which the plasmin cleavage site of the protein was mutated were created. When the plasmin cleavage site was mutated from Arg110/Ala111 to either Arg110/Pro111 (VEGF-A<sub>165</sub><sup>A111P</sup>) or to Lys110/Pro111, the mitogenic properties of the wild type protein were retained, and the potent proteins remain stable upon plasmin digest and in wound fluid obtained from chronic wounds (Lauer et al. 2002). Moreover, *in vivo* experiments were performed in diabetic (db/db) mice employing transfection of the skin by particle bombardment with plasmids carrying either VEGF-A<sub>165</sub> or the plasmin resistant mutant VEGF-A<sub>165</sub><sup>A111P</sup> prior to wounding (Roth et al. 2006). Db/db mice are characterized by a mutation in their leptin receptor gene (Bahary et al. 1990) and represent an established model for the study of impaired wound healing. Importantly, they also show increased plasmin activity in skin wounds (Roth et al. 2006). When VEGF-A<sub>165</sub> or VEGF-A<sub>165</sub><sup>A111P</sup> was expressed in skin of diabetic mice during regeneration, a well-vascularized granulation tissue was induced by day 12, which was not the case in animals receiving a control vector. In comparison to VEGF-A<sub>165</sub>, VEGF-A<sub>165</sub><sup>A111P</sup> induced a more persistent vasculature that regressed later during healing, most likely due to the prolonged stability of VEGF-A<sub>165</sub><sup>A111P</sup> protein at the wound site, which protected endothelial cells from apoptosis and resulted in more efficient recruitment of pericytes (Roth et al. 2006). For all experiments performed in this thesis, a VEGF-A<sub>165</sub> variant in which the plasmin cleavage site was mutated from Arg110/Ala111 to Lys110/Pro111 was used (Figure 5). This isoform is referred to as VEGFmut henceforth.

VEGF <sub>165</sub> wild type	100	K	C	E	C	R	P	K	K	D	<b>R</b>	<b>A</b>	R	Q	E	N	P	C	G	P	C	120	
VEGF <sub>165</sub> mutant	100	K	C	E	C	R	P	K	K	D	<b>K</b>	<b>P</b>	R	Q	E	N	P	C	G	P	C	120	

Figure 5: For experiments performed, a VEGF-A<sub>165</sub> isoform was used, which is resistant to plasmin mediated processing due to a mutation in the major cleavage site from Arg110/Ala111 to Lys110/Pro111. This mutant is denoted as VEGFmut.

### 1.6.2 Targeted delivery of VEGF-A for pro-angiogenic therapies

In a large variety of animal models, delivery of VEGF-A in either plasmid or protein form to induce angiogenesis yielded promising results. However, most double-blinded, placebo controlled clinical trials in humans have been disappointing so far, as VEGF-A treatment failed to prove superior to sham treatments.

Major challenges to overcome in the development of pro-angiogenic therapy using VEGF-A are the tight control of the dosage, the precise local administration and the timely limited exposure of the growth factor (Zisch et al. 2003). The proper local dose is essential for the induction of a

functional and mature vasculature, as VEGF-A acts physiologically in a very narrow range of concentrations (Ozawa et al. 2004). Elevated concentrations of VEGF-A result in the formation of excessive vasculature that is leaky, a fact that together with VEGF-A's ability to induce vascular permeability contributes to the formation of edema, which is a major side-effect observed upon bolus injections. Furthermore, overdose or extended delivery can result in the formation of haemangioma-like structures. Also, this immature and dysfunctional vasculature regresses as the growth factor concentration decreases due to protein diffusion out of the site of application below a biologically effective dose (Zisch et al. 2003).

To overcome these problems, Schense and Hubbell developed a delivery strategy in which recombinant proteins or peptides are covalently coupled to fibrin matrixes when applied to the place of action and released upon cell-mediated fibrin degradation (Schense and Hubbell 1999). Fibrin is a biopolymer forming naturally during wound healing, is non-toxic, and provides cues for degradation and invasion by cells. Thus, fibrin is a very attractive compound for tissue engineering applications.

Its precursor, fibrinogen, consists of three pairs of disulfide-bond linked polypeptide chains. Fibrinogen is converted to fibrin by activity of the protease thrombin that cleaves off N-terminal fibrinopeptides A and B. Thereby, binding sites on the molecule are exposed, allowing for non-covalent interactions with other fibrin molecules, resulting in the generation of double stranded protofibrils that laterally aggregate and built a network. This network is stabilized by covalent crosslinks formed between lysines and glutamines of distinct fibrin chains, a reaction that is catalysed by the transglutaminase factor XIIIa (Figure 6 A). Factor XIII is a heterotetrameric molecule that binds to fibrin(ogen) and is activated by thrombin to factor XIIIa (Mosesson et al. 2001; Weisel 2004). Besides crosslinking fibrin molecules with each other, factor XIIIa also crosslinks  $\alpha_2$ -plasmin inhibitor or fibronectin to fibrin. The factor XIIIa substrate sequence of proteins that become bound to fibrin is known, and hence, by fusing a factor XIIIa substrate sequence to a recombinant protein, it is possible to incorporate it specifically into fibrin matrices. For this purpose, the substrate sequence of  $\alpha_2$ -plasmin inhibitor, NQEQVSPL, is used, as it is an especially efficient substrate of factor XIIIa (Schense and Hubbell 1999). Growth factors fused to this transglutaminase substrate sequence (denoted as TG henceforth) and incorporated into fibrin matrices are released once cells proteolytically degrade the matrix, and thereby they are available when needed by the cells (Figure 6 B). The liberation of growth factors from the matrix can be accelerated by inserting the engineered plasmin sensitive site LIKMKP denoted as PL between the TG sequence and the growth factor (Figure 6 C). Liberation under these circumstances is even more sensitive to the presence of cells (Ehrbar et al. 2005).



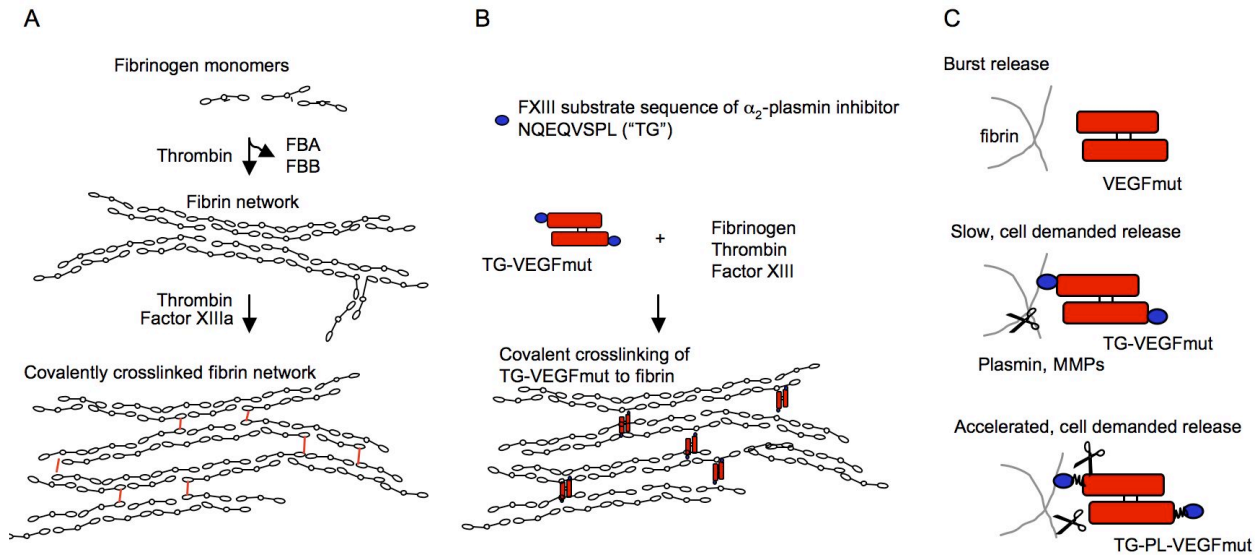


**Figure 6: Fibrin as slow release matrix for the delivery of bioengineered VEGF-A proteins.** (A) Fibrinogen is converted to fibrin by proteolytic processing by thrombin and aggregates to form a network. This network is covalently crosslinked by the activity of the transglutaminase factor XIIIa (Mosesson et al. 2001). (B) Expression of VEGFmut as a fusion protein with the factor XIIIa substrate sequence of  $\alpha_2$ -plasmin inhibitor (TG) allows for the covalent incorporation of the protein into fibrin matrices. (C) Comparison of differential release mechanisms of VEGFmut from fibrin gels. Soluble VEGFmut is thought to result in an uncontrolled burst release. Matrix-bound TG-VEGFmut is released once cells proteolytically degrade the matrix, and this release is more sensitive to the presence of cells, if a plasmin sensitive site (PL) is incorporated between the TG-site and VEGFmut (Ehrbar et al. 2005).

The effect of matrix coupled VEGF- $A_{121}$  has been investigated *in vitro* and *in vivo* by Zisch et al. and Ehrbar et al. They demonstrated that VEGF- $A_{121}$  released from fibrin matrices remains active (Zisch et al. 2001) and that fibrin matrix bound VEGF- $A_{121}$  is able to induce morphologically normal, hierarchical, well-developed vessels in a CAM assay. Matrix binding was shown to improve the effect of VEGF- $A_{121}$  on vessel induction, as no unorganized capillary networks were observed. Moreover, it was shown in the mouse subcutaneous Teflon chamber implant model, that vessels induced by diffusible VEGF- $A_{121}$  were leaky, whereas those induced by matrix bound VEGF- $A_{121}$  did not leak (Ehrbar et al. 2004).

Within the present study, plasmin resistant VEGF- $A_{165}$  proteins were delivered to skin wounds using fibrin matrices in order to limit burst release of the growth factor.

### 1.6.3 Amplification of VEGF- $A_{165}$ induced signals

An additional strategy to increase the angiogenic response of endothelial cells could be to co-stimulate VEGFR-2 and integrin  $\alpha v \beta 3$ . As described above, this integrin plays a prominent role in VEGF-A stimulated angiogenesis, and co-stimulation can result in increased downstream signaling and integrin activation.

For the generation of a bi-functional ligand consisting of VEGFmut and an integrin ligand, the design was inspired by a natural complex forming between VEGF- $A_{165}$  and fibronectin.

Fibronectin is a 430 kDa rod-like protein composed of three different kinds of repeating modules (Figure 7 A) found in the blood and in the extracellular matrix. Fibronectin interacts with several extracellular matrix proteins such as collagen, fibrin and syndecan. Importantly, this molecule comprises various integrin-adhesion sites localized to fibronectin type III domains 9 (FNIII9) and 10 (Pankov and Yamada 2002) that primarily are recognized by integrin  $\alpha 5\beta 1$ . Fibronectin binds to different growth factors including VEGF- $A_{165}$ . Activated thrombocytes were shown to be a source for a fibronectin/VEGF- $A_{165}$  complex. The complex proved to amplify VEGF-A derived signaling in endothelial cells by binding to integrin  $\alpha 5\beta 1$  via the cell-binding domains FNIII9 and 10 on fibronectin, and to VEGFR-2 via VEGF- $A_{165}$  (Wijelath et al. 2002, Figure 7 A). The VEGF- $A_{165}$ -binding domain of fibronectin could be located to FNIII12-14. However, binding of VEGF- $A_{165}$  to recombinant FNIII12-14 is not sufficient to increase the cellular response to the growth factor. Instead, the fibronectin cell binding domains FNIII9/10, which are a ligand for  $\alpha 5\beta 1$ , have to be present in the recombinant VEGF- $A_{165}$ -binding protein to trigger a strong cellular response. The minimal fibronectin based construct permissive for synergistic downstream signaling in that context thus consisted of the cell binding type III domains 9 and 10 as well as the VEGF-A-binding domains III12-14 (Wijelath et al. 2006).

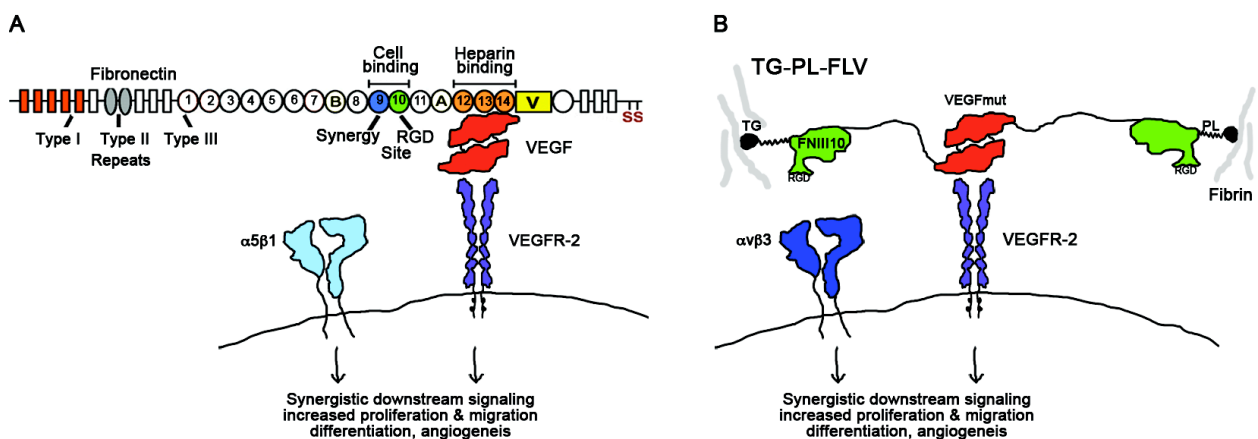


**Figure 7: The design of a bi-functional protein for the induction of synergistic signaling between VEGFR-2 and integrin  $\alpha 5\beta 3$  was inspired by nature. (A)** A complex released from activated thrombocytes consisting of fibronectin and VEGF- $A_{165}$  was shown to induce synergistic downstream signaling in endothelial cells by co-activation of VEGFR-2 and integrin  $\alpha 5\beta 1$  (fibronectin domain structure from Wierzbicka-Patynowski and Schwarzbauer 2003). **(B)** Generation of a bi-functional construct consisting of VEGF- $A_{165}$ mut and FNIII10 is thought to mimic this co-stimulation but to signal via VEGFR-2 and integrin  $\alpha 5\beta 3$ . This construct is to be delivered in fibrin matrices.

Interestingly, different fibronectin fragments have distinct affinities to various integrins. Thus, large fragments comprising FNIII9 and 10 were shown to bind to integrin  $\alpha 5\beta 1$ , whereas small fragments consisting of FNIII10 bound preferentially to integrin  $\alpha 5\beta 3$  (Pytela et al. 1985).

FNIII10 is the location of the minimal site required to promote integrin-mediated attachment, the tripeptide RGD, which is recognized by both integrins. However, for enhanced activation of  $\alpha 5\beta 1$ , additional portions of FNIII9 are required, that consist in a synergy site comprising a PHSRN sequence.

To mimic the enhanced biological activity of fibronectin-bound VEGF- $A_{165}$ , the FNIII10 was fused to VEGFmut via a linker peptide, thus giving rise to FNIII10-linker-VEGFmut, referred to as FLV. The RGD-site of FNIII10 is a promiscuous ligand for various integrins. However, in the activated endothelium, integrin  $\alpha v\beta 3$  becomes strongly upregulated (Brooks et al. 1994a), thus the construct is thought to target VEGFR-2 and integrin  $\alpha v\beta 3$  for synergistic downstream signaling (Figure 7 B).

## 2 Hypothesis

Previous investigations show that interactions between VEGF-A isoforms and the extracellular matrix are of crucial importance for the formation of a functional vascular network. VEGF-A isoforms bound to the extracellular matrix permit the formation of a growth factor tissue gradient, which is essential for the formation of tip cells and guidance of growing vessels. Furthermore, cells can discriminate between matrix bound and soluble VEGF-A, and both forms result in distinct downstream signaling. Finally, matrix binding of VEGF-A is considered important for the generation of local VEGF-A depots and can be used for the development of therapeutic strategies to promote angiogenesis.

In this thesis, the following questions were investigated:

1. How does non-covalent binding of VEGF-A<sub>165</sub> to fibrin influence wound angiogenesis as compared to covalent binding? To answer this question, the binding of a plasmin-resistant VEGF-A<sub>165</sub> molecule (VEGFmut) was artificially increased by covalent coupling of the molecule to fibrin. To that end, VEGFmut was expressed as a fusion protein to a substrate sequence of the transglutaminase factor XIIIa, which under these conditions mediates the formation of covalent crosslinks between fibrin fibers and VEGFmut. VEGFmut covalently linked to a fibrin gel was delivered to full-thickness wounds of diabetic mice and its proangiogenic potential and tissue repair activities were examined.
2. Does the simultaneous co-stimulation of integrin  $\alpha v \beta 3$  and VEGFR-2 by a bioengineered protein result in increased angiogenesis? To investigate this question, bi-functional fusion proteins comprising VEGFmut fused to fibronectin type III domain 10 were generated (FLV) in order to co-ligate VEGFR-2 and integrin  $\alpha v \beta 3$ , and their biological activities were investigated *in vitro* and *in vivo*.

The recombinant proteins generated can be used as experimental tools to gain new insights into the biology of growth factor-matrix interactions and to elucidate mechanisms underlying the increased cellular responses upon integrin and growth factor receptor co-stimulation. Furthermore, the use of the recombinant fusion proteins in combination with fibrin matrices might also represent a potential pro-angiogenic approach for the treatment of impaired wound healing conditions due to defective angiogenesis.

### 3 Results

#### 3.1 Design of VEGF-A based fusion proteins for the co-stimulation of VEGFR-2 and integrin $\alpha\beta3$

##### 3.1.1 Domain organization of engineered VEGF-A proteins

To allow for simultaneous activation of VEGFR-2 and integrin  $\alpha\beta3$ , a novel fusion protein was designed based on the plasmin-resistant VEGFmut. As ligand for integrin  $\alpha\beta3$ , FNIII10 was chosen, which due to its RGD binding site is a promiscuous integrin-ligand and is also recognized by integrin  $\alpha\beta3$ . These functional domains were interconnected by a linker. Additional functional domains employed were the TG-site for factor XIIIa-mediated covalent coupling of the proteins to fibrin, and a plasmin-sensitive sequence for facilitated release of the protein from the fibrin gel upon cell invasion. Eight different constructs were cloned into expression vectors and purified as described in section 3.2. An overview on the domain organization is given in Figure 8.

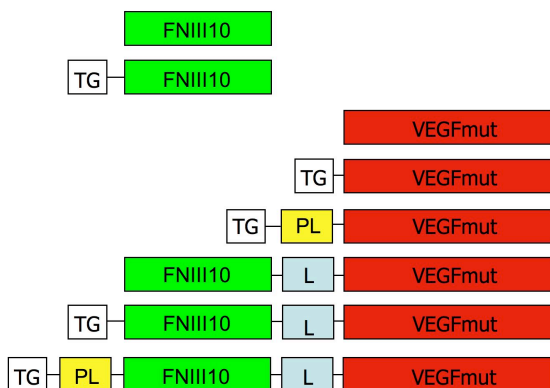


**Figure 8: Domain organization of recombinant fusion proteins expressed and purified.** Abbreviations: FNIII10: fibronectin type III domain 10, TG: transglutaminase substrate sequence of  $\alpha_2$ -plasmin inhibitor (NQEQVSPL), VEGFmut: plasmin-resistant variant of VEGF-A<sub>165</sub>, PL: plasmin-sensitive site (LIKMKP), L: linker.

##### 3.1.2 Design of the linker interconnecting FNIII10 and VEGFmut in the bi-functional constructs

For the functionality of the system it is essential to choose a linker long enough to allow coincident stimulation of VEGFR-2 and integrin  $\alpha\beta3$ . To estimate the required linker length, the diameters of both receptors were determined using Pdb-viewer, added and divided by two (Figure 9). 15% of the length was added as recommended by Crasto and Feng (2000).

The required linker length was calculated to be 112 angstroms. Assuming that one amino acid is 3.25 angstroms long (Craigo and Feng 2000; Huston et al. 1988), the required linker is 34 amino acids long.

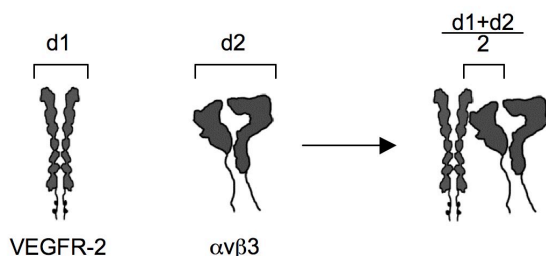


**Figure 9: The required length of the linker was roughly calculated by determining the diameters of the dimeric VEGFR-2 and  $\alpha v\beta 3$ .** The diameters  $d_1$  and  $d_2$  were added and divided by two and additionally 15% of the length was added. The required linker length is 112 angstroms.

Furthermore, the amino acid sequence of the linker can influence the function of the recombinant fusion protein. In general, the linker should be flexible and have an extended conformation, while at the same time it should not interfere with folding of the protein. It is possible to search databases for natural linkers according to their length. These interconnect domains of native proteins with each other but have no enzymatic activity on their own. Another approach is the use of a repetitive GGGGS-linker, which is frequently and successfully used in the production of recombinant single-chain antibodies. Due to its high glycine content, this linker is very flexible, and hydrophilic serine residues promote an extended conformation (Huston et al. 1991). Additionally, it is unlikely to be immunogenic, and no protease cleavage site was predicted within the linker using the PeptideCutter tool available on the ExPASy Proteomics server (Swiss Institute of Bioinformatics, Lausanne). For the interconnection of FNIII10 and VEGFmut, the linker (GGGGS)<sub>6.5</sub> was used.

## 3.2 Production and identification of the recombinant fusion proteins

### 3.2.1 Expression of GST-tagged proteins in *E. coli*

#### 3.2.1.1 Purification of FNIII10 and TG-FNIII10

FNIII10 and TG-FNIII10 were purified as GST-fusion proteins. Figure 10 shows typical chromatograms and protein gels monitoring the purification processes. In the first step of purification (Figure 10 A), GST-fusion proteins were retained in the GSH-column, and proteins not binding to the column were found in the first peak. Upon addition of elution buffer,

GST-FNIII10 or GST-TG-FNIII10 was eluted from the column, represented by the second peak. Following thrombin mediated cleavage, a second step of purification was performed removing the protease and the cleaved-off tag from the sample (Figure 10 B). FNIII10 or TG-FNIII10 was found in the fractions collected from the first peak. The second peak represented GST, and the third set of peaks corresponded to thrombin (Figure 10 B). Samples from the peaks denoted in Figure 10 A and B were investigated by Coomassie stained reducing SDS-PAGE gels (Figures 10 C and D). GST-FNIII10 and GST-TG-FNIII10 were detected at 35 kDa. The GST-tag was efficiently cleaved off by thrombin, and upon thrombin digest, GST was detected at 25 kDa and FNIII10 and TG-FNIII10 at 12 kDa. Both final products revealed high purity. From 1 L of bacterial culture, 3 mg of pure recombinant FNIII10 and 10 mg of TG-FNIII10 were purified, respectively. Yields of all protein productions performed are summarized in Table 1.

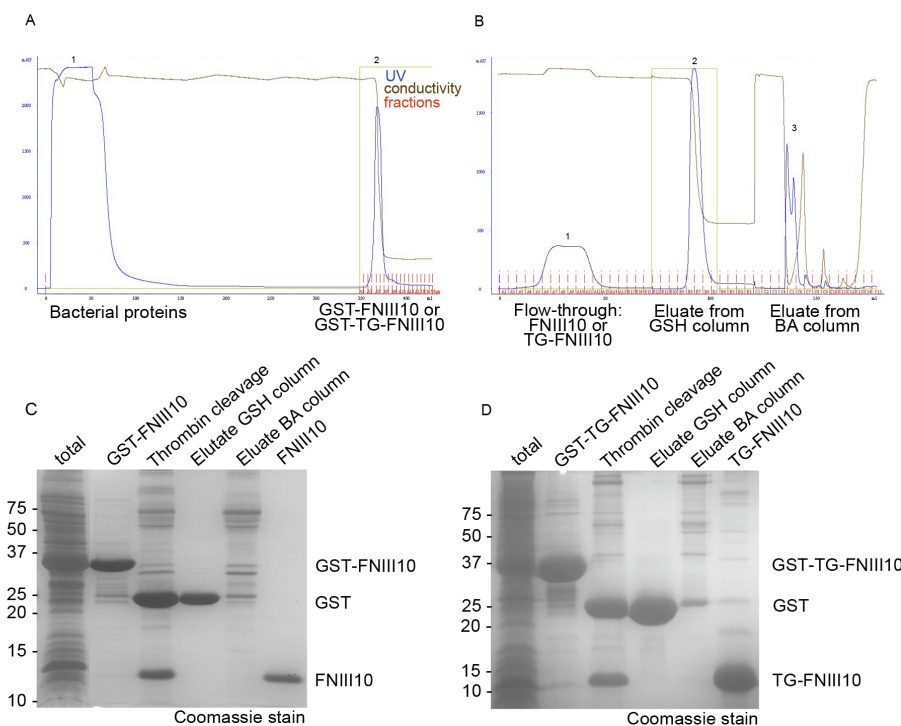


**Figure 10: Purification of FNIII10 and TG-FNIII10 as GST-fusion proteins resulted in high yields and final products of good purity. (A)** Chromatogram showing the first step of purification, capturing GST-FNIII10 and GST-TG-FNIII10 from the soluble fraction of bacterial lysates exploiting their GSH-binding affinity. **(B)** Chromatogram showing the second purification step, in which the sample was applied to a GSH-packed column and to a benzamidine (BA) column to remove GST and thrombin. **(C, D)** The purification process was monitored by SDS-PAGE and subsequent protein staining.

### 3.2.1.2 Purification of TG-PL-FLV and VEGFmut as GST-fusion proteins

For GST-TG-PL-FLV, the thrombin digestion was optimized first. The protein was completely digested within 8 hours by 1 U of thrombin per mg of protein. Figure 11 A shows a western blot using a primary antibody directed against VEGF-A monitoring the digestion of the protein over

time. Prior to thrombin digest, two bands were visible: GST-TG-PL-FLV at about 65 kDa, and a truncated form of GST-TG-PL-FLV, which had a molecular weight of about 50 kDa. Upon thrombin digest, TG-PL-FLV was detectable at 37 kDa, which corresponded well to its predicted molecular weight. Surprisingly, two additional bands became visible upon thrombin digestion. The band at about 25 kDa corresponded to a truncated form of TG-PL-FLV, and the other band was detected at 20 kDa. This latter band seemed to be another thrombin cleavage product resulting from processing of TG-PL-FLV because this 20 kDa band increased in intensity whereas the 37 kDa and the 25 kDa band decreased in intensity with prolonged thrombin incubation. Indeed, for GST-TG-PL-FLV, a second thrombin cleavage site was predicted by ExPASy Proteomic Server's PeptideCutter tool (Swiss Institute of Bioinformatics), which is situated in the RGD domain of FNIII10. Cleavage in this site would give rise to linker-VEGFmut, and the predicted molecular weight of this fragment is in agreement with a band at about 20 kDa on SDS-PAGE gels.

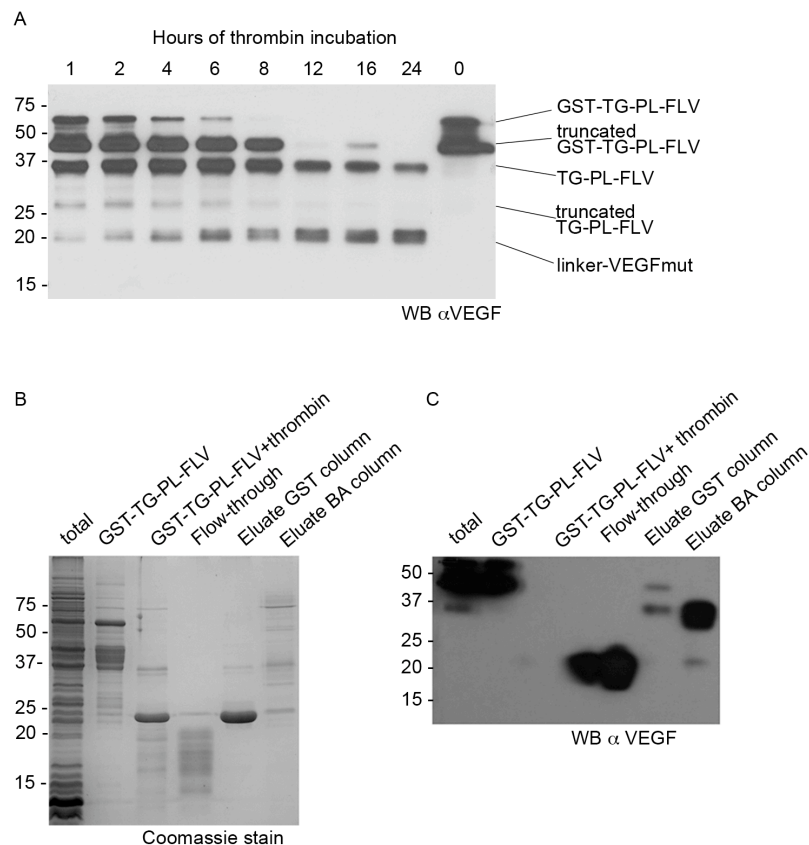


**Figure 11: GST-TG-PL-FLV was processed by thrombin to yield TG-PL-FLV, but purification was not possible due to the protein's affinity to benzamidine. (A)** Western blot using an antibody directed against VEGF monitoring the thrombin digest of GST-TG-PL-FLV over time using 1 U per mg of protein. **(B)** Coomassie blue stain and **(C)** VEGF-specific western blot on samples taken during the purification process.



TG-PL-FLV was attempted to be purified in two steps as described above and monitored by Coomassie blue staining and western blot (Figure 11 B and C). GST-TG-PL-FLV was detected on Coomassie blue stained SDS-PAGE gels at 65 kDa (Figure 11 C). The GST-tag was cleaved off by thrombin and detected at 25 kDa, while TG-PL-FLV was observed at 37 kDa. In the flow-through, where TG-PL-FLV was expected, exclusively linker-VEGFmut was found in a band at 20 kDa. TG-PL-FLV by contrast efficiently bound to benzamidine, which is used to remove thrombin from the sample. The identity of these bands was confirmed by western blot using an antibody directed against VEGF as primary antibody (Figure 11 C). Therefore, it was impossible to remove thrombin from the protein sample. Due to this benzamidine affinity, the purification of TG-PL-FLV following standard protocols was not possible.

The production of VEGFmut as a GST-fusion protein was not feasible following this protocol either. During large-scale thrombin digest, the recombinant VEGFmut regularly precipitated.

Thus, VEGF-based proteins were purified from bacterial inclusion bodies.

### **3.2.2 Purification of VEGFmut-containing proteins from bacterial inclusion bodies**

#### **3.2.2.1 Purification of VEGFmut by heparin affinity chromatography**

The purification of VEGFmut was done as described previously (Zisch et al. 2001). Briefly, bacterial protein expression of the recombinant protein was induced with IPTG for 3 hours, inclusion bodies were then harvested and solubilized, and VEGFmut was refolded in decreasing concentrations of urea and dimerized in a GSH redox system. The dimeric protein was then purified by heparin affinity chromatography and eluted with NaCl.

To increase both yield and purity of the sample, two modifications of the original protocol were established. First, protein production was induced overnight, to increase quantity as well as purity, since the relative amount of contaminating protein is expected to decrease in inclusion bodies as the relative amount of recombinant protein increases (Carrio et al. 1998). Second, the sample was pre-cleared prior to purification by adjusting the pH to 3.5, at which most impurities precipitated (Fiebich et al. 1993). Prolonged induction time resulted in higher recombinant protein content in inclusion bodies as exemplified for the expression of TG-VEGFmut (Figure 12 A), and acetic precipitation increased the purity of the sample for both, VEGFmut and TG-PL-FLV as shown on Coomassie stained SDS-PAGE gels (Figure 12 B).

Both modifications of the protocol were therefore included in subsequent protein productions.

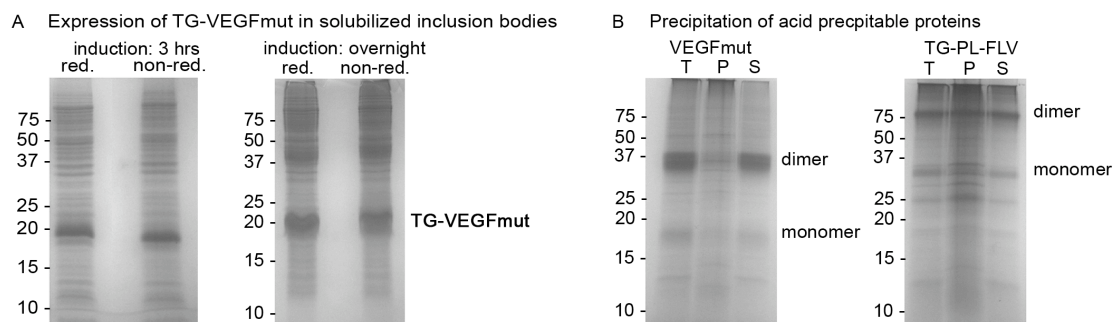


**Figure 12: Prolonged induction time and removal of acetic precipitable proteins from the sample resulted in higher content of target proteins in inclusion bodies and purer samples as monitored by SDS-PAGE and Coomassie blue staining. (A) Effect of induction time on recombinant protein content in inclusion bodies. (B) Pre-clearing by acetic precipitation. T – total, P – pellet, S – supernatant.**

The purification of VEGFmut following this modified protocol is shown in Figure 13. The solubilized inclusion bodies were enriched in monomeric VEGFmut detectable at 20 kDa (Figure 13 A). The refolded, dimerized and pre-cleared protein sample contained good amounts of dimeric VEGFmut, and the dimeric VEGFmut is detectable at 37 kDa under non-reducing conditions on Coomassie blue stained SDS-PAGE gels (Figure 13 B). The sample denoted as supernatant in Figure 13 B was applied to a heparin column and eluted in one step after extensive washing (Figure 13 C).

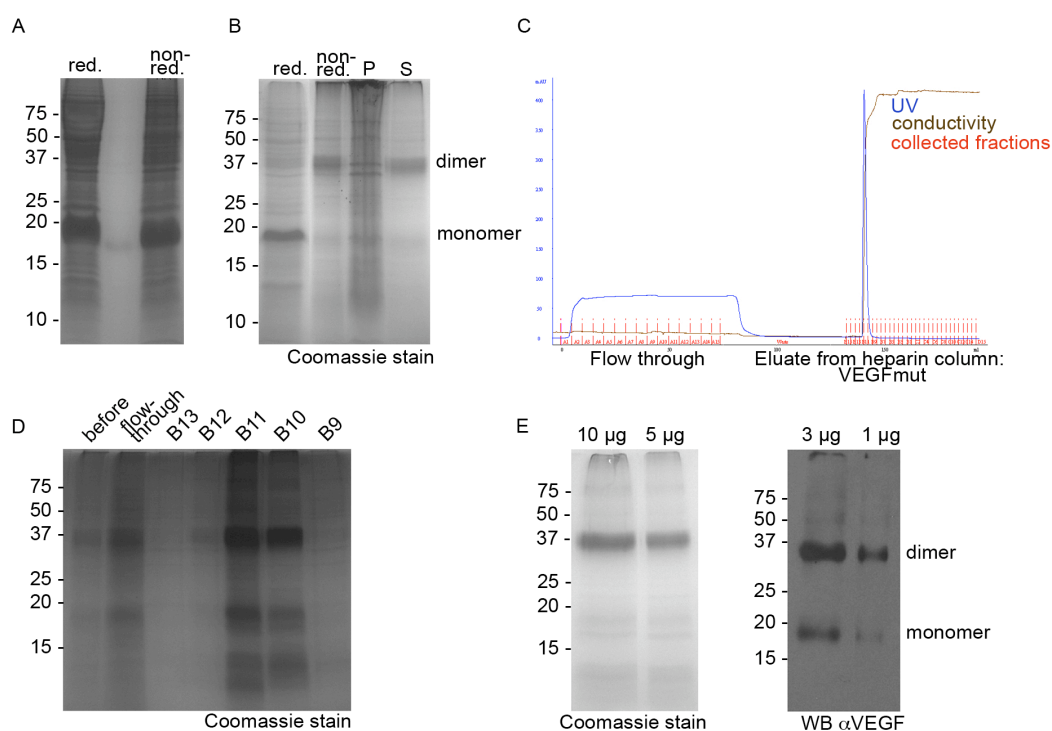


**Figure 13: VEGFmut was purified according to the modified protocol, and the final protein product was of good purity and mainly composed of the dimeric protein. (A, B, D) Coomassie stained SDS-PAGE gels and (C) chromatogram monitoring the purification process. (E) Final product as detected by Coomassie stain and western blot. P – pellet, S – supernatant.**

Investigation of obtained fractions by non-reducing SDS-PAGE and Coomassie blue staining identified several fractions highly enriched with dimeric VEGFmut (Figure 13 D). Similar fractions (B11 and B10) were pooled, and the final product exhibited good purity as shown by Coomassie blue staining and western blotting using an antibody raised against VEGF-A (Figure 13 E). In several purifications, 2.1 mg of VEGFmut were obtained from 4 L of bacterial culture (Table 1).

### **3.2.2.2 Purification of the engineered VEGF-proteins**

VEGF<sub>165</sub>wt, TG-VEGFmut, TG-PL-VEGFmut, FLV, TG-FLV and TG-PL-FLV were purified according to the optimized protocol as well. The final products are shown on non-reducing Coomassie blue stained SDS-PAGE gels in Figure 14, and the yields are summarized in Table 1. VEGF<sub>165</sub>wt was dimerized successfully and dimers were detected at 37 kDa. Several fractions enriched in the protein were pooled, and the final product is very pure (Figure 14 A). The yield from 3 L of bacterial culture was 6 mg.

TG-VEGFmut was well dimerized and showed good purity (Figure 14 B). Similar fractions were pooled and frozen separately from fraction C8, in which the TG-VEGFmut content was higher. Dimeric TG-VEGFmut was visible at 36 kDa, and the final yield from 2 L of bacterial culture was 4.8 mg.

Also of TG-PL-VEGFmut, several pure fractions were obtained. The dimeric protein was detected in a band at 37 kDa on a non-reducing SDS-PAGE gel (Figure 14 C). Fractions C3 and C5 were pooled and frozen separately from fraction C4. By this purification, 1.8 mg of TG-PL-VEGFmut were obtained from a 2 L culture.

Purification of FLV yielded one pure fraction, which was used for subsequent experiments (Figure 14 D). The final product consisted of dimeric FLV at 75 kDa, and monomers detected below 37 kDa. Also higher ordered structures were detectable. This purification yielded 1.1 mg of FLV from a 2 L culture.

TG-FLV was detected at around 74 kDa in its dimeric form and at 37 kDa as a monomer. Fractions containing the dimeric protein were pooled. The resulting product was rather pure as judged by Coomassie blue staining; however, precipitates and monomers remained detectable (Figure 14 E). 200 µg of TG-FLV were purified from a 2 L bacterial culture.

The longest construct, TG-PL-FLV, was visible at 75 kDa upon successful dimerization, while bands of the monomeric protein were detected at 35 kDa on non-reducing, Coomassie blue stained SDS-PAGE gels (Figure 14 F). Similar fractions (C2, C3, and C6) were pooled and

frozen separately from higher concentrated fractions C4 and C5. The final product mainly consisted of dimeric TG-PL-FLV, but monomers and precipitates were detected as well. The total yield was 1.3 mg from 6 L of bacterial culture.

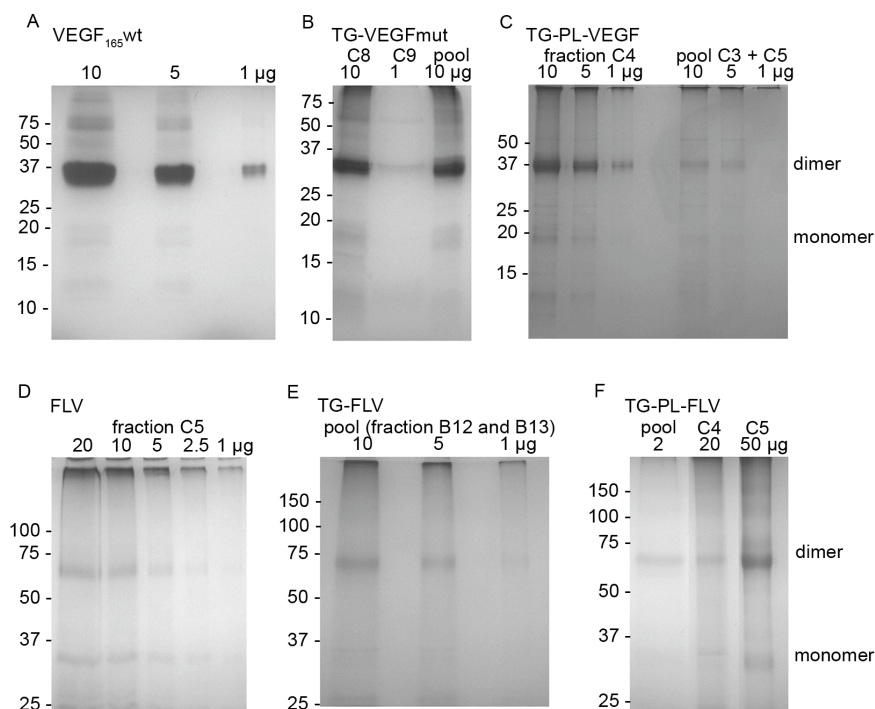


**Figure 14: Purification of VEGF-constructs from bacterial inclusion bodies yielded pure protein preparations mainly consisting of dimeric proteins, but also containing higher ordered precipitates and monomers.** Non-reducing, Coomassie blue stained SDS-PAGE gels showing the final product of (A) VEGF<sub>165</sub>wt, (B) TG-VEGF, (C) TG-PL-VEGF, (D) FLV (E) TG-FLV and (F) TG-PL-FLV.

### 3.2.3 Protein expression in eucaryotic cells

Especially expression of the bi-functional constructs in *E. coli* was a challenge because the dimerization was usually incomplete and a high amount of precipitates was present in the preparations. Thus, the constructs FNIII10, TG-FNIII10, VEGFmut, TG-VEGFmut, FLV and TG-FLV were subcloned into the eucaryotic expression vector pCEP-V97 and expressed according to a protocol established by professor Dr. Manuel Koch as His-tagged proteins in human embryonic kidney (HEK) 293-EBNA cells and purified from conditioned cell supernatants.

The proteins obtained were investigated by Coomassie blue staining under reducing and non-reducing conditions to assess overall purity and dimerization. Results are shown in Figure 15, and Table 2 summarizes final yields. FNIII10 and TG-FNIII10 run at around 15 kDa under both reducing and non-reducing conditions as these are monomeric proteins. Of FNIII10, 3.2 mg of protein were purified from 2.3 L of conditioned media, while 1.5 mg of TG-FNIII10 were

purified from 1.2 L of media. VEGFmut and TG-VEGFmut monomers were observed at 30 kDa and the dimers at 55 kDa. 715 µg of VEGFmut were obtained from 2 L of culture supernatant, and of TG-VEGFmut, 490 µg were purified from 2.2 L. FLV and TG-FLV dimers were found to run at 70 kDa, and monomers were observed at 45 kDa. The yield of FLV was 1100 µg from 1.6 L of conditioned media, and 860 µg of TG-FLV were purified from 3.6 L. Comparison between reducing and non-reducing conditions revealed good dimerization for all engineered VEGF proteins. Remaining monomers seemed to be found exclusively in the TG-forms. Generally, proteins were of very good purity, and no precipitates were observed.

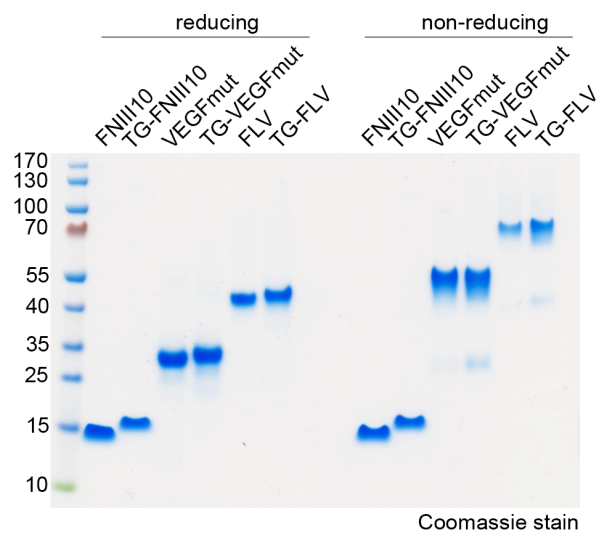


**Figure 15: Recombinant protein preparations purified from HEK293-EBNA cell supernatants were pure and well dimerized.** On the Coomassie blue stained gel, the final products are shown. Loading: 2 µg/lane.

### 3.2.4 Confirmation of the identity of recombinant proteins produced

The identity of the purified proteins was confirmed by liquid chromatography followed by liquid chromatography tandem mass spectrometry (LC-MS/MS) and subsequent peptide mass fingerprinting (PMF). Analysis was performed at the Proteomic Core Facility at Ecole Polytechnique Fédérale de Lausanne, Switzerland by Diego Chiappe or at Zentrale Bioanalytik at Zentrum für Molekulare Medizin, Köln, Germany by Dr. Stefan Müller and Andrea Grün.

### 3.2.5 Determination of protein concentrations

As a first approach to determine protein concentrations of the obtained fractions expressed in *E. coli*, a BCA assay was performed. Working concentrations were determined by human VEGF-A specific ELISA, and concentrations were calculated in comparison to a VEGF-A standard curve. This has the major advantage that the concentration is already normalized for its VEGF-content and thus corresponds to the effective concentration. Often, the protein concentration determined using the ELISA was markedly lower than the concentration determined by BCA-assay (see Table 1). This discrepancy was particularly dramatic when determining protein concentrations of FLV, TG-FLV and TG-PL-FLV, and was not abolished when the concentration determined by ELISA was corrected taking into account the molecular weight of the proteins (for example, the molecular weight of TG-PL-FLV is approximately 1.7 times higher than the molecular weight of VEGFmut, thus the concentrations obtained by ELISA might be too low). A reasonable explanation for this was the presence of aggregates particularly enriched in protein preparations containing the bi-functional constructs produced in *E. coli*. For this reason, protein concentrations determined by ELISA measurements were considered more precise than these determined by BCA assay, and these concentrations were used in subsequent experiments. The calculations of the molar concentrations were based on the concentrations obtained by ELISA and corrected for the molecular weight. Molecular weights were predicted using ExPASy's ProtParam tool. For FNIII10 and TG-FNIII10, protein concentrations were determined by UV measurement and corrected by the extinction coefficient (labeled with an asterisk).

For engineered VEGF proteins prepared from cell supernatants, there were also enormous differences in concentrations determined by BCA assay as compared to concentrations determined by human VEGF-A ELISA (Table 2). However, concentrations determined by ELISA appeared too low compared to intensities of protein bands observed on Coomassie blue stained gels, and again this effect was particularly prominent when comparing values obtained for bi-functional constructs. As in these purifications, neither precipitates nor contaminations were observed that could account for these discrepancies, the concentration was determined by BCA assay, and values obtained were corrected for the molar VEGF-content of the protein to determine the effective concentration. These corrected values were used for subsequent experiments characterizing the bioactivity of these proteins. The calculation of the molarity was

## Results

based on uncorrected concentrations determined by BCA-assay, and the molecular weight was predicted using the ProtParam tool (ExPASy). FNIII10 and TG-FNIII10 protein concentrations were determined by UV-spectrometry and corrected as described above.

Proteins produced in <i>E. coli</i>								
Protein	Molecular weight [kDa]	Culture volume	Fraction	BCA [ $\mu\text{g/mL}$ ]	ELISA [ $\mu\text{g/mL}$ ]	ELISA corrected [ $\mu\text{g/mL}$ ]	Molarity [ $\mu\text{M}$ ]	Yield [ $\mu\text{g}$ ]
FNIII10	11.2	1 L		2250*			200.90	3000
TG-FNIII10	12.48	1 L		3379*			270.65	10000
VEGFwt (dimer)	38.59	1 L		25.6	54.54	54.54	1.41	1000
VEGFwt (dimer)	38.59	2 L	C4-C6	641.4	844.7	844.7	21.89	5000
VEGFmut (dimer)	38.59	2 L	B15	282.1	379.85	379.85	9.84	760
	38.59		A15+B14	25.9	33.11	33.11	0.86	130
VEGFmut (dimer)	38.59	2 L	B11+B10	356.6	321.52	321.52	8.33	1280
TG-VEGFmut (dimer)	40.81	2 L	C8	524.1	241.26	255.01	6.25	510
	40.81		C5-7+C10	1026.2	515.22	544.59	13.34	4300
TG-PL-VEGFmut (dimer)	42.57	2 L	C4	2899.9	671.55	740.72	17.40	1500
			C3+C5	1410.4	79.8	88.02	2.07	350
FLV (dimer)	63.44	2 L	C5	910	340.8	560.28	8.83	1120
TG-FLV (dimer)	66.21	2 L	B12+B13	696.1	30.25	51.88	0.78	200
TG-PL-FLV (dimer)	67.96	2 L	C5	3178.6	258.1	454.57	6.69	910
	67.96		C4	1105	13.71	23.34	0.34	45
TG-PL-FLV (dimer)	67.96	2 L	C4+C5	390	32.05	56.46	0.83	225
TG-PL-FLV (dimer)	67.96	2 L	C4	1105	33.87	59.66	0.88	120

**Table 1: Summary of protein concentrations and yields of protein expression in *E. coli*.** Protein concentrations were determined by BCA-assay or by VEGF-specific ELISA. The values obtained by ELISA were considered more precise and used in subsequent experiments (see text for details). Asterisks indicate the determination of protein concentration by UV-spectrometry.

Proteins produced in HEK293-EBNA cells							
Protein	Molecular weight [kDa]	Supernatant volume	BCA [ $\mu\text{g/mL}$ ]	BCA corrected [ $\mu\text{g/mL}$ ]	ELISA [ $\mu\text{g/mL}$ ]	Molarity [ $\mu\text{M}$ ]	Yield [ $\mu\text{g}$ ]
FNIII10	11.96	2.3 L	679*			56.77	3200
TG-FNIII10	13.35	1.2 L	600*			44.96	1500
VEGFmut (dimer)	42.71	2.0 L	188.17	188.17	85.45	4.41	710
TG-VEGFmut (dimer)	44.93	2.2 L	188.81	179.48	89.47	4.20	490
FLV (dimer)	67.56	1.6 L	302.06	190.9	18.75	4.47	1100
TG-FLV (dimer)	70.33	3.6 L	333.55	202.46	19.07	4.74	860

**Table 2: Summary of yield and concentration of proteins purified from HEK293-EBNA cell supernatants.** Concentrations obtained by the BCA-assay were in agreement with the intensity of bands observed on Coomassie-blue stained gels and calculations of the molarity are based on these concentrations. Asterisks indicate the determination of protein concentrations by UV-spectrometry.

### 3.2.6 Endotoxin test

The endotoxin content of recombinant protein samples was determined by Dr. Gabriela Bald in the laboratories of Bayer Schering Pharma (Wuppertal, Germany) by the LAL-test. The endotoxin contents of individual preparations are given in Table 3.

It was evident, that proteins obtained from HEK293-EBNA cells showed a very low endotoxin content as compared to proteins produced in *E. coli*. In general, the endotoxin content seemed to increase with increasing molecular weight of the constructs.

Endotoxin content of protein preparations			
Construct	Expression system	Purification	EU/ $\mu$ g
FNIII10	HEK	His-tag	0.0035
FNIII10	<i>E. coli</i> , cytosol	GST-tag	0.026
TG-FNIII10	<i>E. coli</i> , cytosol	GST-tag	11.6
VEGFwt	<i>E. coli</i> , inclusion bodies	Heparin affinity C4-6	2.55
VEGFmut	HEK	His-tag	0.01
VEGFmut	<i>E. coli</i> , inclusion bodies	Heparin affinity B11+10 a)	0.56
VEGFmut	<i>E. coli</i> , inclusion bodies	Heparin affinity B11+10 b)	21.5
TG-VEGFmut	<i>E. coli</i> , inclusion bodies	Heparin affinity C8	2.35
TG-VEGFmut	<i>E. coli</i> , inclusion bodies	Heparin affinity C5-7+10	15.15
TG-PL-VEGFmut	<i>E. coli</i> , inclusion bodies	Heparin affinity C4	13.4
FLV	HEK	His-tag	0.15
FLV	<i>E. coli</i> , inclusion bodies	Heparin affinity C5	69.5
TG-FLV	<i>E. coli</i> , inclusion bodies	Heparin	31000

Table 3: Summary of the endotoxin content of recombinant protein preparations as determined by the LAL-test.

The endotoxin limit for the planned animal experiments was calculated as suggested by Malyala and Singh (2004) as follows:

$$\text{Endotoxin limit} = \frac{K}{M} \quad (\text{parenteral administration})$$

K: Threshold human pyrogenic dose per kg of body weight = 5 EU/kg  
M: Dose per kg body weight and hour in  $\mu$ g/h Dosis

Weight diabetic mouse 50 g = 0.05 kg      Dose: Mouse obtains 4.8  $\mu$ g of protein = 0.0048 mg

$$M_{\text{mouse}} = \frac{\text{dose}}{\text{Body weight}} = \frac{0.0048 \text{ mg}}{0.05 \text{ kg}} = 0.096 \text{ mg/kg}$$

$$\text{Endotoxin limit}_{\text{mouse}} = \frac{K}{M} = \frac{5 \text{ EU/kg}}{0.096 \text{ mg/kg}} = 52 \text{ EU/mg protein}$$

0.052 EU/ $\mu$ g protein

As all recombinant proteins produced in *E. coli* show an endotoxin content markedly above this value, exclusively proteins produced in HEK293-EBNA cells were used for animal experimentations.



### 3.3 Functional characterization of recombinant proteins

#### 3.3.1 Covalent incorporation of engineered VEGF-proteins into fibrin matrices

##### 3.3.1.1 Retention of proteins produced in *E. coli* equipped with a TG-sequence in fibrin gels

Recombinant VEGF proteins were to be delivered to wounds in fibrin gels. To test the functionality of the TG-site, fibrin gels were formulated from 10 mg/mL fibrinogen containing either VEGFmut, TG-VEGFmut, TG-PL-VEGFmut, FLV or TG-PL-FLV and were washed for two days with shaking at 37°C. The gels were then degraded by plasmin incubation, and the lysate was investigated by western blot analysis using an antibody raised against VEGF-A. As shown in Figure 16, the soluble variants VEGFmut and FLV could not be detected by this approach. In contrast, the constructs containing the TG-sequence were readily identified by western blot. For TG-VEGFmut, TG-PL-VEGFmut and TG-PL-FLV, several prominent bands were detected, which is indicative for the presence of fibrinopeptides still coupled to the growth factor.

In regard to the constructs containing a plasmin cleavage site, this result is surprising, as the construct should be released without fibrinopeptides, therefore, one single band would be expected. Possibly, the digestion was incomplete.

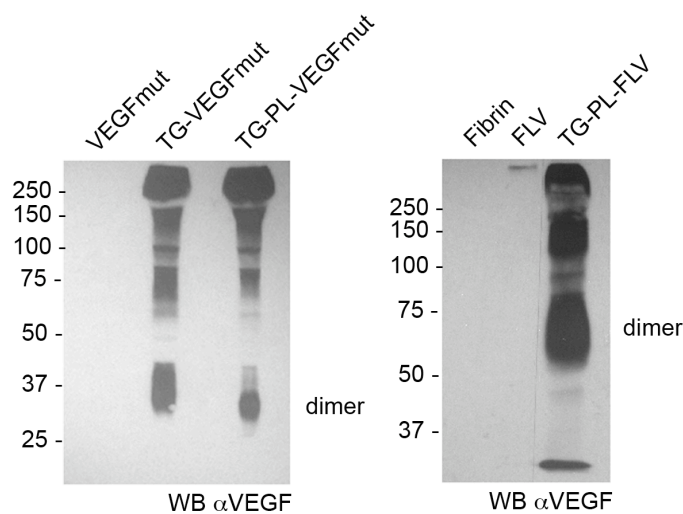


**Figure 16: Bioengineered VEGF-proteins comprising a TG site are retained in fibrin gels upon washing.** VEGF-specific western blot on lysates of fibrin gels formulated with various VEGF proteins after washing, non-reducing conditions.

Furthermore, VEGF concentrations in the wash buffer were determined at different time points of washing by ELISA in two independent experiments using 2 U/mL or 10 U/mL of factor XIII (Figure 17). Factor XIIIa used in these experiments was provided by Baxter.

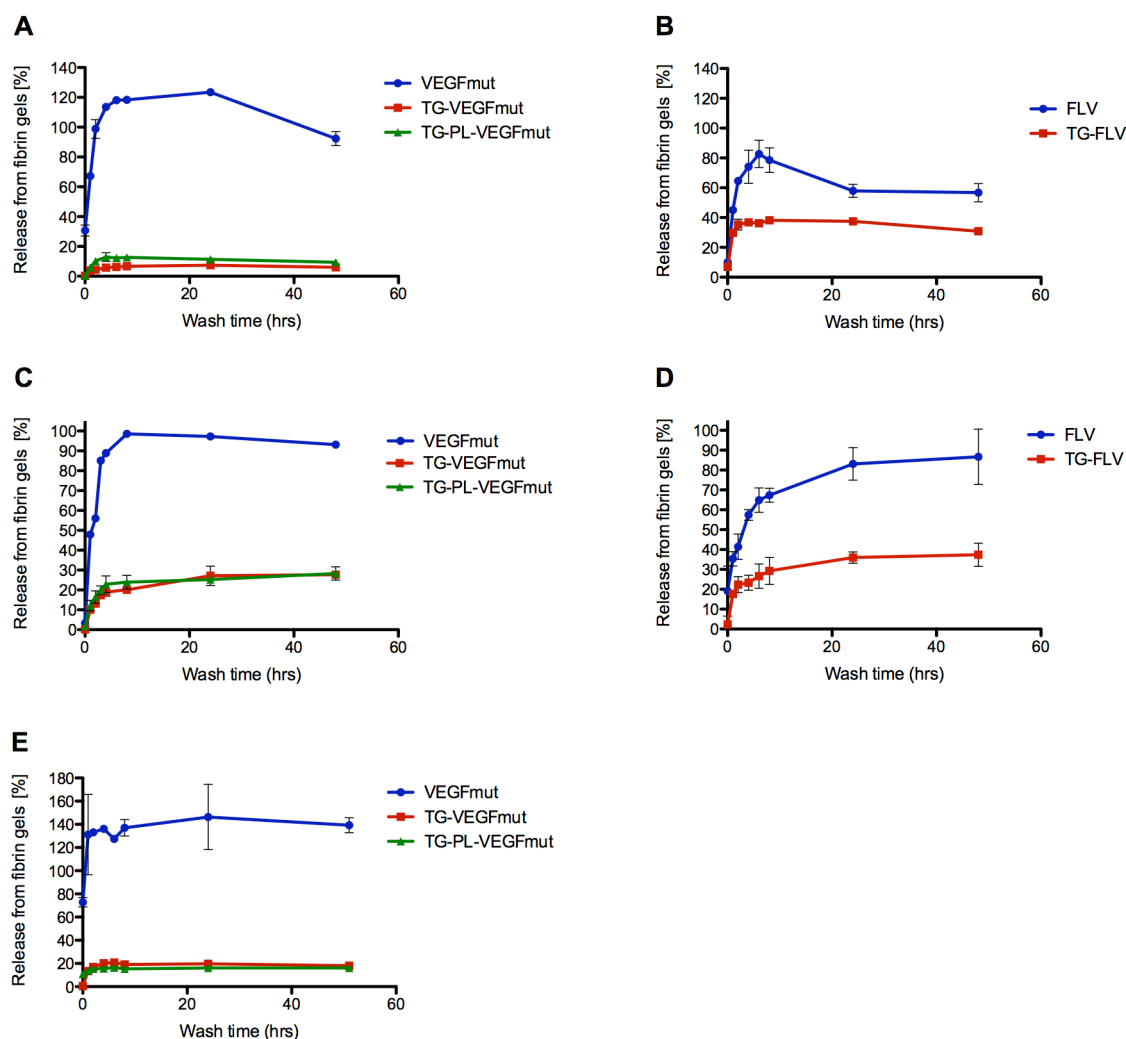


**Figure 17: Prolonged retention of VEGF-variants comprising a TG-site produced in *E. coli* in fibrin gels.** Graphs monitoring the release of proteins from fibrin gels formulated with 2 U/mL (A, B) or 10 µg/mL (C, D) of factor XIIIa provided by Baxter, as compared to the release from fibrin gels crosslinked with 10 U/mL of factor XIII obtained from CSL Behring (E).

Under both conditions, the soluble form VEGFmut was entirely released during the first 8 hours of washing, whereas both TG-VEGFmut and TG-PL-VEGFmut were retained at a minimum of 70 % in the matrix (Figure 17 A and C). These results are in good agreement with data published previously (Ehrbar et al. 2004; Ehrbar et al. 2005). The results obtained for the bi-functional constructs tested were similar. Also in these experiments, the non-coupled form was largely released in a burst release within the first 8 hours of washing. TG-PL-FLV was retained by approximately 60 % during washing (Figure 17 B and D). Furthermore, the release of FLV

appeared to be delayed from fibrin gels formulated with 10 U/mL factor XIIIa. However, additional experiments would be necessary to confirm this tendency.

The same experiment was repeated using a different, commercially available factor XIIIa, obtained from CSL Behring as Fibrogamin. For fibrin gels formulated, 10 U/mL of factor XIIIa were used. Release kinetics of the VEGF-isoforms investigated (Figure 17 E) were very similar to those observed using factor XIII obtained from Baxter (Figure 17 C and D). The soluble VEGFmut is released during the first hours of washing, whereas only around 20 % of both TG-VEGFmut and TG-PL-VEGFmut produced in *E. coli* were found in the washing buffer at the time points indicated.

### 3.3.1.2 Release of proteins produced in HEK293-EBNA cells from fibrin gels

The release of engineered VEGF proteins produced in the eucaryotic expression system from fibrin gels was investigated in similar experiments as described above. Release kinetics from fibrin matrices formulated with either 2 U/mL (Figure 18 A and B) or 10 U/mL (Figure 18 C and D) factor XIIIa from CSL Behring closely resembled the release observed from fibrin gels formulated with proteins produced in *E. coli*.

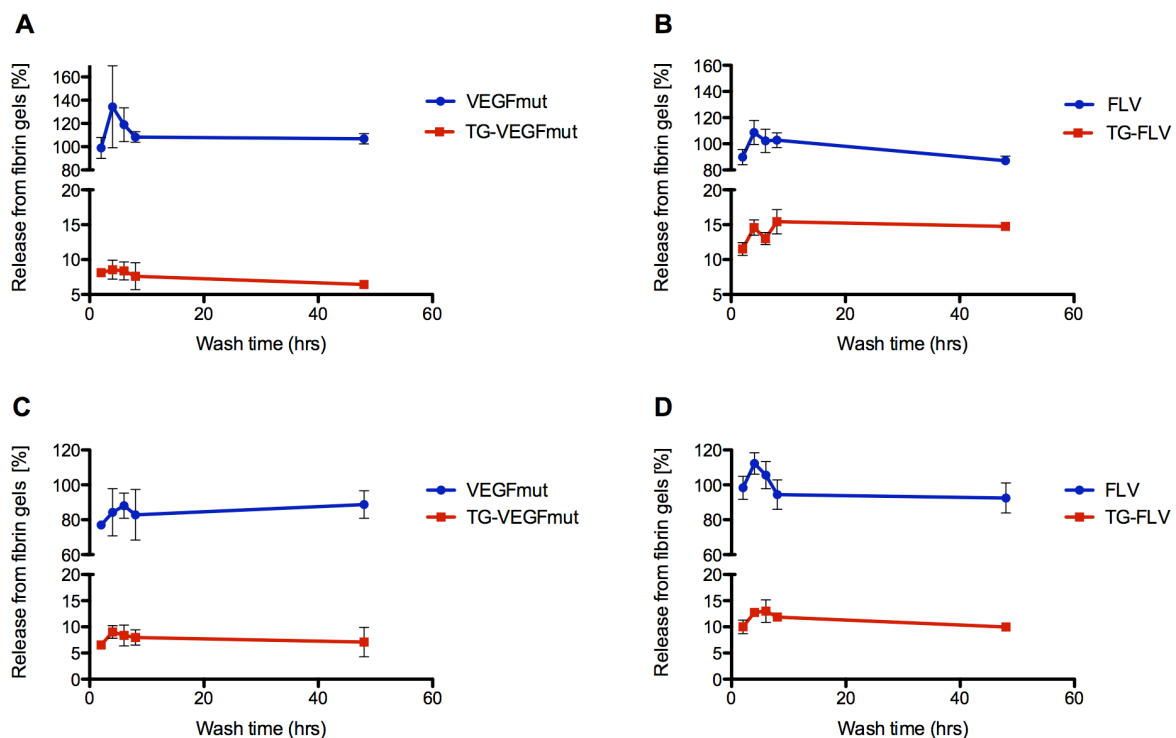


**Figure 18:** The release kinetics of proteins produced in HEK293-EBNA cells closely resemble those of proteins produced in *E. coli*. Graphs showing the release of VEGF proteins from fibrin gels formulated with 2 U/mL (A, B) or 10 U/mL (C, D) factor XIIIa (CSL Behring).

The soluble proteins VEGFmut and FLV were quickly released during the first hours of washing. By contrast, TG-VEGFmut and TG-FLV, which become covalently bound to fibrin by factor XIIIa, were retained in the gel by up to 85 %. Interestingly, the retention of TG-FLV was similar to the retention of TG-VEGFmut observed in these experiments, which was unlike in previous experiments employing proteins obtained from inclusion bodies. A likely explanation for this is the absence of aggregates in the final product obtained from HEK293-EBNA cells, as aggregates may fail to become incorporated into fibrin gels due to misfolding possibly resulting in an inaccessible TG-site.

### 3.3.2 HUVEC attachment to TG-FNIII10 is partially dependent on integrin $\alpha v \beta 3$

To assess the bioactivity of TG-FNIII10 produced in *E. coli*, cell attachment assays using human umbilical vein endothelial cells (HUVECs) were performed (Figure 19 A). When HUVECs were allowed to attach to various concentrations of TG-FNIII10, attachment proved to be dependent on the concentration of the ligand plated. The difference in attachment observed between 0.01  $\mu\text{M}$  and 0.1  $\mu\text{M}$  of TG-FNIII10 plated was significant ( $p < 0.05$ ). Pre-treatment of cells with function-blocking integrin specific antibodies prior to seeding revealed that adhesion of cells to fibronectin was not influenced by anti- $\alpha v \beta 3$ , but partially inhibited by anti- $\alpha 5$  ( $p < 0.05$ , Figure 19 B). By contrast, anti- $\alpha v \beta 3$  strongly inhibited attachment to TG-FNIII10 by 30 % ( $p < 0.05$ ), whereas pre-incubation with anti- $\alpha 5$  had a less pronounced effect on attachment to this fibronectin domain (Figure 19 C).

By this experiment, it was shown that indeed  $\alpha v \beta 3$  is targeted by FNIII10, as intended by the expression of the bi-functional constructs containing FNIII10 and VEGFmut.

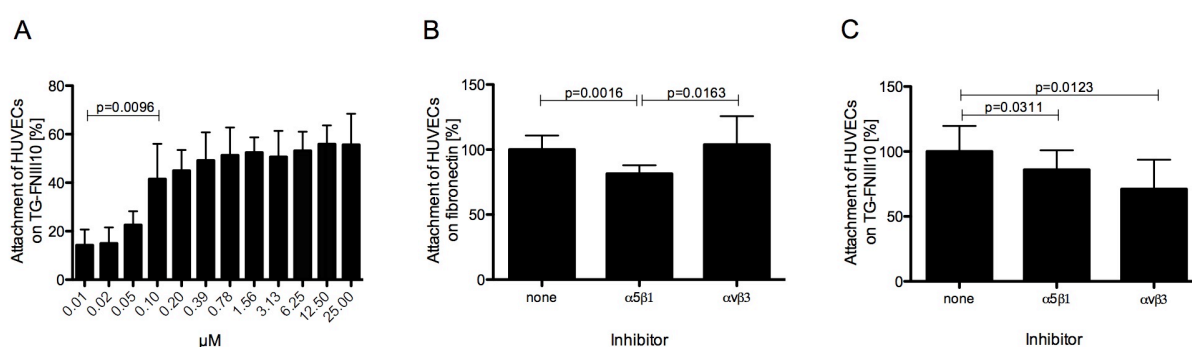


**Figure 19: HUVEC attach to TG-FNIII10 in a concentration dependent manner, and attachment is partially dependent on integrin  $\alpha v \beta 3$ .** Graphs summarize the investigation of cell attachment to TG-FNIII10. (A) Cells were seeded on increasing concentrations of TG-FNIII10. (B, C) Cells were incubated with integrin adhesion-blocking anti-integrin antibodies and seeded on fibronectin or TG-FNIII10. Significance was accepted for  $p < 0.05$  and p-values were determined by paired t-tests.

### **3.3.3 FLV and FNIII10 promote cell attachment and spreading of HUVECs**

In order to investigate cell attachment and spreading of HUVECs on the recombinant proteins produced in HEK293-EBNA cells, microscopy slides were coated with FNIII10, VEGFmut, FLV and poly-L-lysine as a negative control. The coating density employed took into account that FLV as a dimeric protein comprises two FNIII10-sites per molecule, and for this reason, 0.4  $\mu\text{M}$  of FNIII10 and 0.2  $\mu\text{M}$  of FLV and VEGFmut were used for the coating, thus providing equal amounts of functional domains. Cells were allowed to attach for two hours, fixed and stained for actin filaments and the focal adhesion protein vinculin (Figure 20 A).

On poly-L-lysine, cells remained rounded and no spreading was observed. Cells on VEGFmut behaved similar. On FNIII10 by contrast, various degrees of spreading were observed. While only few cells were rounded, most cells were well attached to the substrate and spread. Some cells also showed stress fibers and focal adhesion assembly indicated by vinculin staining. On FLV, cell spreading observed was maximal, and cells were enriched in stress fibers ending in vinculin-positive focal adhesion sites. Cells in five random fields of view were counted per condition. Low cell numbers on poly-L-lysine and VEGFmut indicated weak attachment to these substrates (Figure 20 B). By contrast, cell numbers on FLV and FNIII10 were approximately 6fold higher than on poly-L-lysine.

These results indicate that cell attachment and cell spreading are promoted by FNIII10 and FLV, and that spreading on FLV is more efficient than on FNIII10.

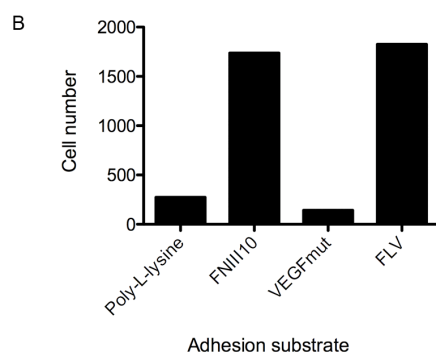
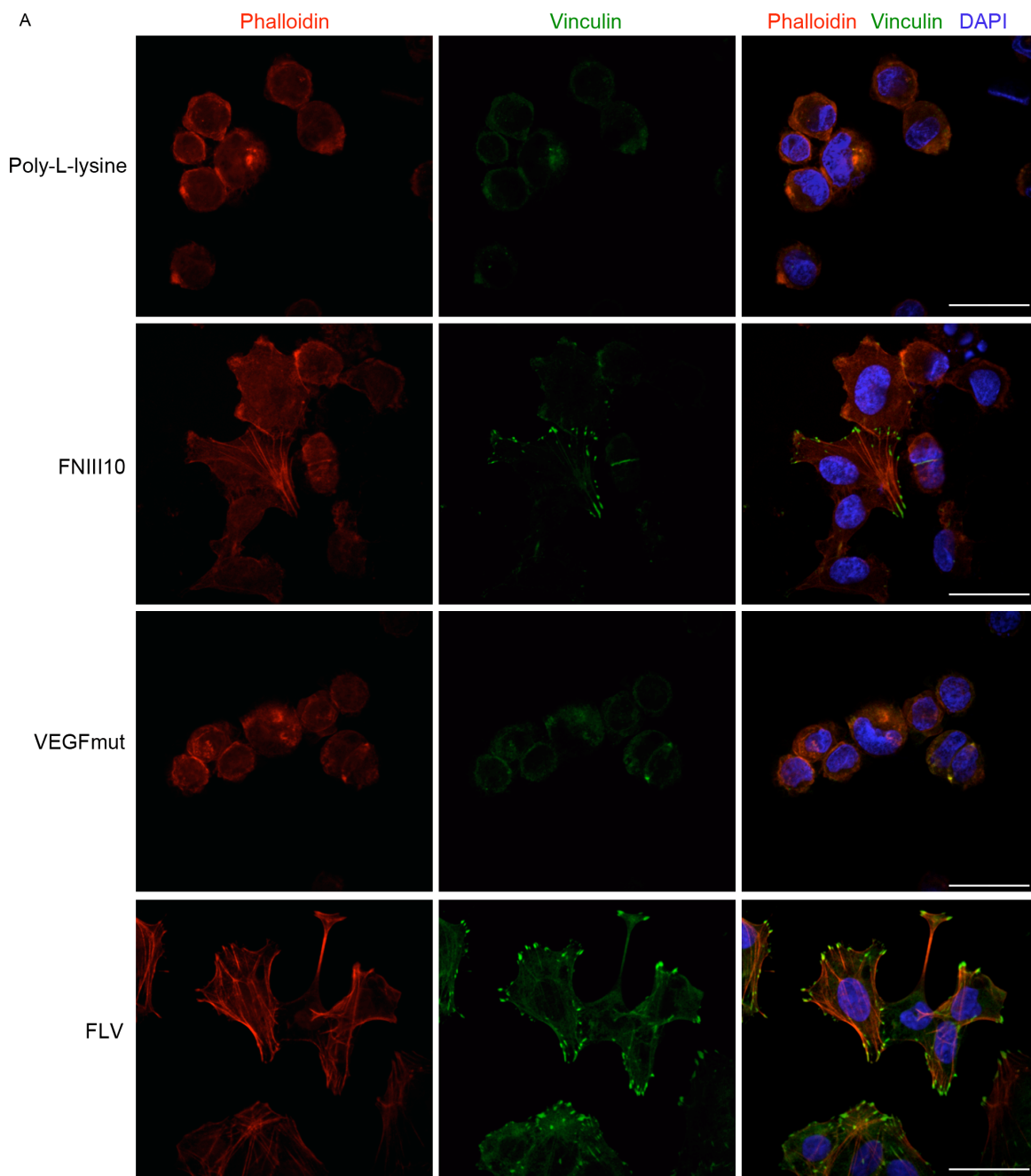


**Figure 20: FLV promotes cell attachment and spreading.** (A) Confocal images of HUVECs seeded on poly-L-lysine, FNIII10, VEGFmut or FLV, stained for F-actin (red), vinculin (green) and nuclei (blue). Scale bars: 30  $\mu$ m. (B) Graph summarizing the quantification of adherent cells in five random fields of view.

### 3.3.4 Recombinant VEGF-proteins produced in *E. coli* promote VEGFR-2 phosphorylation

To answer the question if the designed proteins were biologically active *in vitro*, they were tested for their ability to promote VEGFR-2 phosphorylation. Serum starved HUVECs in 3.5 cm dishes were stimulated for 5 minutes with 1.3 nM of commercial VEGF<sub>165</sub> (Invitrogen), VEGF<sub>165</sub>wt, VEGFmut, TG-VEGFmut, TG-PL-VEGFmut, FLV and TG-PL-FLV produced in *E. coli* (corresponding to 50 ng/mL effective VEGFmut concentration). By western blotting, VEGFR-2 phosphorylation was detected by a primary antibody raised against phosphotyrosine 1175 in VEGFR-2 (Figure 21), which is one of the major autophosphorylation sites of the receptor (Takahashi et al. 2001). By contrast, no phosphorylation of this residue was observed in non-stimulated cells or upon stimulation with 4.46 nM FNIII10 (corresponding to 50 ng/mL). Detection of VEGFR-2 on the same blot indicated equal loading. These data clearly showed that the engineered VEGF proteins produced are active.

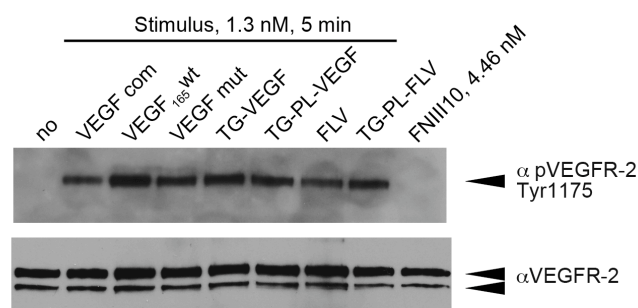


**Figure 21: Recombinant VEGF-proteins purified from inclusion bodies promote VEGFR-2 phosphorylation.** Western blot anti phospho-VEGFR-2 and anti VEGFR-2 on lysates obtained from HUVECs stimulated with 1.3 nM (50 ng/mL) of VEGF proteins or 4.46 nM (50 ng/mL) FNIII10.

### 3.3.5 VEGFR-2 phosphorylation is induced by VEGF-proteins produced in eucaryotic cells

#### 3.3.5.1 The activity of bi-functional proteins is reduced as compared to VEGFmut-proteins as determined by western blot

The activity of recombinant proteins produced in HEK293-EBNA cells was tested by assessing their ability to promote VEGFR-2 phosphorylation on tyrosine residue 1175 following stimulation with 1.17 nM (corresponding to 50 ng/mL effective VEGFmut concentration) of recombinant VEGF proteins. Additionally, phosphorylation of the VEGFR-2 downstream signaling molecules Erk 1/2 was investigated. Representative western blots are shown in

Figure 22. At all time points investigated, VEGFmut and TG-VEGFmut constructs induced a stronger VEGFR-2 phosphorylation than FLV or TG-FLV, while autophosphorylation of VEGFR-2 on tyrosine 1175 was strongest upon stimulation with commercial VEGF-A<sub>165</sub> (denoted as VEGF com). For Erk 1/2, analysis proved difficult, as the kinase seemingly became activated once the media were changed for stimulation. However, as a tendency, Erk 1/2 became activated upon stimulation with commercial VEGF<sub>165</sub>, VEGFmut and TG-VEGFmut at all time points investigated. Upon stimulation with FLV and TG-FLV, phosphorylation of Erk 1/2 remained at background levels, and only after 30 minutes of stimulation a slight increase in phosphorylation was detectable. The same blots were reprobbed for total VEGFR-2 and  $\beta$ -actin as loading controls, and indicated similar loading.

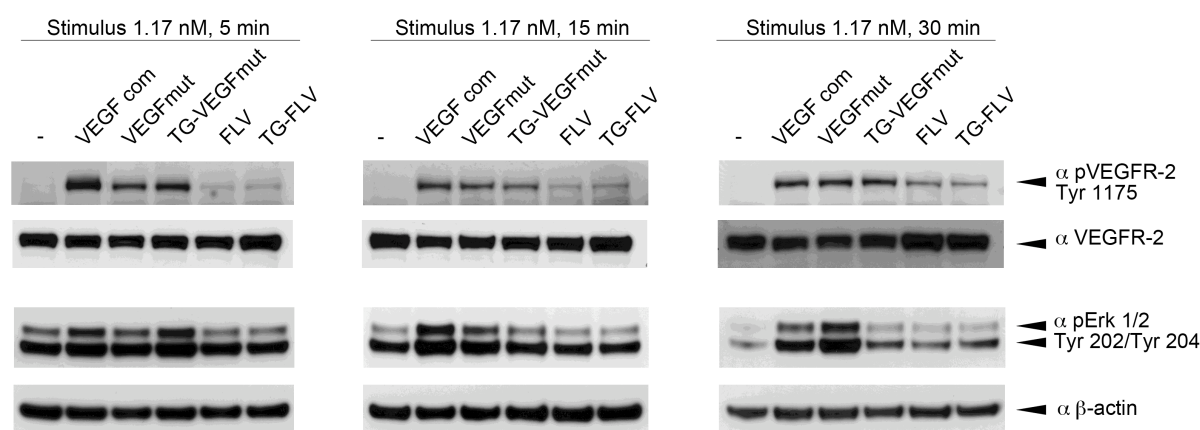


**Figure 22: VEGF-constructs purified from HEK293-EBNA cell supernatants promote VEGFR-2 phosphorylation, but no synergistic signaling was observed upon stimulation with bi-functional constructs.** Western blot on HUVEC lysates stimulated with engineered VEGF proteins for the time indicated, detecting phosphorylation of VEGFR-2 and Erk 1/2 and showing loading controls.

In summary, no increase in phosphorylation was detected neither on the receptor level nor on the level of downstream signaling molecules Erk 1/2 upon stimulation with FLV as compared to stimulation with VEGF.

### 3.3.5.2 The overall VEGFR-2 phosphorylation detected by ELISA reproduces phosphorylation on tyrosine 1175

VEGFR-2 becomes phosphorylated at multiple tyrosine residues upon VEGF-stimulation. To clarify whether phosphorylation of tyrosine 1175 reflects the phosphorylation state of overall VEGFR-2, phosphorylation was investigated by an ELISA detecting all phosphorylated tyrosines of VEGFR-2 captured by a VEGFR-2 specific primary antibody (Figure 23).



## Results

---

A dose response was determined in a first experiment. HUVECs were stimulated for 15 minutes with 0.02, 0.23, 1.17 and 2.34 nM (corresponding to 1, 10, 50 and 100 ng/mL effective VEGF-A concentration, respectively) of commercial VEGF, VEGFmut, TG-VEGF, FLV and TG-FLV. Under these conditions, higher concentrations of commercial VEGF-A<sub>165</sub>, VEGFmut, TG-VEGFmut, FLV and TG-FLV resulted in higher VEGFR-2 phosphorylation (Figure 23 A). Phosphorylation was maximal for stimulation with either 50 or 100 ng/mL. Also in this ELISA, stimulation with the bi-functional constructs led to a markedly decreased VEGFR-2 phosphorylation as compared to phosphorylation induced by VEGF-isoforms investigated. Stimulation with commercial VEGF-A, VEGFmut or TG-VEGF led to an increase of up to 140 % in VEGFR-2 phosphorylation, while FLV and TG-FLV increased phosphorylation by maximally around 20% as compared to non-stimulated controls.

Furthermore, the time-course of VEGFR-2 phosphorylation was investigated upon stimulation with 1.17 nM (corresponding to 50 ng/mL effective VEGF-A concentration) VEGF proteins in an independent experiment (Figure 23 B). Commercial VEGF-A<sub>165</sub> induced a dramatic increase of VEGFR-2 phosphorylation within 5 minutes of stimulation. Phosphorylation decreased over time, but still remained high 30 minutes after stimulation (50fold increase over non-stimulated control). VEGFmut and TG-VEGFmut triggered a less dramatic increase in VEGFR-2 phosphorylation, but the signal was elevated during the time investigated and showed a 50 % increase over non-stimulated controls. Again, upon stimulation with FLV and TG-FLV, phosphorylation was low, and a maximal increase of 11 % over non-stimulated controls was observed.

However, when comparing the signal intensities detected for phosphorylated VEGFR-2 obtained in this experiment to the data generated when investigating the VEGFR-2 dose response, it was evident that signal intensities differed markedly between both experiments. In general, the VEGFR-2 phosphorylation upon stimulation with VEGFmut and TG-VEGFmut was much lower in the second experiment as compared to the first one, as can be seen by direct comparison of the phosphorylation triggered by stimulation with 50 ng/mL of the proteins for 15 minutes determined in both experiments (Figure 23 C).

By this ELISA, it could be ruled out that reduced VEGFR-2 phosphorylation upon stimulation with FLV or TG-FLV as compared to stimulation with VEGFmut or TG-VEGFmut is specific to tyrosine 1175. The results obtained by western blotting hence reflect well overall VEGFR-2 phosphorylation.

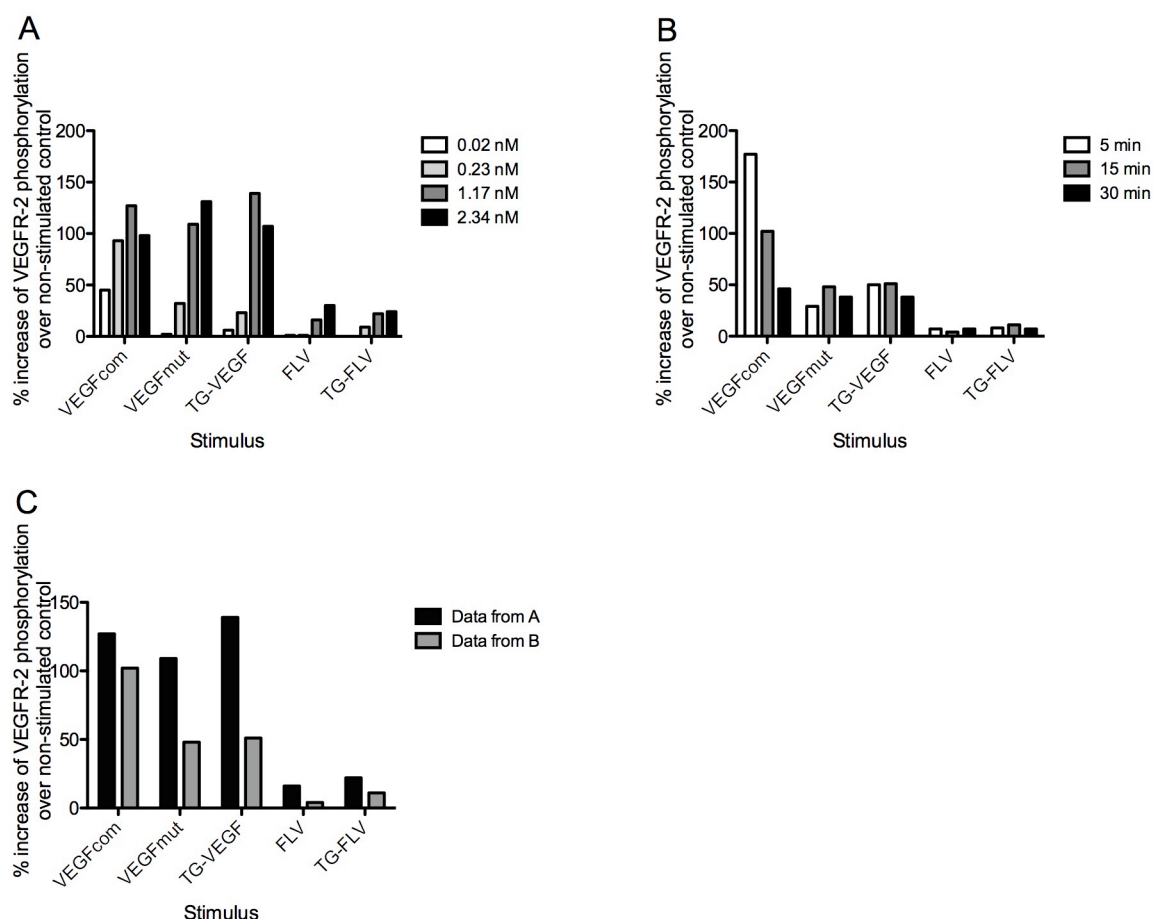


**Figure 23: Detection of overall VEGFR-2 phosphorylation by ELISA confirmed reduced phosphorylation levels upon stimulation with FLV and TG-FLV as compared to VEGFmut and TG-VEGFmut.** Graphs showing the phosphorylation of VEGFR-2 upon stimulation with VEGF proteins from a commercial source or produced in HEK293-EBNA. **(A)** Dose response and **(B)** time response of VEGFR-2 phosphorylation. **(C)** Comparison of VEGFR-2 phosphorylation detected in the two separate experiments upon stimulation with 1.17 nM (50 ng/mL) of the proteins for 15 minutes.

### 3.3.6 VEGFmut and FLV bind to VEGFR-2 with high affinities: Surface plasmon resonance binding studies

One possible reason for the lower VEGFR-2 phosphorylation observed upon stimulation with these proteins might be an altered conformation inhibitory to interaction with the receptor. To characterize the binding of the bi-functional constructs to VEGFR-2 in comparison to binding of VEGFmut to the receptor, surface plasmon resonance (SPR) biosensor binding studies were carried out in collaboration with professor Dr. Stefan Höning. Representative sensograms are shown in Figures 24 A and B. Association rate constants  $k_a$ , dissociation rate constants  $k_d$  and the resulting equilibrium dissociation constant  $K_D$  are summarized in Table 4.

## Results

VEGFmut bound to immobilized VEGFR-2 Fc with an association rate constant  $k_a = 1.34 \cdot 10^6 \pm 2.63 \cdot 10^5 \text{ M}^{-1}\text{s}^{-1}$ . This value is comparable with the association rate constant  $k_a = 3.71 \cdot 10^6 \pm 0.7 \cdot 10^5 \text{ M}^{-1}\text{s}^{-1}$  published in the literature for VEGF-A<sub>165</sub> (Cunningham et al. 1999). For FLV,  $k_a = 2.31 \cdot 10^5 \pm 5.69 \cdot 10^4 \text{ M}^{-1}\text{s}^{-1}$  was determined. Binding of FLV to VEGFR-2 Fc was markedly weaker than binding of VEGFmut, but FLV still bound the receptor with high affinity. The decreased affinity of FLV to the receptor was not due to too low concentrations of FLV employed, as shown in the western blot performed on reduced protein samples used for the SPR binding studies (Figure 24 C).

Due to the high affinity both molecules showed to VEGFR-2 Fc, determination of the dissociation rate constant was difficult and not precise under the experimental conditions used, as seen by the lack of a drop in the sensograms shown in Figures 24 A and B at the end of injection, indicating that all recombinant protein injected remains bound to the receptor. The dissociation rate constant determined was  $k_d = 1 \cdot 10^{-3} \text{ s}^{-1}$  for both molecules. Cunningham et al. measured  $k_d = 1.34 \cdot 10^{-4} \pm 0.19 \cdot 10^{-4} \text{ s}^{-1}$  for VEGF-A<sub>165</sub>. Based on these values, for VEGFmut  $K_D = 7.81 \cdot 10^{-10} \pm 1.87 \cdot 10^{-10} \text{ M}$ , and for FLV,  $K_D = 4.55 \cdot 10^{-9} \pm 1.16 \cdot 10^{-9} \text{ M}$  were calculated, and for VEGF<sub>165</sub>,  $3.71 \cdot 10^{-11} \pm 4.9 \cdot 10^{-11} \text{ M}$  are published. Due to differences in  $k_d$ ,  $K_D$  determined for VEGFmut compared less well to the  $K_D$  published for VEGF-A<sub>165</sub>.

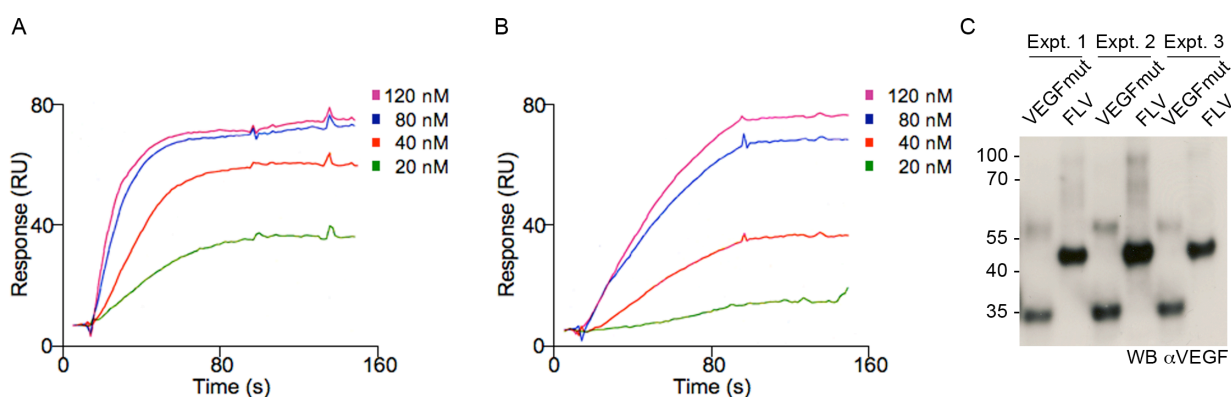


**Figure 24: SPR biosensor binding studies revealed high affinity binding of VEGFmut and FLV to VEGFR-2. (A)** Sensogram illustrating the binding of VEGFmut to VEGFR-2-Fc. **(B)** Sensogram describing the binding of FLV to VEGFR-2-Fc. **(C)** Western blot anti-VEGF-A on 200 ng of the protein samples used for the experiments.

	$k_a \text{ [M}^{-1}\text{s}^{-1}\text{]}$	$k_d \text{ [s}^{-1}\text{]}$	$K_D \text{ [M]}$
VEGFmut	$1.34 \cdot 10^6 \pm 2.63 \cdot 10^5$	$1 \cdot 10^{-3}$	$7.81 \cdot 10^{-10} \pm 1.87 \cdot 10^{-10}$
FLV	$2.31 \cdot 10^5 \pm 5.69 \cdot 10^4$	$1 \cdot 10^{-3}$	$4.55 \cdot 10^{-9} \pm 1.16 \cdot 10^{-9}$
VEGF <sub>165</sub> (Cunningham et al. 1999)	$3.6 \cdot 10^6 \pm 0.7 \cdot 10^5$	$1.34 \cdot 10^{-4} \pm 0.19 \cdot 10^{-4}$	$3.71 \cdot 10^{-11} \pm 4.9 \cdot 10^{-11}$

**Table 4: Table summarizing  $k_d$ ,  $k_a$  and  $K_D$  determined as compared to values found in the literature.**

For an appropriate description of the dissociation kinetics, additional experiments would be necessary. However, experiments performed clearly affirm specific binding of both, VEGFmut and FLV, to VEGFR-2 Fc, and the association rate constant of VEGFmut is comparable to that of VEGF-A<sub>165</sub>. Performed experiments thus provide the answers required for this work.

### 3.4 *In vivo* characterization of engineered VEGF proteins applied to wounds in fibrin matrices

Subsequent experiments explored the angiogenic properties of recombinant proteins produced in HEK293-EBNA and delivered in fibrin gels *in vivo*, using full thickness skin wounds as a clinically relevant model. Punch biopsy wounds were created on the back of male db/db mice, and fibrin gels supplemented with 0.468  $\mu$ M (corresponding to 20  $\mu$ g/mL effective VEGFmut concentration) of either soluble VEGFmut, TG-VEGFmut, TG-FLV, or no growth factor were allowed to polymerize *in situ*. After gel formation, the wounds were covered by a piece of non-adherent Adaptic<sup>®</sup> and a semipermeable wound dressing to prevent drying of the gels (Figure 25). Tissue samples were collected on day 10 and 14/15 post wounding.

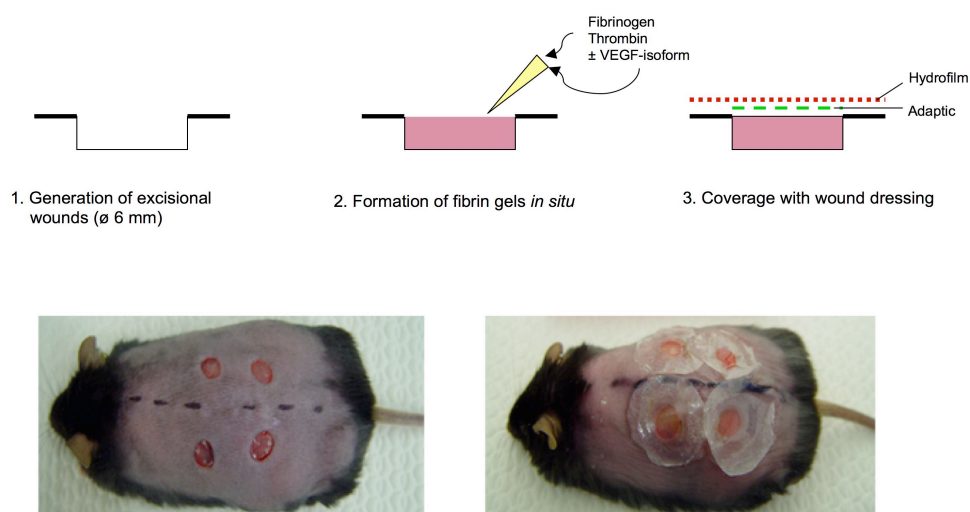


Figure 25: Schematic overview of the wounding procedure and the optimized wound care applied.

### **3.4.1 Cellular invasion of fibrin gels and induction of angiogenesis in day 10 and day 15 wounds**

To get a first impression on angiogenesis and the wound healing response upon the described treatment, wounds from a total of 6 mice were harvested on day 10 and 15 post injury. The overall histology of these wounds was investigated by hematoxylin and eosin (H&E) stained paraffin sections, and Masson's Trichrome (TM) staining was performed to distinguish the extracellular matrix and to highlight erythrocytes (Figure 26).

Based on this histological analysis, the fibrin gel was always evident in day 10 wounds. In some day 15 wounds, it could still be seen, even though it largely became substituted by granulation tissue. The fibrin gel seemed to be incorporated by the regenerating tissue, as cells invaded the fibrin gel under all conditions investigated. This was particularly evident in day 10 wounds, where the hyperproliferative epithelium of the wound margins seemed to migrate over the gel, whereas the gel was integrated in the cell-rich granulation tissue that formed beneath the epithelium (Figure 26). Fibrin alone had little effect on angiogenesis. Upon inclusion of diffusible VEGFmut in fibrin gel, some vascular structures filled with erythrocytes were visible. Vascular structures were more numerous and showed increased vessel diameters in wounds treated with the matrix bound proteins TG-VEGFmut or TG-FLV.

Also 15 days post wounding, in some of the wounds the fibrin matrix was still detectable, and became replaced by the granulation tissue (Figure 26). Furthermore, on day 15, the angiogenic response detected was more pronounced in wounds treated with TG-VEGFmut than with VEGFmut, but decreased as compared to day 10 wounds. Also in wounds treated with TG-FLV, erythrocyte numbers were increased as compared to the fibrin treated control. In wounds with the matrix-bound growth factors, TG-VEGFmut and TG-FLV, the granulation tissue appeared highly cellular with a dense extracellular matrix.

For both time points, plain fibrin matrices resulted in the weakest response in angiogenesis and granulation tissue formation. In contrast, VEGFmut, TG-VEGFmut and TG-FLV seemed to stimulate granulation tissue formation when compared to the control. Both granulation tissue formation and angiogenesis appeared slightly higher on both day 10 and day 15 when fibrin gels contained soluble VEGFmut. Granulation tissue formation and angiogenesis was most pronounced in fibrin matrices formulated with TG-VEGFmut and TG-FLV.

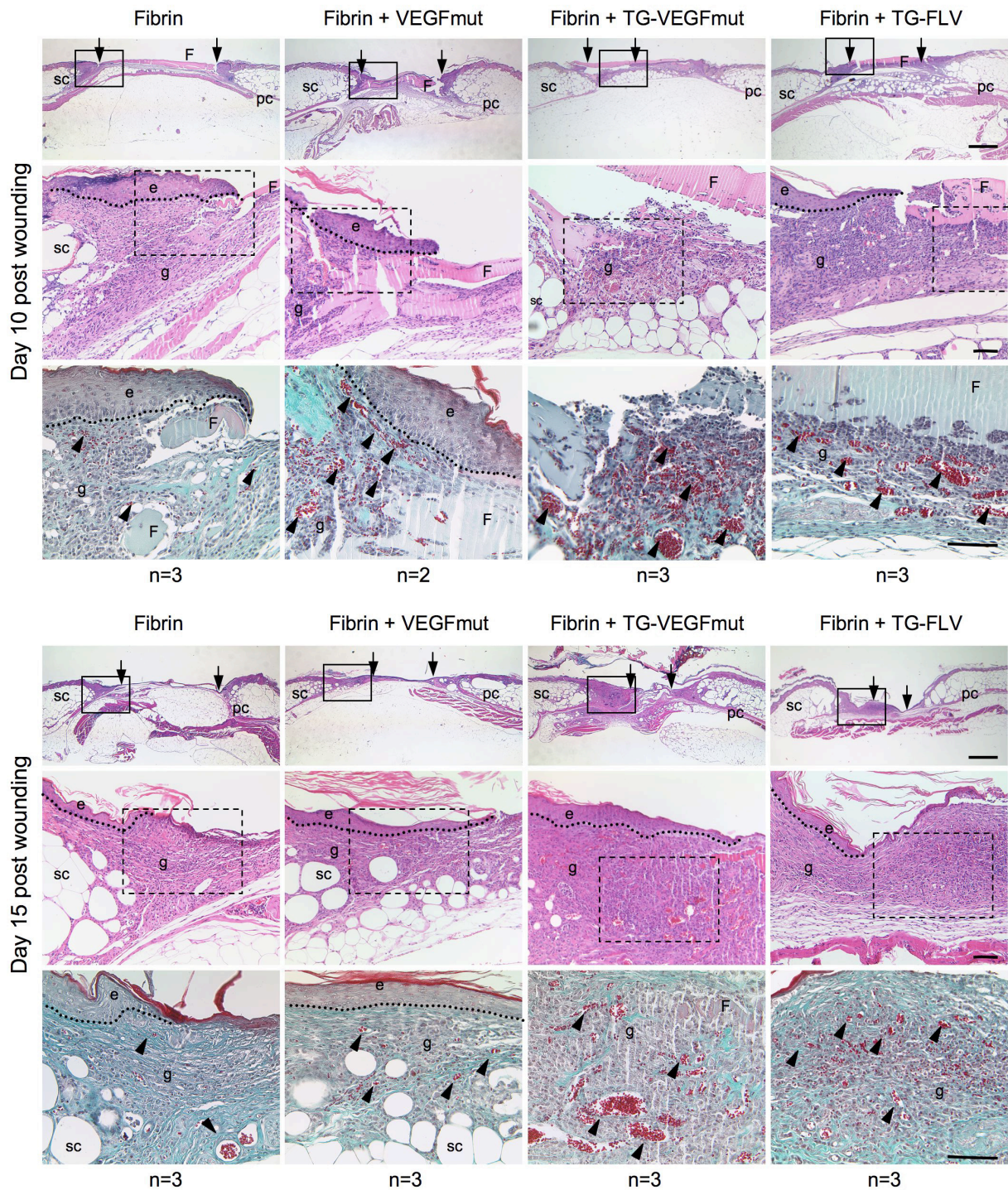


**Figure 26: Investigation of skin wounds treated with recombinant VEGF proteins in a fibrin gel revealed that matrix bound isoforms were particularly efficient at inducing angiogenesis.** Wound sections from day 10 and day 15 wounds were stained with H&E and Masson's Trichrome staining. Magnifications shown: 1.5x (scale: 1000  $\mu$ m), 10x, 20x (scales 100  $\mu$ m). Abbreviations used: e – epidermis, g – granulation tissue, F – fibrin, sc – subcutaneous fat tissue, pc – panniculus carnosus. Frames and dashed frames highlight area of interest, on which was focused in higher magnification.

### 3.4.2 TG-VEGFmut and TG-FLV induce a prominent angiogenic response, but differ in their potency to recruit pericytes

For a more sophisticated analysis of the wound healing response, cryosections were prepared from the wounds of 12 mice sacrificed on day 10 or 14 after wounding treated as described above. Sections were probed for CD31, an endothelium-specific marker, and for desmin, in the wound mainly expressed by pericytes. The effect of these treatments on the wound healing response was assessed histomorphometrically, and distance between the epithelial tips, the amount of granulation tissue and the distance between the ends of the panniculus carnosus determined are summarized in Figure 27.

When compared to fibrin only treated control wounds, wound closure was accelerated upon treatment with fibrin plus diverse VEGF proteins (Figure 27 A). Whereas 4 out of 6 wounds treated with fibrin were still open on day 10, 1 out of 6 treated with VEGFmut/fibrin and 1 out of 7 treated with TG-FLV/fibrin showed incomplete epithelialization by day 10. All 7 wounds treated with TG-VEGF/fibrin were closed by this time. By day 14 post injury, all wounds revealed complete reepithelialization.

Although at day 10 post injury the mean deposition of granulation tissue was increased in VEGF-isoform treated wounds versus fibrin alone treated wounds, this difference was not statistically significant (Figure 27 B). Furthermore, wound contraction was not significantly altered at day 10 or day 15 post injury in VEGF-isoform treated wounds versus control wounds (Figure 27 C).

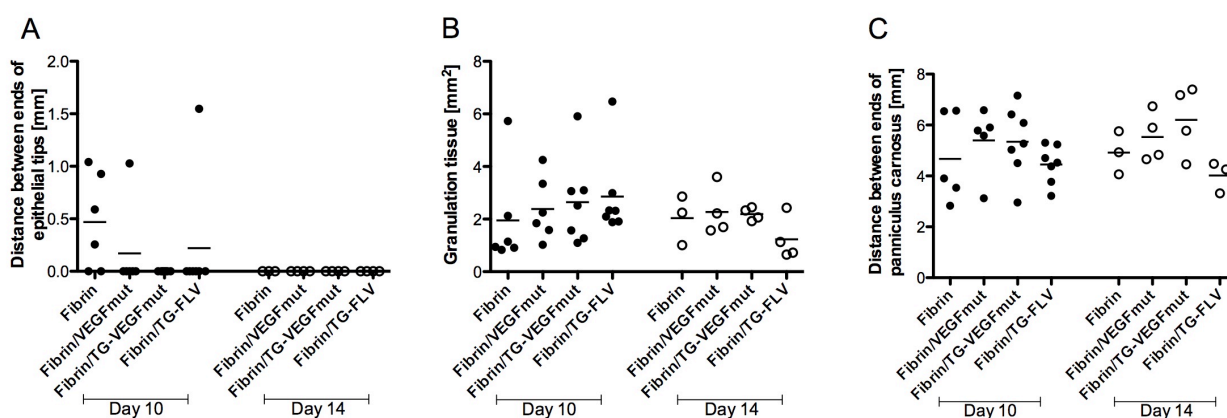


**Figure 27: Accelerated wound closure and a tendency toward increased amounts of granulation tissue were evident in wounds treated with recombinant VEGF proteins.** Morphometric analysis of wound healing on CD31/desmin stained cryosections at day 10 and 14 post injury, treated with either fibrin alone, VEGFmut/fibrin, TG-VEGFmut/fibrin or TG-FLV/fibrin. Graphs summarize (A) distance between ends of epithelial tips, (B) area of granulation tissue, (C) distance between ends of panniculus carnosus. Each data point represents the wound tissue of a different mouse.

The vascular response during granulation tissue formation was investigated in cryosections co-stained for CD31 and desmin and quantified in a semiquantitative fashion. Statistical significance was accepted for p-values  $<0.05$  in the paired student's t-test. Representative images of wound tissue 10 days post injury are shown in Figure 28, and the quantification is summarized in Figure 29.

Wounds treated with fibrin only showed few short capillaries invading the granulation tissue (Figures 28 and 29). Generally, these sparse vascular structures were associated with desmin positive perivascular cells.

When soluble VEGFmut was incorporated into the fibrin gel, the length of vascular structures appeared slightly increased when compared to control wounds (Figure 28), however the mean area within the granulation tissue that stained positive for CD31 was similar to that observed in control wounds (Figure 29 A, B). Wounds treated with fibrin showed an average of 7.2 % of granulation staining positive for CD31, and wounds treated with VEGFmut 6.5 %. Also the area staining positive for desmin was comparable to that observed in control wounds (Figure 29 D, E).

The most prominent increase in the density and length of vascular structures within the granulation tissue was found in wounds treated with TG-VEGFmut in fibrin (Figures 28 and 29 A, B), where an average area of 18.8 % of the granulation tissue stained positive for CD31. Despite the dramatically increased vascular network, vascular structures were covered with abundant desmin positive perivascular cells (Figure 29 C, D). The density of perivascular cells associated with vascular structures was comparable to fibrin only treated wounds as well as VEGFmut/fibrin gels (Figure 29 E). The relative area covered by endothelial cells or pericytes was significantly increased as compared to the other treatment options (Figure 29 B, D).

Also TG-FLV loaded fibrin gels significantly increased the density of vascular structures within the granulation tissue when compared with control wounds or wounds treated with VEGFmut, as an average of 12.5 % of the granulation tissue was found positive for CD31 (Figure 28 and 29 B).



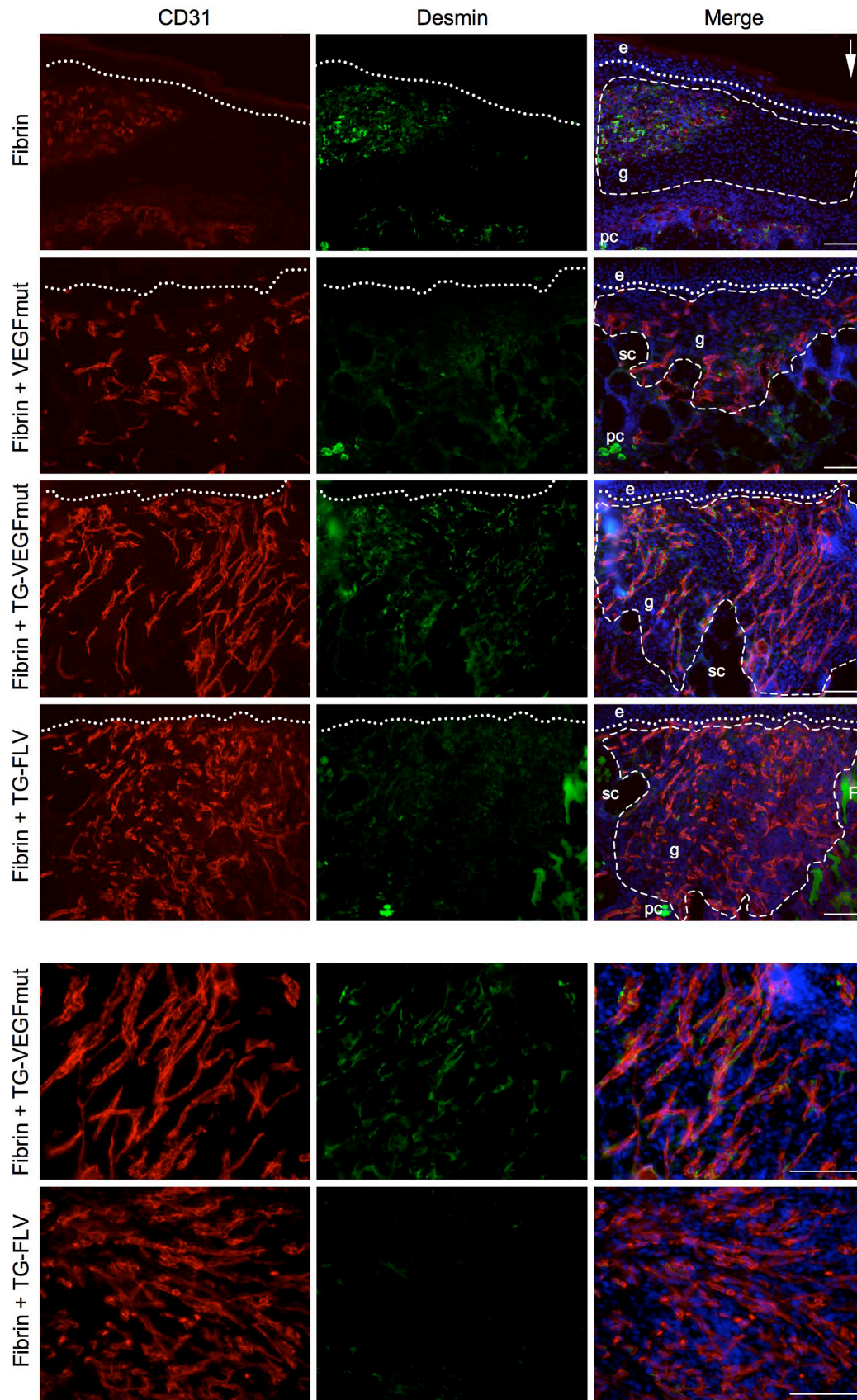


**Figure 28:** Treatment of skin wounds with the matrix bound variants TG-VEGFmut and TG-FLV in fibrin gels induced more vessels as compared to the fibrin only control and to soluble VEGFmut. CD31/desmin stained cryosections of day 10 wounds treated as indicated. Magnifications shown: 10x, 20x. Scale bar 100  $\mu$ m. Abbreviations: e – epidermis; g – granulation tissue; sc – subcutaneous fat tissue; pc – panniculus carnosus; F – fibrin gel. Arrow indicates direction of wound edge.

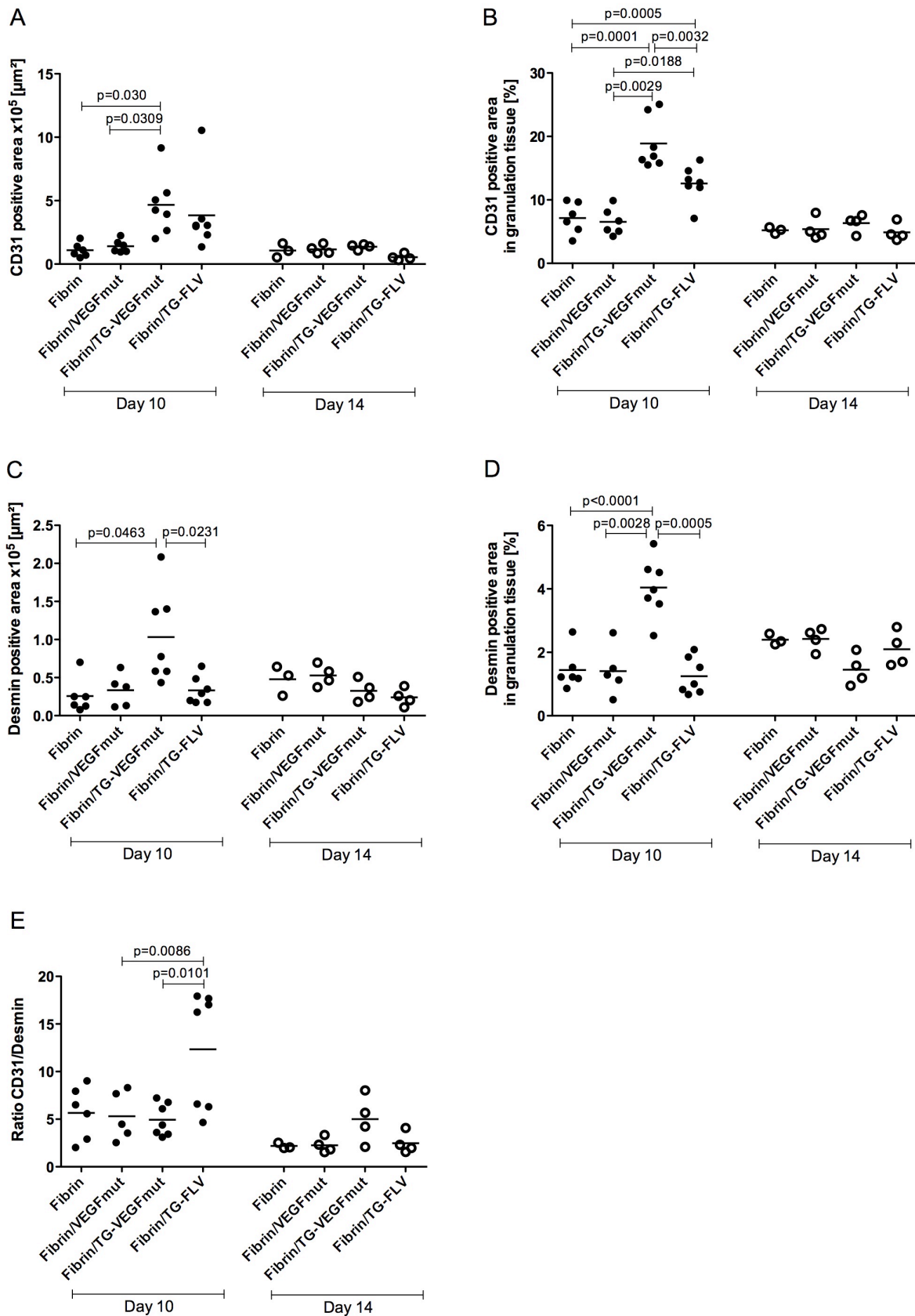


**Figure 29: Quantification of the angiogenic response within the granulation tissue of day 10 and day 14 wounds reveals a significantly increased angiogenesis in wounds treated with TG-VEGF and TG-FLV in fibrin gels. (A, B) Graphs show the result of the quantification of CD31 positive areas. (C, D) Graphs summarize the quantification of desmin positive areas. (E) Graph indicating the ratio of CD31 to desmin positive areas. Each data point represents the wound tissue of a different mouse. Statistical significance was tested by paired t-tests and accepted for  $p<0.05$ .**

Interestingly, the increased vascularity found in wounds treated with TG-FLV was not accompanied with proportional recruitment of perivascular cells, as the area covered by pericytes was similar in wounds treated with fibrin only or soluble VEGFmut (Figure 29 C, D). Thus, the ratio of vascular structures to desmin positive perivascular cells expressed as the ratio of CD31 signal to desmin signal was significantly increased when compared to wounds treated gels containing VEGFmut or TG-VEGFmut (Figure 29 E). In control wounds, as well as in wounds treated with VEGFmut or TG-VEGFmut in fibrin, around 5 endothelial cells are found per pericyte, while in the TG-FLV treated wounds, this ratio of endothelial cells to pericytes is increased to 12 (Figure 29 E).

At day 14 post injury, all treatment options revealed a reduced vascular network when compared to day 10 post injury wounds, indicating vascular remodeling and regression following wound closure (Figure 29).

## 4 Discussion

### 4.1 Covalent binding of VEGF-A<sub>165</sub> to fibrin matrices is superior to soluble VEGF-A<sub>165</sub> to induce sustained angiogenesis during wound repair

This study aims at the optimization of angiogenesis induced by bioengineered VEGF-A variants in combination with advanced delivery strategies. To this end, the produced VEGF-A proteins VEGFmut, TG-VEGFmut and TG-FLV were delivered to full-thickness wounds in diabetic mice, which represent a well-established model for impaired wound healing characterized by delayed angiogenesis. The vessel growth was compared to wounds treated with a fibrin gel only. In this setting, growth factors comprising the TG-peptide become covalently bound to fibrin during coagulation. This delivery strategy allows for cell-demanded, locally controlled release in a sustained manner, hypothesized to be critical for the induction of a functional vasculature.

Wounds treated with fibrin in combination with the various VEGF-A proteins showed accelerated wound closure by day 10 post-wounding as compared to wounds treated with fibrin alone. This observation is in agreement with previous studies, in which the delivery of VEGF-A to wounds either as a protein, as a plasmid or by genetically modified cells accelerated re-epithelialization (Brem et al. 2009; Michaels et al. 2005; Romano Di Peppe et al. 2002; Roth et al. 2006). Major differences between the various treatments were observed in the induction of angiogenesis, as the vessel density at day 10 in wounds treated with the matrix-bound forms was significantly increased as compared to wounds treated with fibrin only. Importantly, soluble VEGFmut did not increase angiogenesis over control levels.

Previous reports underline the importance of matrix coupling for the induction of a functional and well-organized vasculature. Ehrbar et al. showed in a CAM assay, that soluble VEGF-A<sub>121</sub> induced many brush-like vessels and altered the hierarchical organization of the vessels. An increase in intussusception and abrupt vessel diameter changes were observed. By contrast, vascular networks induced by TG-VEGF-A<sub>121</sub> appeared well organized and showed none of these abnormalities. Furthermore, Teflon chambers filled with fibrin with soluble VEGF-A<sub>121</sub> and subcutaneously implanted induced non-functional, leaky vessels in mice, which were not observed upon delivery of TG-VEGF-A<sub>121</sub> in the same model (Ehrbar et al. 2004). By contrast, in the wounding experiments performed in this study, no obvious vascular disorganization upon

treatment with soluble VEGFmut was detectable. As described, VEGFmut is a mutated form of VEGF-A<sub>165</sub>, and thus, the intrinsic capability of VEGF-A<sub>165</sub> to interact with fibrin (Sahni and Francis 2000) may prevent vessel abnormalization. However, a more likely explanation for this phenomenon may consist in different time points chosen for the read-out of the experiments. In the experiments performed by Ehrbar et al., early angiogenic effects were detected. Alterations in the vasculature of the CAM were detected after two days of exposure to VEGF-A functionalized fibrin matrices. Also the mouse experiments performed by this group were terminated after 4 days (Ehrbar et al. 2004). By contrast, wounding experiments conducted during this study were terminated after 10 days. In these experiments, diabetic mice characterized by a delayed wound healing response caused by reduced angiogenesis were investigated as a clinically relevant model. In diabetic mice, the angiogenic response is generally sparse, and therefore, tissue harvest was performed at the time point of maximal vessel growth. In untreated wounds, the maximum angiogenic response was observed between days 8 and 11 following wounding (Roth et al. 2006). Therefore, by the experiments performed, it could not be excluded that an abnormal vessel growth took place during the induction of angiogenesis at earlier time points of the treatment with soluble VEGFmut. By the time of tissue harvest, normalization of the vasculature may have taken place following a decrease in local VEGFmut-concentrations, and by the recruitment of pericytes. The weak angiogenic response observed upon treatment with soluble VEGFmut suggests an earlier depletion of the growth factor depot by a burst release of the growth factor. This was surprising, as VEGF-A<sub>165</sub> is thought to bind to fibrinogen and fibrin with high affinity (Sahni and Francis 2000), and for this reason has been frequently delivered as admixture to fibrin glue in various systems. As also the *in vitro* experiments investigating the release kinetics of VEGFmut showed that the soluble VEGFmut was quickly washed out of the fibrin gels, the delivery of VEGF-A<sub>165</sub> by simple addition of the growth factor to the gel may need to be reconsidered.

A major advantage of the delivery system employed here is the tight control of local VEGF-A doses. VEGF-A is a very potent inducer of angiogenesis, and physiologically induces angiogenesis in a very narrow concentration range. This was shown in a series of elegant experiments, in which myofibroblasts engineered to express various concentrations of VEGF-A were implanted into muscle of mice. In this setting it was demonstrated, that not the total VEGF-A dose delivered was critical for the induction of a functional vasculature, but that rather the local dose in the microenvironment determined the outcome of vessel growth (Ozawa et al. 2004). Control over the local VEGF-A dose upon delivery of the growth factor covalently

coupled to fibrin gels is accomplished by cell-controlled release from the matrix. The engineered, covalently fibrin bound VEGF-A is specifically released upon matrix degradation by proteases located to the cell surface. By this approach, the natural storage function of the extracellular matrix is mimicked, and cell demanded release kinetics allow for a controlled and prolonged releases at low concentrations (Zisch et al. 2001). Importantly, in wounds of diabetic mice, elevated plasmin concentrations were detected (Roth et al. 2006), and the stability of the fibrin gel within the wounds initially was not clear. However, this was a critical parameter, as fibrinolysis is directly linked to the controlled release of VEGF-A from the gel. Results of the wounding experiments performed indicated, that the fibrin gels employed were stable within the wound for at least 10 days, as the gels were microscopically still detectable at the wound site at this time point. This system thus represents a delivery mode, which might be beneficial for the treatment of human non-healing wounds enriched in proteases as well.

Additionally, the covalent coupling of VEGF-A to fibrin matrices not only functions as feedback controlled local growth factor depot, but also provides a steep local VEGF-A-gradient between the gel and the surrounding wound tissue. The formation of gradients depends on extracellular matrix-VEGF-A interactions mediated by VEGF-A isoforms equipped with a heparin-binding site during development. In mice solely expressing the soluble variant VEGF-A<sub>120</sub>, guidance during the post-natal vascularization of the retina was severely impaired. Similar effects were observed when the extracellular VEGF-A gradient in wild-type mice was disturbed by injections of VEGF-A<sub>120</sub> protein (Gerhardt et al. 2003; Ruhrberg et al. 2002; Stalmans et al. 2002). Importantly, in the delivery system applied here, the incorporation of TG-VEGFmut and TG-FLV into fibrin gels by factor XIIIa is incomplete as shown by *in vitro* release experiments performed in this study. Approximately 10-15 % of the growth factor remained soluble. As also VEGF-A<sub>165</sub> is thought to retain some diffusibility within the tissue (Houck et al. 1992; Park et al. 1993), it may be possible that low amounts diffusing out of the fibrin gel could locally activate endothelial cells, thus prime the angiogenic response, and provide local gradients guiding cells into the gel. The induced tip cells may sense VEGF-A localized within the fibrin gel far from the cell body by the extension of multiple, highly dynamic filopodia enriched in VEGFR-2 (Gerhardt et al. 2003). They then guide invasion of the gel in the direction of transcellular gradients, with highest VEGF-A-concentrations at the filopodial tips. Furthermore, the membrane-anchored MMP, MT1-MMP, was shown to be expressed in tip cells during angiogenesis (Yana et al. 2007). Localization of this protease to filopodia would allow for a highly localized matrix degradation and release of VEGF-A at the tip of the migrating cell, and allow for gradient shaping in collaboration with interstitial flow (Fleury et al. 2006; Helm et al.

2005). However, these possible mechanisms of gradient formation and guidance were not investigated within this study and remain to be elucidated in detail in the future.

Many previous experiments, in which VEGF-A was delivered into wounds either employed genetically modified cells engineered to over-express VEGF-A, or delivered VEGF-A protein daily in high doses to the wound (Galiano et al. 2004; Roth et al. 2006). The delivery approach chosen here has the major advantage that it is effective in diabetic mice upon one single application. Furthermore, it provides advantages for the clinical use, as overcomes security concerns when using genetically modified cells in patients, it is more feasible in wound care as daily application of the growth factor is not necessary, and more cost efficient, as lower doses of VEGF-A are delivered.

### **4.2 FNIII10 fusion to VEGF-A<sub>165</sub> promotes enhanced cell attachment and spreading *in vitro* compared to FNIII10 and VEGF-A<sub>165</sub> alone**

Another approach towards the optimization of angiogenesis aimed at the activation of synergistic signaling downstream of  $\alpha v\beta 3$  and VEGFR-2 by a novel fusion molecule consisting of VEGFmut and FNIII10 interconnected by a linker and denoted FLV. The design of this molecule was motivated by findings from various *in vitro* and *in vivo* models indicating that integrin  $\alpha v\beta 3$  is required for the full activation of VEGFR-2 (Mahabeleshwar et al. 2006; Soldi et al. 1999). Ligation of this integrin was interpreted to be critical for angiogenesis, as its inhibition by RGD-mimetics or specific antibodies counteracted vessel growth (Brooks et al. 1994b). It was demonstrated that VEGF-A stimulation results in activation of  $\alpha v\beta 3$ , and that the functional consequence of this crosstalk is enhanced migration on  $\alpha v\beta 3$  substrates (Byzova et al. 2000), in which FAK and SAPK2 are involved (Masson-Gadais et al. 2003). Endothelial cell migration proved to depend on a sustained activation of Erk, which in turn was abolished in CAMs by treatment with integrin  $\alpha v\beta 3$  inhibitors (Eliceiri et al. 1998). Work by Mahabeleshwar et al. demonstrated that the molecular interplay between both receptors is of a reciprocal nature, as ligand binding of the integrin triggered basal VEGFR-2 activation and *vice versa*. Upon stimulation, a complex comprising  $\alpha v\beta 3$  and VEGFR-2 is formed (Soldi et al. 1999), in which both receptors are phosphorylated and  $\alpha v\beta 3$  integrin is activated (Byzova et al. 2000; Mahabeleshwar et al. 2006). For the formation of a VEGFR-2/ $\alpha v\beta 3$  complex, the tyrosine

residues on the  $\beta 3$  cytoplasmic tail which become phosphorylated upon integrin activation are critical, as in endothelial cells obtained from DiYF knock-in mice, in which these tyrosine residues are mutated, showed severe defects in various *in vitro* and *ex vivo* angiogenesis assays. Endothelial cells failed to form tubes in matrigel, also outgrowth from aortic rings as well as migration on  $\alpha v\beta 3$ -ligands was impaired, and no sustained Erk-activation was detected in response to VEGF-stimulation (Mahabeleshwar et al. 2006). Nevertheless, these mice developed normally.

To test whether the FNIII10 subunit indeed is a specific ligand for integrin  $\alpha v\beta 3$ , cell attachment assays were performed using TG-FNIII10 as attachment substrate. The TG-sequence consists of only 8 amino acids, and these 8 amino acids were considered to have a smaller effect on the overall conformation of the FNIII10 domain than the expression of FNIII10 outside of the context of full-length fibronectin. The cell attachment assays performed firstly indicated that attachment of HUVECs to TG-FNIII10 correlated with the concentration of the recombinant protein plated, and secondly showed, that this attachment could be reduced by 30 % by function blocking antibodies raised against integrin  $\alpha v\beta 3$ . This antibody was more efficient in inhibiting attachment to TG-FNIII10 than a function-blocking antibody directed against the  $\alpha 5$  integrin subunit. On full-length fibronectin by contrast, the  $\alpha v\beta 3$  function blocking antibody had no inhibitory effect on cell attachment, but attachment was reduced upon pre-treatment with the  $\alpha 5$  function blocking antibody proving the functionality of this antibody. This was to be expected, because  $\alpha v\beta 3$  is the major integrin binding to the RGD site on FNIII10 in the absence of the synergy site on FNIII9 (Danen et al. 1995). On full-length fibronectin by contrast, binding to the RGD-site on the FNIII10 domain is preferentially mediated by integrin  $\alpha 5\beta 1$ , even though this site is recognized by many different integrins. Integrin  $\alpha 5\beta 1$  recognizes the so called synergy site on FNIII9 in addition to the RGD-site localized in FNIII10, which in turn is required for efficient binding of cells to fibronectin allowing near maximum cell adhesion (Aota et al. 1994; Grant et al. 1997). By this experiment, it was shown that indeed  $\alpha v\beta 3$  is targeted by FNIII10, as intended by the expression of the bi-functional constructs containing FNIII10 and VEGF-A<sub>165</sub>.

Another functional question concerning the bi-functional proteins was, whether their RGD-site within the FNIII10 domain was functional. During the expression of the protein as GST-tagged fusion protein, it seemed that GST-TG-PL-FLV had another thrombin cleavage site besides the one employed to cleave the tag off the protein, as thrombin-mediated cleavage resulted in



additional cleavage products. Indeed, for this protein, a cleavage site within the RGD-site is predicted, which seemingly is not processed by thrombin digestion of GST-TG-FNIII10, as cells can still attach to this protein. Thus, it seemed possible that the RGD-site was non-functional in the bi-functional proteins. To answer this question, HUVECs were allowed to attach to microscopy slides coated with the bi-functional protein FLV. Interestingly, cell attachment and spreading on FLV was enhanced as compared to attachment and spreading to FNIII10 or VEGFmut alone. On FLV, cells appeared maximally spread and showed many stress fibers ending in well-established focal contacts. By contrast, on FNIII10, less advanced cell spreading was observed, cells showed fewer focal contacts and stress fibers, and some cells remain rounded. On VEGFmut, cells did not spread. This was surprising, as Hutchings et al. observed good cell spreading on VEGF-A<sub>165</sub> as compared to spreading on poly-L-lysine, and the formation of numerous membrane protrusions resulting in stellate-like cell shapes (Hutchings et al. 2003). As their VEGF-A concentration plated was lower and the time during which cells were allowed to attach was shorter, this difference most likely is due to the use of different primary endothelial cells, namely human umbilical arterial endothelial cells and bovine retinal endothelial cells in these experiments.

In summary, a clear synergism in the promotion of cell spreading on the novel hybrid protein FLV was shown. These data apparently conflict with other *in vitro* results obtained in this study, as VEGFR-2 and Erk 1/2 phosphorylation upon stimulation of adherent subconfluent HUVECs with FLV was reduced as compared to the stimulation with VEGFmut, thus no synergism could be detected under these conditions. However, integrins are mechanosensors, which can distinguish soluble ligands from sequestered ligands. This idea is based on the observation, that soluble RGD-mimetics raised against  $\alpha v\beta 3$  induce apoptosis endothelial cells (Brooks et al. 1994b). Binding to soluble ligands does not permit the generation and transmission of force to the actin cytoskeleton, and does not support integrin activation (Cheresh and Stupack 2008). The *in vitro* experiments performed within this study underscored thus the importance of the proper presentation of the molecule to endothelial cells to allow for functional signaling. Apparently, sequestered FLV was capable to produce synergistic signaling towards enhanced cell spreading, while no synergism was observed when FLV was applied to the cells in solution. Future investigations should therefore investigate synergistic VEGFR-2 and Erk1/2 signaling in cells plated to immobilized FLV.

### **4.3 Covalent binding of FLV to fibrin is not superior to covalently fibrin-bound VEGF-A<sub>165</sub> in the induction of wound angiogenesis**

Based on the literature it was hypothesized that the collaboration between integrin  $\alpha\beta3$  and VEGFR-2 may be beneficial for the promotion of wound angiogenesis as well, and might result in improved tissue regeneration due to a better perfusion in wound healing impaired mice. To investigate this question, the hybrid protein consisting of the FNIII10 domain and VEGFmut was fused to a substrate sequence for the transglutaminase factor XIIIa and delivered to full thickness lesions in diabetic mice covalently bound to a fibrin gel. In this wound healing model, the angiogenesis induced by fibrin-bound TG-FLV was significantly increased over control levels. However, in wounds treated with TG-FLV, the area covered by vascular structures was reduced as compared to wounds treated with TG-VEGFmut, thus no synergistic signaling could be detected. By the *in vitro* stimulation of HUVECs with bi-functional fusion proteins it was demonstrated that both FLV and TG-FLV were biological active, as they triggered the phosphorylation of VEGFR-2 and downstream signaling partner Erk 1/2. Yet, also in this experiment, the bi-functional proteins they failed to induce increased or sustained activation of VEGFR-2 and Erk 1/2 phosphorylation upon stimulation as compared to the stimulation with VEGFmut.

The most important question at this point was to determine, whether the bi-functional protein was still able to interact with the VEGFR-2 or if the presence of FNIII10 within the same molecule would interfere with VEGFR-2 binding. SPR binding studies demonstrated, that FLV bound to immobilized VEGFR-2-Fc with high affinity. As compared to VEGFmut, the affinity was slightly decreased. However, it is not clear if differences in binding affinity between VEGF-A isoforms to VEGFR-2 directly translate into differences in their signaling capabilities. Even though VEGF-A<sub>121</sub> showed a reduced binding to VEGFR-2 as compared to VEGF-A<sub>165</sub>, both isoforms induced comparable phosphorylation and endothelial cell migration, yet endothelial sprouting from spheroids was decreased upon stimulation with VEGF-A<sub>121</sub> (Pan et al. 2007). By contrast, experiments performed by another group indicated that VEGF-A<sub>165</sub> stimulation of HUVECs induced a stronger and sustained phosphorylation of MEK and ERK as compared to VEGF-A<sub>121</sub>, while VEGF-A<sub>121</sub> appeared to activate Src, which was not the case for VEGF-A<sub>165</sub> (Zhang et al. 2008). Also VEGF-A<sub>165b</sub> binds to VEGFR-2 with the same affinity as VEGF-A<sub>165</sub>. Both molecules differ only by their 6 C-terminal amino acids (Woolard et al. 2004). However, VEGF-A<sub>165b</sub> does not induce VEGFR-2 phosphorylation and does not promote

angiogenesis (Cebe Suarez et al. 2006). Thus, the interaction strength of VEGF-A with VEGFR-2 does not forcedly correlate with the signaling output. By contrast, the interplay of VEGF-A isoforms with co-receptors might have a stronger effect on the signaling than their actual affinity to VEGFR-2, as co-receptors may optimize VEGF-A presentation to the receptor and enhance their binding. This view is supported by the finding that VEGF-A<sub>165b</sub> only weakly binds to HSPGs, and retains no affinity to Nrp-1, which may attribute to the more transient signaling observed downstream of VEGFR-2 (Cebe Suarez et al. 2006; Grunewald et al. 2010).

Another possible explanation for the lack of synergism may be that the density of RGD-ligands within the clot is very high, as fibrin possesses two RGD-sites within its A $\alpha$  chain (Henschen et al. 1983), which are recognized by integrin  $\alpha\beta3$  expressed on endothelial cells (Cheresh 1987). For this reason, the addition of additional integrin ligands may not further induce angiogenic signaling. Also, too many integrin ligands may have adverse effects on cell migration, as they can slow focal adhesion dynamics, as cells attach too strongly (Cheresh and Stupack 2008). By contrast, there is strong evidence based on experiments performed by Hall et al. that additional integrin  $\alpha\beta3$  ligands within the fibrin gel can promote angiogenic sprouting in the absence of growth factors. In these experiments, the 6<sup>th</sup> Ig-like domain of the cell adhesion molecule L1 (L1Ig6), which contains a RGD site and is a specific ligand for integrin  $\alpha\beta3$  (Blaess et al. 1998), was expressed as a fusion to the factor XIIIa substrate sequence and incorporated into fibrin matrices. These L1Ig6 functionalized fibrin gels promoted HUVEC process extension from microcarrier beads and angiogenesis in the CAM (Hall et al. 2004). The presence of additional integrin  $\alpha\beta3$  ligands is thus unlikely to hinder angiogenesis.

It appears more likely, that for the detection of synergistic signaling, a lower concentration of the growth factor should be delivered to wounds within the fibrin gels. In the experiments performed, 1.6  $\mu\text{g}$  of each protein (effective VEGF-A concentration) were delivered to one wound. In combination with the targeted delivery system employed, it seems reasonable that this dosage induced the maximal angiogenic response possible, and that doses below a saturation level should be investigated for the detection of synergistic signaling. Importantly, the physiological density of the vascular network induced is tightly regulated. Thus, the biological activity of TG-FLV to promote angiogenesis *in vivo* observed most likely was to be attributed to its presentation in a covalently matrix bound form, while synergistic effects remain to be elucidated in future experiments.

#### **4.4 Recombinant fusion proteins composed of various protein domains raise the possibility of synergistic signaling and novel biological functions**

The availability of recombinant cloning techniques allows the combination of various functional domains to assemble novel molecules with altered or additional properties. Within this study, bioengineering strategies were employed first to improve the delivery of VEGF-A<sub>165</sub> for biomedical applications, second to potentiate the biologic activity of the growth factor, and third to fine-tune the angiogenic response induced by VEGF-A<sub>165</sub> in non-healing wounds. This section will compare the bioengineering strategies employed in this study to other possible, published strategies, in which similar outcomes were targeted by molecular modifications of biologically active molecules.

The targeted delivery and the controlled release of potent growth factors to the desired site of treatment is recognized to be critical for positive outcome of treatments using recombinant proteins. In this study, VEGF-A<sub>165</sub> was fused to the  $\alpha_2$ -plasmin inhibitor substrate sequence of factor XIIIa, and this fusion allows specific covalent binding of the protein to fibrin by the crosslinking activity of factor XIIIa. As detailed above, this VEGF-A<sub>165</sub> form delivered in fibrin gels proved to be more efficient in the induction of angiogenesis in chronic wounds than soluble VEGF-A<sub>165</sub>, and these results were in agreement with investigations on the induction of angiogenesis with matrix-bound VEGF-A<sub>121</sub> (Ehrbar et al. 2004). In previous studies, the delivery of other growth factors in covalent binding to fibrin proved to have superior biological effects as compared to the soluble growth factor in fibrin gels in various *in vitro* and *in vivo* models. A fibrin-bound form of  $\beta$  nerve growth factor induced increased neurite process extension from embryonic chick dorsal root ganglia (Sakiyama-Elbert et al. 2001), and fibrin-bound bone morphogenic protein-2 promoted healing in critical size cranial defects (Schmoekel et al. 2005), respectively. Further, the delivery of growth factors by the covalent binding of heparin-binding peptides to fibrin (Sakiyama-Elbert and Hubbell 2000), as well as the delivery of DNA via covalently bound DNA-nanoparticles (Trentin et al. 2006) is feasible by this approach.

Similarly, also other growth factors engineered for improved matrix binding have been shown to be more potent as compared to soluble ones due to their prolonged retention time. To accomplish prolonged retention of growth factors in tissues, another strategy consists in their fusion to a collagen-binding domain. As connective tissue mainly consists of collagen, this should increase

residence and bioavailability of the growth factor. Fusion of a collagen-binding domain to VEGF-A was shown to prolong its residency in muscle or wound tissue (Ishikawa et al. 2006; Yan et al. 2010), and similarly, collagen-binding HGF, PlGF and FGF variants were designed (Kitajima et al. 2007; Lin et al. 2006; Pang et al. 2010).

The second strategy employed in this study aimed at the potentiation of the biologic activity of VEGF-A<sub>165</sub>. To this end, a VEGF-A<sub>165</sub> variant with a cell adhesion site naturally found in fibronectin, the FNIII10 domain was designed, aiming at increased angiogenic signaling by co-stimulation of VEGFR-2 and integrin  $\alpha\beta$ 3. In the approach employed here, FNIII10 was fused to the N-terminus of VEGF-A<sub>165</sub>, and both functional domains were interconnected by a linker calculated to be long enough to allow simultaneous interaction of both ligand domains with their respective receptors. The finding that this bi-functional protein retains the ability to bind to VEGFR-2 and to induce its activation *in vitro* is in agreement with previous reports, indicating that the N-terminal modification included is permissive for the bioactivity of the VEGF-A molecule (Backer and Backer 2001). The most important finding of this study was, that these hybrid proteins indeed have the potential to induce synergistic signaling. FLV was shown to promote cell adhesion of HUVECs to a greater extent than both functional domains alone. On FLV, HUVECs were maximally spread, showed many stress fibers and focal contacts. Also on FNIII10, spreading was efficient, but stress fiber organization and focal contact formation were dramatically reduced as compared to cells on FLV. On VEGF-A<sub>165</sub> by contrast, no spreading was observed. Thus, the fusion of cell-binding domains to growth factors can promote increased cell spreading.

This phenomenon was also observed using a very similar hybrid protein design, in which FGF-1 or -2 were directly fused to the fibronectin type III domains 9 and 10 (FNIII9/10). Also these bi-functional fusion proteins increased cell attachment to the hybrid construct over cell attachment observed on FNIII9/10 alone (Jang and Chung 2004; Jeon et al. 2009). Besides, FGF1-FNIII9/10 promoted increased proliferation, Erk1/2 phosphorylation and osteoblastic differentiation in a human osteosarcoma cell line compared with cells seeded on FNIII9/10 or FGF1 alone (Jeon et al. 2009). These results indicate, that the assembly of multiple functional domains in new fusion proteins may not only have an additive effect on biologic responses, but also can result in novel biological responses not observed in response to the single domains.

The third bioengineering strategy employed aimed at the fine-tuning of the angiogenic response, as pro-angiogenic therapies for chronic wounds and other treatments require the induction of a

mature, persistent, non-leaky and well organized vasculature. The highly proteolytic environment of non-healing wounds constitutes an additional challenge for the treatment with recombinant protein formulations, as it requires a stabilization of the growth factor delivered. Previous work by Roth et al. showed that gene delivery of a plasmin-stabilized mutant VEGF-A<sub>165</sub> form to skin lesions on the back of diabetic mice resulted in sustained vascular ingrowth due to pericyte recruitment and reduced apoptosis, most likely due to the increased persistence of the stabilized VEGF-A<sub>165</sub> in the wound (Roth et al. 2006). Similarly, the delivery of a mutant form of VEGF-A<sub>165</sub> covalently linked to fibrin gels in the same wound healing model proved to induce mature vessels abundantly covered with pericytes. Thus, the combination of a stable VEGF-A<sub>165</sub> isoform and targeted delivery is a good strategy for the induction of mature vessels.

An alternative approach using bioengineered VEGF-molecules aimed at the induction of a mature vasculature by specific targeting of VEGFR-2. It was hypothesized, that VEGF-A's ability to recruit inflammatory cells and to induce vascular leakage might delay mature vessel formation during wound healing. This consideration motivated Zheng et al. to design a chimeric VEGF-E<sub>NZ7</sub> molecule. VEGF-E is a potent, Orf-virus encoded VEGF-family member binding specifically to VEGFR-2, and thus incapable to act as a chemoattractant for inflammatory cells, as this response is mediated by VEGFR-1 signaling. For humanization, non-essential portions of VEGF-E<sub>NZ7</sub> were replaced by sequences from PlGF-1 (Zheng et al. 2007). When injected subcutaneously, this novel molecule accelerated wound closure and angiogenesis in full thickness wounds on diabetic mice, and this was attributed to the absence of tissue edema and the lack of a sustained infiltration of inflammatory cells (Zheng et al. 2007).

Furthermore, Ang1 is an emerging compound for the promotion of therapeutic angiogenesis. In binding to its receptor, the receptor tyrosine kinase Tie-2, Ang1 is known to promote vascular maturation, to prevent vascular leakage, and to contribute to angiogenic vascular growth (Asahara et al. 1998; Gamble et al. 2000). Ang1 binding to its receptor is mediated by its C-terminal fibrinogen-like domain, and a coiled-coil domain and a superclustering domain in the N-terminus of the protein accomplish the formation of bioactive oligomers. For its use as pro-angiogenic drug however, difficulties concerning its purification as a recombinant protein had to be overcome. Due to its superclustering domain, the purified protein tends to form aggregates reducing its bioavailability. For this reason, the natural oligomerization domains of Ang1 were replaced by the coiled-coil domain of the cartilage oligomeric matrix protein (COMP). This modification resulted in the preferential formation of COMP-Ang1 pentamers (Cho et al. 2004). In endothelial cells, this bioengineered protein promoted the protection from apoptosis, the

induction of migration, tube formation and sprouting to a greater extent than native Ang1 *in vitro*. Interestingly, COMP-Ang1 induced an angiogenic response similar to that observed upon stimulation with VEGF-A in the corneal micropocket assay, while native Ang1 didn't promote angiogenesis. A major benefit of COMP-Ang1 in comparison to VEGF-A in the induction of angiogenesis was the formation of a non-leaky vasculature (Cho et al. 2004).

These examples indicate, that the optimization of the molecular properties of bioactive compounds by recombinant techniques may provide additional benefits for pro-angiogenic therapies.

## 5 Perspectives

The overall objective of the present study was the amelioration of wound angiogenesis in response to recombinant VEGF-A<sub>165</sub> by optimizing bioavailability and potency of the growth factor.

One major finding was, that VEGF-proteins engineered for the covalent binding to fibrin had a superior effect on the induction of angiogenesis *in vivo* compared to soluble VEGF-A<sub>165</sub>. However, the hypothesized superiority of a bi-functional protein comprising FNIII10 fused to VEGF-A<sub>165</sub> targeting integrin  $\alpha\beta3$  and VEGFR-2 for synergistic pro-angiogenic signaling was not detectable in this wound healing model. One possible reason may be that the amount of VEGFmut and FLV delivered covalently bound to fibrin matrices induced maximum wound angiogenesis, as the amount of recombinant proteins delivered to wounds was high. Thus, future experiments should be performed to determine the optimal dose of recombinant matrix bound VEGF-proteins to be delivered. Also, it is likely that for the distinction of synergistic signaling in response to bi-functional proteins, a lower concentration range might be required.

Also, when HUVECs were stimulated with soluble VEGF-A<sub>165</sub> or FLV, no synergistic signaling was detected on the level of VEGFR-2 or Erk1/2 phosphorylation. By contrast, when HUVECs were plated on the immobilized ligands, cell spreading in response to FLV was markedly enhanced as compared to cell spreading on FNIII10 or VEGF-A<sub>165</sub>. These results indicate, that for the detection of synergistic signaling, the presentation of the immobilized ligand is crucial, and future experiments thus will focus on differences in cellular signaling in cells plated on VEGF-A<sub>165</sub> or FLV. The signaling output under this condition may be very different.

Furthermore, even though the functional domains FNIII10 and VEGF-A<sub>165</sub> are biologically active and can bind to their respective ligands as shown by cell attachment assays and by surface plasmon resonance measurements, respectively, the direct proof of simultaneous binding of both receptors to both ligands is still lacking. This evidence might be obtained by the performance of crosslinking experiments, during which the ligands are covalently crosslinked to cell surface receptors. The crosslinked complexes can be investigated for the presence of  $\alpha\beta3$  and VEGFR-2 by western blot. These experiments are currently ongoing.



The delivery system employed and the fusion proteins generated provide the possibility to study the impact of VEGF-A interactions with the extracellular matrix in angiogenesis and the role of the VEGFR-2 – integrin  $\alpha v \beta 3$  crosstalk. Additionally, the combination of fibrin matrices with protease stabilized VEGF-A proteins holds promising potential also for various pro-angiogenic therapeutic approaches, such as the treatment of healing-impaired wounds.

## 6 Materials and methods

### 6.1 Chemicals

Used chemicals were of analytical purity grade and obtained from Roth (Karlsruhe, Germany), Sigma Aldrich (St. Louis, USA), Riedel de Haen (Seelze, Germany), Applichem (Darmstadt, Germany) or Merck (Darmstadt, Germany) unless specified otherwise.

### 6.2 Special equipment

Chromatograph:	ÄKTApurifier™ (GE Healthcare, Fairfield, USA)
UV spectrometer:	NanoDrop-1000 (Thermo Fisher Scientific Inc., Waltham, USA)
ELISA plate readers:	VICTOR <sup>3</sup> (Perkin Elmer, Waltham, USA) Safire <sup>2</sup> (Tecan, Männedorf, Switzerland)
Electrophoresis systems:	PROTEAN II Electrophoresis Cell (Bio-Rad Laboratories GmbH, Munich, Germany) XCell SureLock™ Mini-Cell (Invitrogen, Paisley, UK)
Western blotting systems:	Mini Trans-Blot® cell (Bio-Rad) XCell II™ Blot Module (Invitrogen)
Microscopes:	Leica DM 4000B (Leica Camera AG, Solms, Germany) Nikon eclipse E 800 (Nikon, Melville, USA) Nikon A1 (Nikon, Melville, USA)

### 6.3 Bacterial cell culture

#### 6.3.1 *Escherichia coli* (*E. coli*) strains

##### *E. coli* strains used for cloning

DH5 $\alpha$  was purchased from Invitrogen and used for routine subcloning. This strain has several mutations that make it particularly useful for cloning and DNA-amplification, such as reduced homologous recombination to stabilize the insert and a reduced endonuclease activity that allows for higher yields. The genotype is F-  $\phi$ 80lacZ $\Delta$ M15  $\Delta$  (lacZYA-argF)U169 recA1 endA1 hsdR17(rk-, mk+) phoA supE44 thi-1 gyrA96 relA1  $\lambda$ -.

SCS110 was purchased from Stratagene (Santa Clara, USA) and is also a strain used for plasmid amplification due to its endonuclease deficiency. Additionally, it carries mutations in the DNA methylases Dam and Dcm, so the DNA isolated from these cells can be digested using methylation-sensitive restriction enzymes. The genotype is *rpsL*, (*Str<sup>r</sup>*), *thr*, *leu*, *endA*, *thi-1*, *lacY*, *galK*, *galT*, *ara*, *tonA*, *tsx*, *dam*, *dcm*, *supE44*, *d(lac-proAB)*, [*F' traD36, proAB, lacI<sup>d</sup>D M15*].

### ***E. coli* strains used for protein expression**

BL21 was purchased from GE Healthcare and is deficient in the proteases lon and ompT and hence a strain commonly used for the expression of recombinant proteins. The genotype is *B F*, *dcm*, *ompT*, *hsdS* (*r<sub>B</sub><sup>-</sup>*, *m<sub>B</sub><sup>-</sup>*), *gal* [*malB<sup>+</sup>*]<sub>K-12</sub>( $\lambda^S$ ).

BL21(DE3)pLys was obtained from Stratagene. As compared to BL21, the expression of recombinant proteins is more tightly controlled. The genome contains a T7 polymerase gene under the control of lacUV5. Expression of the T7 polymerase is induced by the addition of IPTG. Furthermore, this strain carries the plasmid pLysS encoding for the T7 lysozyme, a T7 RNA polymerase inhibitor to prevent leaky expression of the target gene in uninduced cells. The genotype is *B, F*, *dcm*, *ompT*, *hsdS*(*r<sub>B</sub><sup>-</sup>m<sub>B</sub><sup>-</sup>*), *gal* $\lambda$ (DE3) [pLysS Cam<sup>r</sup>].

### **6.3.2 General culture conditions**

For the culture of *E. coli*, sterile plastic ware and sterile technique was used. *E. coli* propagated for cloning purpose or for the expression of recombinant proteins were cultivated in liquid cultures in Lysogeny broth (LB), Super optimal broth with catabolite repression (SOC) or 2x yeast extract and tryptone (YT) medium as specified, at 37°C under shaking at 180 rpm using the appropriate selection antibiotics obtained by Applichem when indicated (Table 5).

For the selection of clones, liquid cultures were plated on LB agar plates and allowed to grow overnight at 37°C. For the investigation of the clones (for example for the detection of an insert during cloning or for the identification of a good protein producer), liquid cultures were inoculated from a single colony. Plates were stored at 4°C for up to 3 weeks.

<b>LB</b>		<b>SOC</b>		<b>2x YT</b>		<b>Antibiotics</b>	
0.5 %	Yeast extract	0.5 %	Yeast extract	1.6 %	Tryptone	Ampicillin	0.1 mg/mL
1 %	Tryptone	2 %	Tryptone	1 %	Yeast extract	Chloramphenicol	0.03 mg/mL
1 %	NaCl	10 mM	NaCl	0.5 %	NaCl		
(1.5%)	Agar)	2.5 mM	KCl				
		10 mM	MgCl <sub>2</sub>				
		10 mM	MgSO <sub>4</sub>				
		20 mM	Glucose				

**Table 5: Media and antibiotics used for the culture of *E. coli*.**

### **6.3.3 Generation of chemical competent bacteria using calcium chloride (Cohen et al. 1972)**

A single colony of bacteria was picked from a plate, transferred into 100 mL of LB and grown to an OD<sub>600</sub> of 0.4. Cells were harvested by centrifugation at 4°C and the pellet was resuspended in 30 mL of ice-cold 80 mM MgCl<sub>2</sub>, 20 mM CaCl<sub>2</sub> solution. Following another centrifugation step, the pellet was resuspended in 4 mL of 0.1 M CaCl<sub>2</sub>. For the preparation of a frozen stock, 140 µL of DMSO were added to the suspension and incubated for 15 minutes on ice. An additional 140 µL of DMSO were added, and cells were dispensed into working aliquots, snap-frozen in liquid nitrogen, and stored at -80°C until use (Sambrook 2001).

### **6.3.4 Transformation of chemical competent bacteria**

For transformation, cells were rapidly thawed, and 10 ng of plasmid DNA or 10 µL of ligation assays were added to 100 µL of cell suspension. After an incubation on ice of 15 minutes, cells were heat shocked in a 42°C water bath for 2 minutes and allowed to recover in SOC-medium with shaking for 1 hour at 37°C prior to plating on LB-agar plates containing the appropriate antibiotics for the selection of transformants.

### **6.3.5 Generation of bacterial frozen stocks**

To overnight cultures of positive clones in LB containing selection antibiotics, 30 % sterile glycerol were added to a total volume of 1 mL, and cultures were stored at -80°C.

## **6.4 Culture of eucaryotic cells**

### **6.4.1 Eucaryotic cells**

Human embryonic kidney (HEK) 293-EBNA cells were a kind gift from professor Dr. Manuel Koch. This cell line constitutively expresses the Epstein Barr Virus EBNA1 gene from the vector pCMV/EBNA. EBNA1 binds to EBV origin of replication (oriP) on eucaryotic expression vectors (Frappier and O'Donnell 1992).

Human umbilical vein endothelial cells (HUVECs) were obtained from either Promocell (Heidelberg, Germany) or Lonza (Basel, Switzerland).

## **6.4.2 General culture conditions**

Cell culture and experiments using cultured cells were performed under a laminar flow hood, applying sterile solutions and devices and using sterile technique. In general, media and solutions applied to the cells were pre-warmed to room temperature or to 37°C. Cells were cultured in cell culture plastic ware obtained from BD (Franklin Lakes, USA) in a cell culture incubator adjusted to 37°C and 5 % CO<sub>2</sub>. Media were supplemented with 100 U/mL penicillin (Biochrom, Berlin, Germany), 100 µg/mL streptomycin (Biochrom) and 0.05 mg/mL ascorbic acid (Sigma-Aldrich).

### **6.4.2.1 Culture of HEK293-EBNA cells**

HEK 293-EBNA were cultured on collagen I coated flasks in DMEM (Invitrogen) supplemented with 10 % FCS (PAA, Pasching, Austria).

### **6.4.2.2 Culture of HUVECs**

HUVECs were cultured according to the protocol from the supplier and using the growth media recommended by the supplier, either endothelial cell growth medium 2 (Promocell) or EGM<sup>®</sup>-2 BulletKit<sup>®</sup> (Lonza). These media are defined as they do not contain bovine brain extract, and the final serum concentration is 2 %. Cells were grown in culture flasks coated with either collagen I (BD, 50 µg/mL in 0.02 M acetic acid) or gelatin (Sigma Aldrich, 0.01% in water). At 70-90% confluency, cells were subcultured as recommended by the supplier. HUVECs were used for experiments between passages 5 and 7.

## **6.5 General protein biochemical methods**

### **6.5.1 Determination of protein concentration**

#### **6.5.1.1 Determination of protein concentration by spectrometry**

The concentration of a protein solution can be determined by its absorbance at 280 nm, but needs to be corrected by the extinction coefficient. The extinction coefficient is protein specific and was predicted based on the amino acid composition of the protein of interest at the ExPASy Proteomics Server (Swiss Institute of Bioinformatics, Lausanne, Switzerland), using the ProtParam tool. Concentrations of FNIII10-constructs were determined by this approach using a NanoDrop 1000 spectrometer. However, in proteins lacking tryptophan residues, this prediction

is very imprecise, hence other ways to determine protein concentrations are required, such as the bicinonchonic acid (BCA) assay or protein-specific enzyme-linked immunosorbent assays (ELISA).

#### **6.5.1.2 Determination of protein concentration by the BCA assay**

The BCA protein assay kit (Pierce, Thermo Fisher Scientific, Waltham, USA) is based on the reduction of  $\text{Cu}^{+2}$  to  $\text{Cu}^{+1}$  by proteins, and the colorimetric detection of  $\text{Cu}^{+1}$  by complexation with BCA. The absorbance of the complex at 562 nm is proportional to the protein concentration over a wide range of concentrations, and protein concentration is determined in comparison to a bovine serum albumin (BSA) standard curve. Protein concentrations of the VEGF-variants or of cell lysates were determined using the microplate procedure as described by the supplier.

#### **6.5.1.3 Determination of protein concentration by VEGF specific ELISA**

A VEGF-A sandwich ELISA, either from R&D (Minneapolis, USA, Quantikine Human VEGF immunoassay) or Peprotech (Hamburg, Germany, Human VEGF ELISA Development Kit), was used for the determination of concentrations of proteins purified from *E. coli* and for the investigation of the release kinetics of proteins from fibrin gels in comparison to a VEGF-standard curve following the manufacturer's manual.

### **6.5.2 Sodium dodecylsulfate polyacrylamide gel electrophoresis (SDS-PAGE)**

SDS-PAGE is a method to separate proteins according to their molecular weight in a polyacrylamide gel. SDS is negatively charged and binds to proteins in a constant ratio, so that the charge of a SDS-protein complex is proportional to its mass. Interaction with SDS denatures proteins and prevents their interaction. Subjected to an electric field, the negatively charged proteins migrate to the anode. During their migration in the gel, large proteins are retained stronger in the polyacrylamide gel than small ones and do not migrate as far. Proteins are first concentrated in a stacking gel with large pore sizes and then separated in a separating gel (Laemmli 1970). Gels for SDS-PAGE were purchased from Invitrogen (NuPAGE system), and NuPAGE<sup>®</sup> Novex<sup>®</sup> Bis-Tris precast gels were run using the XCell SureLock<sup>®</sup> Mini-Cell system in MES/SDS running buffer.

## Materials and methods

Alternatively, the gels were prepared manually and run with the mini PROTEAN II electrophoresis Cell system (Bio Rad) using Tris/glycine/SDS as running buffer. When preparing polyacrylamide gels, the separating gel (Table 6) was cast first, and overlaid with isopropanol to obtain a straight border. Once the separating gel had polymerized, the isopropanol was removed, the stacking gel (Table 6) was cast on top, and the comb creating the gel pockets for the samples was placed in the gel.

Prior to electrophoresis, loading buffer (Table 6) was added to the samples (either recombinant proteins produced or cell lysates), and the mixture was boiled for five minutes at 94°C. In reducing gels, the loading buffer contained  $\beta$ -mercaptoethanol as a reducing agent, thus allows visualization of VEGF monomers.

A protein marker consisting of stained proteins of known size purchased from Bio Rad or Fermentas (Thermo Fisher Scientific), was included on each gel to estimate the molecular weight of given bands.

<b>Stock solutions for SDS-PAGE gels</b>													
	<b>4x Tris-CI/SDS pH 8.8</b>		<b>4x Tris-CI/SDS pH 6.8</b>										
Tris Base	182 g		30.25 g		Acrylamide/Bis-acrylamide (Acr/Bis-Acr), 4 K 30% solution, 37.5:1 (Applichem)								
SDS	4 g		2 g		10% ammonium persulfate (APS) (Sigma)								
HCl	Adjust pH to 8.8		Adjust pH to 6.8		N,N,N,N-tetramethylethylenediamine (TEMED) (Fluka)								
H <sub>2</sub> O	To 1 L		To 500 mL										
<b>Composition of 3 polyacrylamide gels of 1mm thickness:</b>													
<b>Separating gel</b>		<b>Acrylamide concentration (%)</b>										<b>Stacking gel</b>	
<b>Stock solution (mL)</b>		<b>5</b>	<b>6</b>	<b>7</b>	<b>7.5</b>	<b>8</b>	<b>9</b>	<b>10</b>	<b>12</b>	<b>13</b>	<b>15</b>	<b>Stock solution</b>	<b>mL</b>
<b>Acr/Bis-Acr</b>		2.5	3	3.5	3.75	4	4.5	5	6	6.5	7.5	Acr/Bis-Acr	0.65
<b>Tris-CI/SDS pH 8.8</b>		3.75	3.75	3.75	3.75	3.75	3.75	3.75	3.75	3.75	3.75	Tris-CI/SDS pH 6.8	1.25
<b>H<sub>2</sub>O</b>		8.75	8.25	7.75	7.5	7.25	6.75	6.25	5.25	4.75	3.75	H <sub>2</sub> O	3.05
<b>10% APS</b>		0.05	0.05	0.05	0.05	0.05	0.05	0.05	0.05	0.05	0.05	10% APS	0.025
<b>TEMED</b>		0.01	0.01	0.01	0.01	0.01	0.01	0.01	0.01	0.01	0.01	TEMED	0.005
(Current Protocols in Cell Biology, 2007 37:6.1.1-6.1.38. John Wiley & Sons, Inc.)													
<b>Running buffers and loading buffer</b>													
<b>MES/SDS</b>		<b>Tris/glycine/SDS</b>				<b>4x Laemmli loading buffer</b>							
2.5 mM	MES	2.5 mM	Tris, pH 8.3			8 %	SDS						
2.5 mM	Tris base, pH 7.3	19.2 mM	glycine			0.2 M	Tris pH 6.8						
0.005 %	SDS	0.01%	SDS			40 %	Glycerol						
0.05 mM	EDTA					0.01 %	Bromphenol blue						
								(5%	β-mercaptoethanol)				

**Table 6: Solutions and buffers used for SDS-PAGE.**

### 6.5.3 Protein detection on SDS-PAGE gels

For the detection of proteins separated by SDS-PAGE, the gels were stained using the Coomassie blue based stain SimplyBlue™ SafeStain (Invitrogen) according to the manufacture's instructions. Alternatively, staining was performed using Coomassie blue. Gels were covered with the Coomassie blue solution (Table 7) and stained for 2 hours with shaking. Background staining was removed by washing with a destain solution (Table 7) for several hours or over night.

Coomassie blue		Destain solution	
0.01 %	Coomassie blue R-250	10 %	MeOH
50 %	MeOH	10 %	Acetic acid
5 %	Acetic acid		

Table 7: Composition of Coomassie blue and destain solution.

### 6.5.4 Immunoblotting of proteins

#### 6.5.4.1 Western blot transfer

Following SDS-PAGE, separated proteins were transferred onto polyvinylidene fluoride (PVDF)-membranes purchased from Bio Rad or Millipore (Billerica, USA) in order to make them accessible for immunodetection by antibodies. For the transfer, either XCell II™ Blot Module with Bicine/Bis Tris buffer supplemented with 10 % methanol (Invitrogen) or the mini TransBlot system (Bio Rad) with Tris/Glycine as transfer buffer containing 20 % methanol were used (Table 8).

The PVDF membrane was activated in methanol for one minute, and both the PVDF membrane and the gel were washed in the transfer buffer. As mentioned, proteins are charged negatively due to interaction with SDS and migrate toward the anode within an electric field. Thus, the orientation in the module was as follows:

kathode  
sponge  
watson filter paper  
SDS-polyacrylamide gel  
PVDF membrane  
watson filter paper  
sponge  
anode



The transfer was performed at 30 V for 75 minutes in the Invitrogen system, or at 80 V for 60 minutes in the Bio Rad system, respectively.

Transfer buffers			
Bicine/ Bis Tris		Tris/Glycine	
1.25 mM	Bicine	2.5 mM	Tris, pH 8.3
1.25 mM	Bis Tris, pH 7.2	19.2 mM	Glycine
0.05 mM	EDTA	20 %	Methanol
10 %	Methanol		

Table 8: Transfer buffers used for western blot transfers.

### 6.5.4.2 Immunodetection of proteins

Following the transfer to PVDF, unspecific binding sites on the membrane were blocked by incubation in 5 % non-fat milk (Bio Rad or Roth, Karlsruhe, Germany), 1 % BSA (Sigma or PAA) in TBS containing 0.1 % Tween-20 (TBS-T) for at least one hour with shaking. Specific proteins were detected using the primary antibodies given in Table 9.

Antigen	Host species	Supplier	Dilution	Diluent	Incubation time
VEGF A20	Rabbit (polyclonal)	Santa Cruz Biotechnology	1:2000	2.5 % milk	1 hr
VEGFR-2 phosphotyrosine 1175	Rabbit (monoclonal)	Cell signaling Technology	1:1000	5 % BSA	o/n
Flk-1 (A3)	Mouse (monoclonal)	Santa Cruz Biotechnology	1:500	5 % milk	1 hr
Phospho-p44/42 MAPK (Erk1/2)	Rabbit (monoclonal)	Cell Signaling Technology	1:1000	5 % BSA	o/n
β-actin	Mouse (monoclonal)	Santa Cruz Biotechnology	1:1000	5% milk	1 hr

Table 9: List of primary antibodies used for western blot experiments.

For detection of the primary antibodies, the membrane was washed 3x10 minutes in TBS-T, and then incubated with horse radish peroxidase (HRP)-coupled secondary antibodies diluted 1:1000 in 5 % milk for one hour. For detection of glutathione-S-transferase (GST)-tagged proteins, an antibody directly coupled to HRP is available, so no secondary antibody was required (Table 10). Following additional extensive washes, the membrane was incubated with an enhanced chemiluminescence (ECL) system containing luminol (PIERCE or PerkinElmer, Table 10). The HRP mediated oxidation of luminol generates a luminescence signal detected by imposing a Röntgen film on the membrane. The film was then developed using an AGFA (Mortsel, Belgium) developing machine.

HRP-coupled antibodies	Supplier	ECL used	Supplier
Goat anti mouse HRP	Dako	Western Lightning Plus, enhanced	PerkinElmer
Swine anti Rabbit HRP	Dako	chemiluminescence substrate	
Goat anti mouse HRP	Bio Rad	ECL Western Blotting Substrate	PIERCE
Goat anti rabbit HRP	Bio Rad		
Anti GST-HRP	GE Healthcare		

Table 10: Secondary antibodies and ECL solutions used.

## 6.6 Cloning and cloning strategy

Proteins to be expressed were composed from different protein domains and were cloned in subsequent steps into expression vectors by recombinant DNA techniques. The DNA encoding for functional domains of the fusion proteins was amplified by polymerase chain reaction (PCR). The PCR product and the vector into which the sequence is to be cloned were subsequently digested with two restriction endonucleases. Specific PCR primers defining the sequence to be amplified were designed and obtained from Microsynth (Balgach, Switzerland). The sequences of these primers and detailed cloning procedures are given in section 6.6.1.

Initially, the sequences encoding protein domains were cloned into the bacterial expression vector pGEX-4T-1. The sequence encoding for VEGFmut was amplified from pcDNA3.1, FNIII10 was amplified from pFH157, whereas sequences encoding for the transglutaminase substrate sequence TG, the plasmin sensitive site PL and for the linker were ordered as oligonucleotides from Microsynth.

### 6.6.1 DNA and amino acid sequences of protein domains used and cloning into the bacterial expression vector pGEX-4T-1

The protein domains cloned into pGEX-4T-1 in subsequent steps are shown in Figure 30, and were separated by different restriction sites.

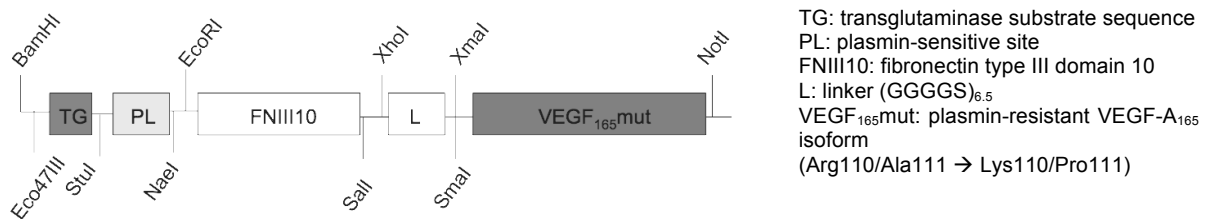


Figure 30: Cloning strategy employed and localization of restriction sites within the construct.

#### Sequence of VEGFmut with the mutated plasmin cleavage site shown in red

```
GCA CCC ATG GCA GAA GGA GGA GGG CAG AAT CAT CAC GAA GTG GTG AAG TTC ATG GAT GTC TAT CAG CGC AGC
TAC TGC CAT CCA ATC GAG ACC CTG GTG GAC ATC TTC CAG GAG TAC CCT GAT GAG ATC GAG TAC ATC TTC AAG
CCA TCC TGT GTG CCC CTG ATG CGA TGC GGG GGC TGC TGC AAT GAC GAG GGC CTG GAG TGT GTG CCC ACT GAG
GAG TCC AAC ATC ACC ATG CAG ATT ATG CGG ATC AAA CCT CAC CAA GGC CAG CAC ATA GGA GAG ATG AGC TTC
CTA CAG CAC AAC AAA TGT GAA TGC AGA CCA AAG AAA GAT AAG CCA AGA CAA GAA AAT CCC TGT GGG CCT TGC
TCA GAG CGG AGA AAG CAT TTG TTT GTA CAA GAT CCG CAG ACG TGT AAA TGT TCC TGC AAA AAC ACA GAC TCG
CGT TGC AAG GCG AGG CAG CTT GAG TTA AAC GAA CGT ACT TGC AGA TGT GAC AAG CCG AGG CGG TGA
```

```
A P M A E G G Q N H H E V V K F M D V Y Q R S Y C H P I E T L V D I F Q E Y P D E I E Y I F K P
S C V P L M R C G G C C N D E G L E C V P T E E S N I T M Q I M R I K P H Q G Q H I G E M S F L Q
H N K C E C R P K K D K P R Q E N P C G P C S E R R K H L F V Q D P Q T C K C S C K N T D S R C K
A R Q L E L N E R T C R C D K P R R
```

**Sequence of FNIII10 with the RGD site shown in red**

GTT CCG AGG GAC CTG GAA GTT GTT GCT GCG ACC CCC ACC AGC CTA CTG ATC AGC TGG GAT GCT CCT GCT GTC  
 ACA GTG AGA TAT TAC AGG ATC ACT TAC GGA GAA ACA GGA GAA AAT AGC CCT GTC CAG GAG TTC ACT GTG CCT  
 GGG AGC AAG TCT ACA GCT ACC ATC AGC GGC CTT AAA CCT GGA GTT GAT TAT ACC ATC ACT GTG TAT GCT GTC  
 ACT GGC **CGT GGA GAC** AGC CCC GCA AGC AGC AAG CCA ATT TCC ATT AAT TAC CGA ACA GAA

V P R D L E V V A A T P T S L L I S W D A P A V T V R Y Y R I T Y G E T G G N S P V Q E F T V P G  
 S K S T A T I S G L K P G V D Y T I T V Y A V T G **R G D** S P A S S K P I S I N Y R T E

**Sequence of the oligonucleotide encoding for TG-PL with TG shown in italic and PL underlined**

TCG GTC GGA TCC AGC GCT AAC CAG GAG CAG GTG AGC CCC CTG AGG CCT CTG ATC AAG ATG AAG CCC GCC GGC  
 GAA TTC TTT ATG

S V G S S A N Q E Q V S P L R P L I K M K P A G E F L M

**Sequence of the oligonucleotide encoding for the linker**

T ATA CTC GAG GGT GGC GGA GGG TCT GGA GGC GGT GGG TCC GGC GGT GGG GGA TCA GGG GGA GGC GGT TCG GGA  
 GGT GGG GGC TCG GGC GGT GGG GGA AGT GGT GGA GGT CCC GGG TTT A

G G G G S G G G G S G G G G S G G G G S G G G G S G G G G S G G G S G G G

**Sequence of TG-PL-FLV with the distinct functional domains highlighted as follows:**

TG PL FNIII10 linker VEGFmut  
 AAC CAG GAG CAG GTG AGC CCC CTG AGG CCT CTG ATC AAG ATG AAG CCC GCC GGC GAA TTC GTT CCG AGG GAC  
 CTG GAA GTT GTT GCT GCG ACC CCC ACC AGC CTA CTG ATC AGC TGG GAT GCT CCT GCT GTC ACA GTG AGA TAT  
 TAC AGG ATC ACT TAC GGA GAA ACA GGA GGA AAT AGC CCT GTC CAG GAG TTC ACT GTG CCT GGG AGC AAG TCT  
 ACA GCT ACC ATC AGC GGC CTT AAA CCT GGA GTT GAT TAT ACC ATC ACT GTG TAT GCT GTC ACT GGC CGT GGA  
 GAC AGC CCC GCA AGC AGC AAG CCA ATT TCC ATT AAT TAC CGA ACA GAA GTC GAC CTC GAG GGT GGC GGA GGG  
 TCT GGA GGC GGT GGG TCC GGC GGT GGG GGA TCA GGG GGA GGC GGT TCG GGA GGT GGG GGC TCG GGC GGT GGG  
 GGA AGT GGT GGA GGT CCC GGG GCA CCC ATG GCA GAA GGA GGA GGG CAG AAT CAT CAC GAA GTG GTG AAG TTC  
 ATG GAT GTC TAT CAG CGC AGC TAC TGC CAT CCA ATC GAG ACC CTG GTG GAC ATC TTC CAG GAG TAC CCT GAT  
 GAG ATC GAG TAC ATC TTC AAG CCA TCC TGT GTG CCC CTG ATG CGA TGC GGG GGC TGC TGC AAT GAC GAG GGC  
 CTG GAG TGT GTG CCC ACT GAG GAG TCC AAC ATC ACC ATG CAG ATT ATG CGG ATC AAA CCT CAC CAA GGC CAG  
 CAC ATA GGA GAG ATG AGC TTC CTA GAG CAC AAC AAA TGT GAA TGC AGA CCA AAG AAA GAT AAG CCA AGA CAA  
 GAA AAT CCC TGT GGG CCT TGC TCA GAG CGG AGA AAG CAT TTG TTT GTA CAA GAT CCG CAG ACG TGT AAA TGT  
 TCC TGC AAA AAC ACA GAC TCG CGT TGC AAG GCG AGG CAG CTT GAG TTA AAC GAA CGT ACT TGC AGA TGT GAC  
 AAG CCG AGG CGG TGA

N Q E Q V S P L R P L I K M K P A G E F V P R D L E V V A A T P T S L L I S W D A P A V T V R Y Y  
 R I T Y G E T G G N S P V Q E F T V P G S K S T A T I S G L K P G V D Y T I T V Y A V T G R G D S  
 P A S S K P I S I N Y R T E V D L E G G G G S G G G S G G G S G G G S G G G S G G G S G G G S G  
 G P G A P M A E G G G Q N H H E V V K F M D V Y Q R S Y C H P I E T L V D I F Q E Y P D E I E Y  
 I F K P S C V P L M R C G G C C N D E G L E C V P T E E S N I T M Q I M R I K P H Q G Q H I G E M  
 S F L Q H N K C E C R P K K D K P R Q E N P C G P C S E R R K H L F V Q D P Q T C K C S C K N T D  
 S R C K A R Q L E L N E R T C R C D K P R R

**Cloning into pGEX-4T-1**

1. Amplification of the sequence encoding for VEGFmut from from pcDNA3.1 using forward primer AAT GTC GAC TC GAG CCC GGG GCA CCC ATG GCA GAA GGA GGA GG and reverse primer TAT TGC GGC CGC TCA CCG CCT CGG CTT GTC ACA TCT GC and cloning into pGEX-4T-1 as SalI/NotI digest gives rise to pGEX-4T-1-VEGFmut.
2. Amplification of the sequence encoding for FNIII10 from pFH157 using forward primer CGC GGT GAA TTC GTT CCG AGG GAC CTG GAA GTT G and reverse primer CGC GCC GTC GAC TTC TGT TCG GTA ATT AAT GGG C, and cloning into pGEX-4T1 as EcoRI/SalI digest gives rise to pGEX-4T-1-FNIII10.
3. Amplification of the ordered oligonucleotide encoding for the TG-PL peptide using forward primer TCG GTC GGA TCC AGC GCT AAC and reverse primer CAA GAA TTC GCC GGC GGG CTT. The sequence was cloned into pGEX-4T-1 as BamHI/EcoRI digest, which results in pGEX-4T-1-TG-PL.

4. Amplification of the sequence encoding for FNIII10 from pFH157 using forward primer CGC GGT *GAA TTC* GTT CCG AGG GAC CTG GAA GTT G and reverse primer CGC GCC *GTC GAC* TTC TGT TCG GTA ATT AAT GGG C, and cloning into pGEX-4T-1-TG-PL as *EcoRI/SalI* digest gives rise to pGEX-4T-1-TG-PL-FNIII10.
5. Digest of pGEX-4T-1-TG-PL-FNIII10 with *StuI* and *NaeI* gives rise to pGEX-4T-1-TG-FNIII10.
6. Amplification of the sequence encoding for VEGFmut from pcDNA3.1 using the forward primer AAT *GTC GAC* CTC GAG CCC GGG GCA CCC ATG GCA GAA GGA GGA GG and the reverse primer *tat TGC GGC CGC* TCA CCG CCT CGG CTT GTC ACA TCT GC and cloning into pGEX-4T-1-TG-PL-FNIII10 as *SalI/NotI* digest gives rise to pGEX-4T-1-TG-PL-FNIII10-VEGFmut.
7. The linker was ordered as oligonucleotide T ATA *CTC GAG* GGT GGC GGA GGG TCT GGA GGC GGT GGG TCC GGC GGT GGG GGA TCA GGG GGA GGC GGT TCG GGA GGT GGG GGC TCG GGC GGT GGG GGA AGT GGT GGA GGT CCC GGG TTT A, and amplified using forward primer ACT TCT ATA CTC GAG GGT GGC and reverse primer AAC TGT AAA *CCC GGG* ACC TCC A. Subsequent cloning as *XhoI/XmaI* digest into pGEX-4T1-TG-PL-FNIII10-VEGFmut gives rise to pGEX-4T-1-TG-PL-FNIII10-linker-VEGFmut.
8. Digest of pGEX-4T-1-TG-PL-FNIII10-linker-VEGFmut with *NaeI* and *StuI* gives rise to pGEX-4T-1-TG-FNIII10-linker-VEGFmut.
9. Digest of pGEX-4T-1-TG-PL-FNIII10-linker-VEGFmut with *Eco47III* and *NaeI* gives rise to pGEX-4T-1-FNIII10-Linker-VEGFmut.
10. Digest of pGEX-TG-PL-FNIII10-VEGF with *NaeI* and *SmaI* gives rise to pGEX-4T-1-TG-PL-VEGFmut
11. Digest of pGEX-4T-1-TG-PL-FNIII10-VEGFmut with *StuI* and *SmaI* gives rise to pGEX-4T-1-TG-VEGFmut.

### 6.6.2 Protein expression vectors used for cloning

pGEX-4T-1 is a bacterial expression vector obtained from GE Healthcare. Target protein over-expression is controlled by the strong tac promoter, inducible by IPTG. The vector further encodes for an N-terminal GST tag separated from the target protein by a thrombin cleavage site (Figure 31 A).

pRSET is a bacterial expression vector from Novagen (Merck, Darmstadt, Germany) and contains a gene encoding for resistance to ampicillin. Target genes are expressed under the control of the strong T7 bacteriophage promoter. The vector used for protein expression in *E. coli*, a kind gift from professor Dr. Andreas Zisch, University Hospital Zurich, was a modified

## Materials and methods

vector, from which the multiple cloning site along with the his-tag was removed, and contained VEGF<sub>165</sub>wt as an insert (Figure 31 B).

pCEP-V97 is an episomal eucaryotic expression vector based on the vector pCEP4 from Invitrogen and was a kind gift from professor Dr. Manuel Koch, Institut für Biochemie II, medizinische Fakultät, Universität zu Köln. The vector carries a cytomegalovirus promoter and the Epstein-Barr virus replication origin for high level protein expression and high-copy replication. For selection in bacteria, an ampicillin-resistance is encoded. pCEP-V97 differs from pCEP4 in the organization of its multiple cloning site, and it further encodes for puromycin resistance, a sorting signal targeting the recombinant protein for secretion, and a C-terminal poly-histidine tag that can be cleaved off by factor X (Figure 31 C).

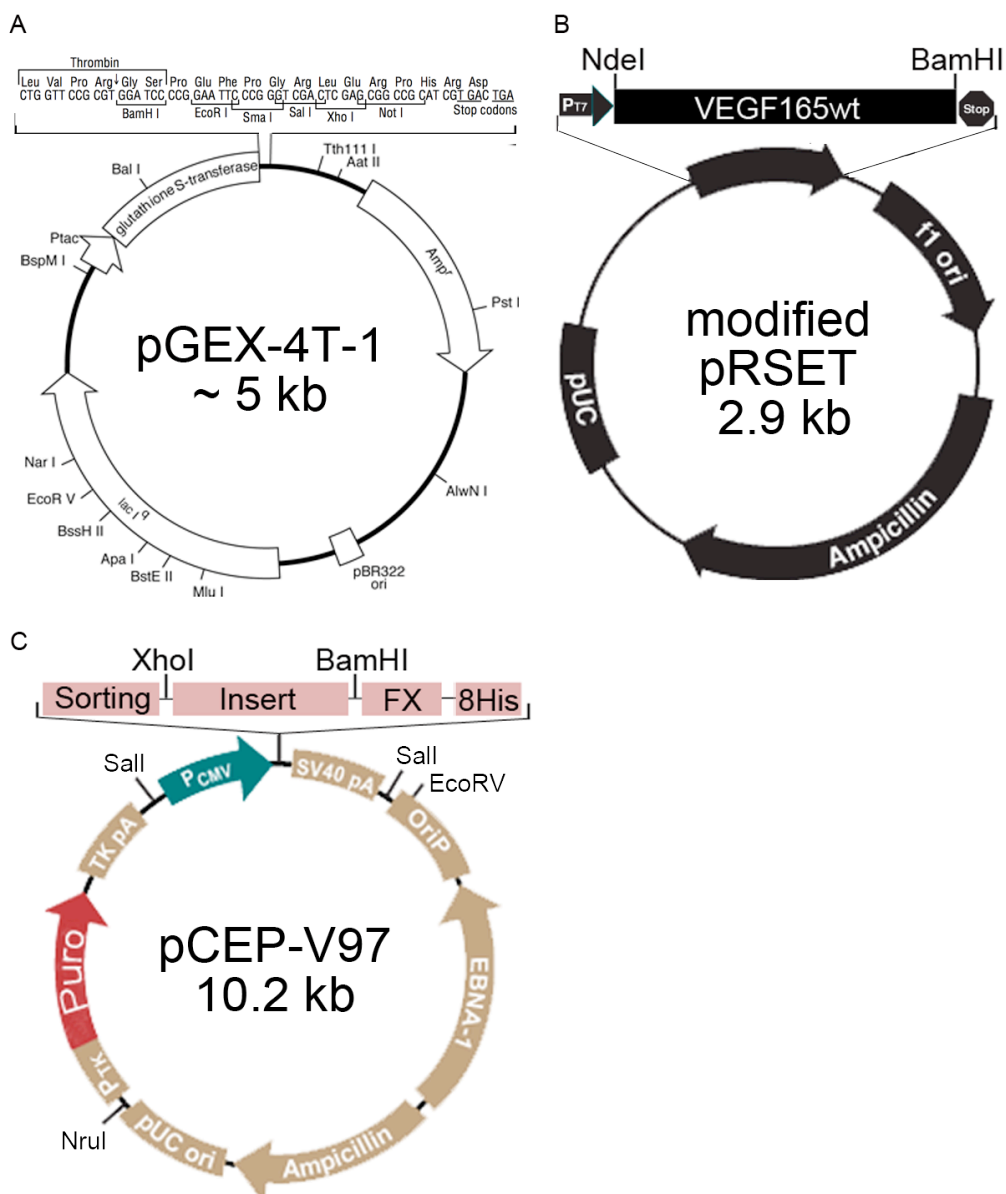


**Figure 31: Vector maps of vectors used.** (A) pGEX-4T-1 and (B) pRSET are bacterial expression vectors, and (C) pCEP-V97 is an eucaryotic expression vector. See text for details.

### 6.6.3 Polymerase chain reaction (PCR)

The PCR reaction is divided into three distinct steps, namely denaturation of the DNA double-strand, annealing of the primers, and extension, that usually are repeated for a total of 35 cycles. Additional steps are included to denature the double-strand prior to the first cycle and for extension of the construct. DNA is denatured at 94°C, and extension using Pfx50 (Invitrogen), a DNA-polymerase with 5'→3' proofreading activity, is performed at 68°C. The annealing temperature is primer specific and was calculated using the program OligoCalculator (University of Pittsburgh), while the extension time depends on the length of the expected PCR product. PCR-programs are summarized in Table 11. The templates were amplified in a standard PCR reaction mixture composed of 5 μM of each primer, 4 ng/μL of the template and 5 U Pfx in 1x polymerase buffer.

PCR-programs used for the amplification of the indicated functional domains:					
<u>TG-PL</u>			<u>FNIII10</u>		
time	temp.		time	temp.	
1'	94°C		1'	94°C	
15"	94°C	35 cycles	15"	94°C	35 cycles
30"	60°C		30"	60°C	
30"	68°C		1'	68°C	
5'	68°C		5'	68°C	
			<u>TG-PL-FLV</u>		
			time	temp.	
			1'	94°C	
			15"	94°C	35 cycles
			30"	60°C	
			1'	68°C	
			5'	68°C	
<u>VEGF</u>			<u>linker</u>		
time	temp.		time	temp.	
1'	94°C		1'	94°C	
15"	94°C	35 cycles	15"	94°C	35 cycles
30"	56°C		30"	58°C	
1'	68°C		30"	68°C	
5'	68°C		5'	68°C	

Table 11: PCR-programs used.

### 6.6.4 DNA agarose gel electrophoresis

To evaluate proper PCR amplification of the inserts or successful digest of the host vector, DNA fragments were routinely investigated by DNA agarose gel electrophoresis. Gels were formulated with 0.5 or 2 % (w/v) agarose in TAE (for digested vectors or PCR-products, respectively). Agarose was dissolved in the buffer by repeated boiling, the solution was chilled and supplemented with GelRed (1:10000, Biotium) or ethidium bromide (0.5 μg/ml) for the visualization of DNA under UV-light. Electrophoresis was performed at 80 V.

Bands of the PCR product or the digested vector corresponding to the expected size were cut out of the gel using a scalpel and purified using the Wizard SV Gel and PCR Clean-up Kit by Promega (Madison, USA) or the E.Z.N.A. Gel Purification Kit by Omega bio-tek (Norcross, USA).

### 6.6.5 DNA restriction digest and 5' dephosphorylation of the vector

The PCR product and the vector were digested for 8 hours using the appropriate enzymes obtained from Promega, Invitrogen or New England Biolabs (Ipswich, USA, Table 12), and conditions as recommended by the supplier. A standard digest comprised 10 µg of vector and 3 µL of the enzyme, or all obtained PCR-product and 0.3 µL of the enzyme in a total volume of 20 µL.

Restriction endonucleases			
BamHI (Promega)	NdeI (New England Biolabs)	Sall (New England Biolabs)	XhoI (New England Biolabs)
Eco47III (Promega)	NheI (New England Biolabs)	SmaI (Promega)	XmaI (New England Biolabs)
NaeI (New England Biolabs)	Not I (New England Biolabs)	StuI (Invitrogen)	

**Table 12: Restriction endonucleases used for cloning procedures.**

After each digest, the restriction endonuclease was heat-inactivated for 15 minutes at 65°C. The digested vector was then purified by running on an agarose gel, and the digested PCR-product was directly purified using Wizard SV Gel and PCR Clean-up Kit (Promega). The second digest was performed in the same way.

The double-digested vector was dephosphorylated on the 5' end if enzymes creating cohesive ends were used for the digest in order to prevent auto-ligation of the vector by addition of 5 µL shrimp alkaline phosphatase (Promega) for 30 minutes at 37°C. Both vector and insert were purified one last time.

### 6.6.6 DNA ligation

Digested vector and inserts were ligated by T4 ligase (New England Biolabs) in three different molar ratios (1:1, 1:3, 1:6) using 100 ng of vector and 1 µL of the enzyme in a total volume of 20 µL per reaction. The ligation was allowed to take place for at least 16 hours at 4°C.

Competent *E. coli* were transfected with 10 µL of the ligation assay and plated onto LB-agar plates containing selection antibiotics. From the colonies formed, small liquid cultures were inoculated, from which the plasmid DNA was isolated using the E.Z.N.A. Plasmid Miniprep Kit I (Omega bio-tek). Presence of an insert was first verified by PCR followed by DNA agarose gel electrophoresis, and the correct DNA sequence was validated by sequencing by either FASTERIS (Geneva, Switzerland) or SEQLAB (Göttingen, Germany).

### 6.6.7 Subcloning

Due to problems with purification of the VEGF-containing constructs as GST-fusion proteins, constructs containing VEGF were subcloned into a modified pRSET vector for the production from inclusion bodies and subsequent purification by heparin affinity. As the obtained batches were of insufficient purity for the bi-functional constructs, constructs FNIII10, TG-FNIII10, VEGFmut, TG-VEGFmut, FLV and TG-FLV were then subcloned into pCEP-V97 comprising a C-terminal His-tag for eucaryotic expression.

For subcloning of VEGF-containing constructs into the modified pRSET vector, the vector was *NdeI/BamHI* digested in order to remove the insert VEGF<sub>165</sub>wt. Other, VEGFmut containing inserts were inserted as *NdeI/BamHI* digest. For amplification of VEGFmut, the forward primer G GAA TTC CAT ATG GCA CCC ATG GCA GAA GGA was used, for constructs containing the TG-sequence, the primer G GAA TTC CAT ATG AAC CAG GAG CAG GTG AGC was used and for sequences starting with the FNIII10 sequence, G GAA TTC CAT ATG AAC CAG GAG CAG GTG AGC was used. The reverse primer was always CGC *GGA TCC* TCA CCG CCT CGG CTT GTC ACA TCT.

The constructs FNIII10, TG-FNIII10, VEGFmut, TG-VEGFmut, FLV and TG-FLV were subcloned into pCEP-V97 as *BamHI/NheI* digests, and amplified using a combination of the following primers: FNIII10 forward C GGT GCT AGC A GTT CCG AGG GAC CTG GAA GTT GTT G; FNIII10 reverse CGC GCC *GGA TCC* TTC TGT TCG GTA ATT AAT GGA AAT TG; VEGFmut reverse GA TAT T *GGA TCC* CCG CCT CGG CTT GTC ACA TCT GCA AG; VEGF forward: C GGT GCT AGC A GCA CCC ATG GCA GAA GGA GGA GGG CAG; TG-sequence forward GT ATG CTA GCA AAC CAG GAG CAG GTG AGC CCC CTG.

## 6.7 Recombinant protein expression in bacteria

Generally, protein expression was induced with isopropyl  $\beta$ -D-1-thiogalactopyranoside (IPTG). IPTG is a mimetic of allolactose not metabolizable by bacteria. IPTG binds to and inhibits the lac-repressor, thus allowing for the expression of target genes under the lac promoter. Protein expression from the expression vector pGEX-4T-1 is directly induced by IPTG in BL21. In BL21(DE3)pLysS cells, IPTG by contrast induces the expression of the T7 RNA polymerase under the control of a lac promoter, and T7 polymerase in turn binds to the T7 promoter on pRSET vector constructs, leading to the expression of the target gene. Additionally, in the latter system, the leaky expression of the target gene is reduced by the expression of pLysS, that



encodes for T7 lysozyme, an inhibitor of T7 polymerase (Davanloo et al. 1984; Moffatt and Studier 1987; Studier and Moffatt 1986). In general, after transformation of bacteria and selection of positive clones, a good producer of the recombinant proteins was identified by induction of protein expression and SDS-PAGE followed by protein staining on the lysate.

### 6.7.1 Expression and purification of GST-tagged proteins

BL21 were transfected with pGEX-4T-1 vectors encoding for the proteins to be produced, and GST-tagged proteins were purified from the bacterial cytosol. For large-scale production, a 5 mL liquid culture was inoculated in 2xYT containing ampicillin and grown overnight. 1L of 2xYT with ampicillin was inoculated with this culture and grown at 37°C with shaking until the OD<sub>600</sub> was about 0.6. At this density, protein expression was induced by addition of 0.6 mM IPTG, and bacteria were grown for 6 hrs at 22°C. The bacteria were collected by centrifugation and lysed by addition of 45 ml phosphate buffered saline (PBS) containing protease inhibitors, 50 mg lysozyme (Merck), and sonication. 500 U of DNase (Sigma Aldrich) and 1% Triton-X-100 were added, and lysis was performed on a spinning wheel at 4°C for 30 min. The lysate was cleared by centrifugation and filtration, and 0.1% NaN<sub>3</sub> was added. The GST-fusion proteins were purified using an ÄTKA-FPLC system and a GSH-column. Elution from the column was accomplished by addition of 50 mM Tris-HCl, 10 mM reduced GSH, pH 8. The protein was subsequently digested by 20 U of thrombin (Sigma Aldrich) per mg of recombinant protein while removing GSH from the sample by dialysis against PBS. A second step of purification was performed using a GST column and a benzamidine column in order to remove GST and thrombin from the sample (Table 13). The protein was concentrated by membrane filtration (Amicon ultra filter systems by Millipore), and the buffer was exchanged to tris buffered saline (TBS). The protein concentration was then determined by absorbance measurement at 280 nm using a NanoDrop1000 spectrometer and corrected by division by the extinction coefficient. Purity of the protein solution was verified by SDS-PAGE and protein staining, and the protein's identity was confirmed by LC-MS/MS and MALDI-TOF.

Buffers and solutions	Columns	Enzymes
PBS containing complete protease inhibitor (Roche)	GSTPrep FF 16/10 20 mL, GE Healthcare	Lysozyme, VWR
Running and wash buffer: PBS	HiTrap Benzamidine FF, 1 mL, GE Healthcare	DNase, Merck
Elution buffer: 50 mM Tris-HCl, 10 mM reduced GSH, pH 8-8.6		Bovine thrombin, Sigma Aldrich
TBS: 135 mM NaCl, 18 mM Tris-HCl, pH 7.4		

Table 13: Buffers and columns used for the purification of GST-tagged proteins.

### **6.7.2 Thrombin processing of GST-VEGFmut and GST-TG-PL-FLV**

To investigate whether the GST-tag could be removed from GST-VEGFmut and GST-TG-PL-FLV by thrombin mediated cleavage, thrombin digestion of these proteins was performed using 1 U of thrombin per mg of recombinant protein and monitored over time by western blotting using a primary antibody directed against VEGF-A.

### **6.7.3 Purification of recombinant proteins from bacterial inclusion bodies**

For the purification of VEGF-isoforms from inclusion bodies, sequences encoding for these isoforms were cloned into a modified pRSET. BL21(DE3)pLys were transfected with pRSET vectors containing VEGF isoforms. A 3 ml culture of a good producer in LB containing ampicillin and chloramphenicol was grown. 1 L of LB with ampicillin was inoculated with this culture and grown at 37°C until an OD<sub>600</sub> of 0.8. Protein expression was induced by addition of 1 mM IPTG and bacteria were grown over night.

The culture was harvested by centrifugation, dissolved in lysis buffer completed with 10 mg lysozyme and lysed for 20 minutes at room temperature. 50000 U of DNase were added to the lysate and incubated overnight at 4°C. The inclusion bodies containing VEGF-A variants were collected by centrifugation and solubilized in extraction buffer containing 8 M urea. Proteins were refolded by subsequential dialysis against decreasing concentrations of urea and dimerized using a redox-system consisting of reduced and oxidized GSH. After removal of GSH from the sample by dialysis, the pH of the sample was set to 3.5. At this pH, many proteins precipitate, whereas VEGF-A remains soluble (Fiebich et al. 1993). The precipitate was removed by centrifugation. VEGF constructs were purified by heparin affinity chromatography after adjusting the pH of the sample to 6.5 and the NaCl concentration to 0.4 M, Bound proteins were eluted in one step with 1 M NaCl, 20 mM Tris pH 7.4 (Table 14). Obtained fractions were investigated by SDS-PAGE followed by protein staining, and similar fractions were pooled, aliquoted, and stored at -80°C.

Subsequent investigations to confirm the identity of the obtained proteins included western blotting, LC-MS/MS and MALDI-TOF. Protein concentration was determined by a BCA-assay using a BSA standard curve (PIERCE, Thermo Scientific) and working concentrations were determined by ELISA (Quantikine ELISA, R&D Systems) compared to a VEGF-A standard curve.

Buffers required		Column used
Lysis buffer	50 mM Tris pH 7.5, 150 mM NaCl, 5 mM EDTA	HiTrap™ Heparin, 5 mL, GE Healthcare
Column equilibration	50 mM Tris, 150 mM NaCl	
Wash buffer	4 M urea, 20 mM Tris pH 8, 150 mM NaCl, 2 mM EDTA	
Extraction buffer	8 M urea, 20 mM Tris pH 8, 150 mM NaCl, 10 mM DDT	
Folding buffers	6 M urea, 50 mM Tris pH 7.5, 150 mM NaCl, 2 mM EDTA	
	4 M urea, 50 mM Tris pH 7.5, 150 mM NaCl, 2 mM EDTA	
	2 M urea, 50 mM Tris pH 7.5, 150 mM NaCl, 2 mM EDTA	
Dimerization buffer:	2 M urea, 50 mM Tris pH 7.5, 150 mM NaCl, 2 mM EDTA, 0.5 mM oxidized GSH, 5 mM reduced GSH	
Elution buffer	50 mM Tris, 1 M NaCl	

**Table 14: Buffers and column used for the purification of VEGF-proteins from bacterial inclusion bodies.**

### 6.7.4 Endotoxin test

Endotoxins, also called lipopolysaccharides (LPS), are components of the outer membrane of Gram-negative bacteria. They are frequently released during normal cell division but particularly during lysis of bacteria. Endotoxins are recognized by the immune system, and hence have very strong biological effects when they enter the blood stream of humans or laboratory animals, including fever and endotoxin shock (Gorbet and Sefton 2005). As these side effects can severely impair the outcome of *in vivo* experiments, it is essential to deliver protein solutions devoid of endotoxins. Endotoxin testing of recombinant proteins was performed in the laboratories of Bayer Schering Pharma with kind support by Dr. Gabriella Bald, Dr. Felix Oehme and Dr. Burkhard Fugmann using the Limulus Amebocyte Lysate (LAL) test. This test represents the standard method for endotoxin detection and quantification in the pharmaceutical industry and is based on the property of the blood cell lysate of the horseshoe crab *Limulus polyphemus* to gel in the presence of endotoxin.

### 6.8 Expression of recombinant proteins in HEK293-EBNA cells

For protein expression in HEK293-EBNA cells, the constructs FNIII10, TG-FNIII10, VEGFmut, TG-VEGFmut, FLV and TG-FLV were subcloned into the eucaryotic expression vector pCEP-V97, which encodes for a signal sequence targeting the recombinant protein for secretion and a C-terminal poly-histidine tag. Recombinant protein expression is under the control of EBV origin of replication. HEK cells were transfected using the Fugene HD transfection reagent (Roche) according to the supplier's instructions. Transfectants were selected by the puromycin-resistance encoded on the plasmid and propagated after secretion of the recombinant proteins to the cell supernatant was confirmed by western blot analysis. Cells were seeded into collagen-

coated triple flasks and serum deprived. Conditioned medium was collected every third day and stored at  $-20^{\circ}\text{C}$  until purification.

For purification, a gelatin sepharose column was used as a pre-column, and the his-tagged proteins were purified using a Ni Sepharose™ (GE Healthcare) packed column. Prior to purification, 1 mM PMSF, 0.07 % Tween-20, and 10 %  $\text{Na}_2\text{HPO}_4$  were added to the supernatant. The proteins were eluted from the column by applying increasing concentrations of imidazol in 20 mM Tris (Table 15), and the fractions were investigated by SDS-PAGE and Coomassie blue staining. Subsequently, fractions containing the recombinant proteins were pooled and dialyzed against TBS prior to aliquoting and storage at  $-80^{\circ}\text{C}$ .

Buffers for protein purification from HEK cell supernatant		Column beds (GE Healthcare)
wash buffer:	20 mM Tris pH 8, 150 mM NaCl	Gelatin Sepharose™ 4B
elution buffers:	5-250 mM Imidazol, 20 mM Tris pH 8, 150 mM NaCl	Ni Sepharose™ 6 Fast Flow

**Table 15: Buffers and column beds used for the purification of his-tagged proteins from conditioned cell supernatants.**

## 6.9 Functional characterization of recombinant proteins

### 6.9.1 Cell attachment to TG-FNIII10 in presence and absence of integrin-specific inhibitors

The protocol applied to assess cell attachment was modified from a basic protocol given in Current Protocols in Cell Biology (1998, 9.1.1-9.1.11, John Wiley & Sons, Inc.).

Wells of a 96 well ELISA plate were coated for one hour at room temperature with 0.001 to 25  $\mu\text{M}$  TG-FNIII10 and subsequently blocked with 0.2% heat-inactivated BSA in PBS for one hour at  $37^{\circ}\text{C}$ . After washing the wells with HBSS,  $3.5 \times 10^4$  HUVECs in 100  $\mu\text{L}$  M-199 were plated per well and allowed to attach for 45 minutes. As a positive control, cells were plated on wells coated with 0.05  $\mu\text{g}/\mu\text{L}$  full-length fibronectin (final coating per well: 5  $\mu\text{g}$ ), which served to define 100 % cell attachment. Non-adherent and loosely attached cells were removed by washing, and cells were then fixed with 5 % glutaraldehyde for 20 minutes. The cells were washed with water and stained with crystal violet for one hour (Table 16). Crystal violet binds to DNA and thereby allows quantification of cells. Following extensive washing, the dye was solubilized with 10 % acetic acid, and absorbance was measured at 570 nm. Each assay was performed in triplicate, and results were obtained in three independent assays.

To test whether integrin  $\alpha v \beta 3$  was involved in the observed attachment, the cell attachment assay was performed using integrin function blocking antibodies. Wells of a 96-well ELISA

plate were coated with 25  $\mu$ M TG-FNIII10 or 5  $\mu$ g fibronectin per well and subsequently blocked with 0.2 % BSA in PBS for one hour at 37°C. A cell suspension containing 35x10<sup>4</sup> cells per ml was prepared and incubated with either 5  $\mu$ g/mL function blocking anti-integrin  $\alpha$ v $\beta$ 3 or anti-integrin  $\alpha$ 5 (Table 16) or without inhibitor for 20 minutes at 37°C. 100  $\mu$ L of the cell suspension were plated per well, and cells were allowed to attach for 45 minutes. The readout was then performed as described above.

Buffers and media		Antibodies		Proteins
M199	Invitrogen	anti-integrin $\alpha$ v $\beta$ 3	Chemicon, MAB1976Z	Fibronectin
HBSS with calcium and magnesium	Invitrogen	anti-integrin $\alpha$ 5	Abcam, JBS5	(Millipore)
PBS	Amimed			
0.1 % (w/v) crystal violet in 200 mM MES				

**Table 16: Buffers, media and antibodies used for cell attachment studies.**

### 6.9.2 Cell spreading assay

To test cell spreading to the recombinant proteins produced in HEK293-EBNA, the chambers of a 8-chamber slide (Lab-Tek™ Chamber Slide™, Nunc, Thermo Scientific) were coated overnight at 4°C with 0.1 % poly-L-lysine, 0.4  $\mu$ M FNIII10, 0.2  $\mu$ M FLV or 0.2  $\mu$ M VEGFmut. FLV was plated at a lower molarity, as the molecule comprises two FNIII10 sites. Unspecific binding sites were blocked with heat-inactivated BSA, and 80000 serum-starved HUVECs were plated per condition in M199 supplemented with 0.1 % BSA. Cells were allowed to attach for 2 hours, washed once with TBS and fixed in 3 % PFA for 15 minutes. The cells were permeabilized with 0.2 % of Triton-X 100 in PBS for 10 minutes, and unspecific binding sites were blocked for 30 minutes with 10 % normal goat serum in PBS. The primary antibody directed against vinculin was diluted 1:500 in 1% BSA and incubated for 1 hour at room temperature. Following several rinses with PBS, the secondary antibody in combination with phalloidin and 1  $\mu$ g/mL 4',6-diamidino-2-phenylindole (DAPI) was applied to the cells for one hour. Antibodies used are summarized in Table 17. Cells were mounted in evanol.

Antibodies and dyes		
Vinculin MAB 3574	1:500	Chemicon
Alexa 488 goat anti mouse IgG1	1:500	Invitrogen
Alexa Fluor 594 phalloidin	1:100	Invitrogen

**Table 17 : Antibodies used for vinculin and actin co-staining.**

### 6.9.3 Investigation of VEGFR-2 activation and downstream signaling by western blot

The activation of VEGFR-2 in response to VEGF-containing constructs was determined by western blot using a phospho-specific primary antibody recognizing phosphorylation of tyrosine 1175 on VEGFR-2. Furthermore, phosphorylation of downstream signaling target Erk 1/2 was investigated using the antibodies specified in table 9. HUVECs were grown to confluence in 6-well plates and starved for 4 hours with M199 medium containing 0.1 % BSA. Then, they were stimulated with 50 ng/mL effective VEGF dose in M199 medium for 5 minutes at 37°C. After washing in M199 medium, cells were lysed on ice in Laemmli loading buffer (see Table 6) supplemented with  $\beta$ -mercaptoethanol, sodium orthovanadate, and protease inhibitors (Sigma Aldrich). The lysate was sonicated and boiled, and samples were subjected to SDS-PAGE.

Alternatively, lysis was performed in RIPA buffer (Table 19) supplemented with protease inhibitors (Sigma) and phosphatase inhibitors (PhosStop, Roche) according to the manufacturer's recommendations. Protein concentration was determined by BCA assay, and equal amounts of protein were loaded on gels and separated by electrophoresis.

After detection of the phosphorylated proteins, the blot was stripped and re-probed with a pan specific VEGFR-2 antibody (Flk-1 sc-6251, Santa Cruz) as loading control. Alternatively, equal loading was verified by detection of  $\beta$ -actin.

RIPA buffer		Stripping buffer	
50 mM	Tris-HCl, pH 7.4	0.2 M	Glycine
1%	NP-40	0.1 %	SDS
0.25%	Sodium-deoxycholate	1 %	Tween-20
150 mM	NaCl	pH 2.2	
1 mM	EDTA		

Table 19: Buffers used for the determination of protein phosphorylation.

### 6.9.4 Determination of VEGFR-2 phosphorylation by ELISA

During western blotting, one single phosphotyrosine on VEGFR-2 was probed. In order to detect overall VEGFR-2 phosphorylation, an ELISA was performed, during which a ELISA plate is coated with a VEGFR-2 specific capture antibody, and the phosphorylated tyrosines are detected by an HRP-coupled secondary tyrosine-specific antibody (Human Phospho-VEGF R2/KDR DuoSet IC, R&D Systems). HUVECs in passage 6 were cultured in T25 flasks and lysed in 500  $\mu$ L of lysis buffer. Following a brief centrifugation, total protein concentration was determined by BCA assay, and lysates were stored at -80°C until further use. The ELISA was

performed according to the manufacturer’s recommendations (Table 20) after equalizing total protein concentration. The positive control supplied with the kit consisted of phosphorylated VEGFR-2 and was used to create a standard curve. The concentration of phosphorylated VEGFR-2 in the samples was calculated according to this standard curve, and values were expressed as percent increase over a non-stimulated control.

Materials and buffers required	
Elisa plate	NUNC MaxiSorp, 96 well
Wash buffer	0.05 % Tween 20 in PBS
Block buffer	1 % BSA, 0.05 % NaN <sub>3</sub> in PBS, pH 7.2
Diluent	20 mM Tris, 137 mM NaCl, 0.05 % Tween20, 0.1 % BSA, pH 7.2
Lysis buffer	1% NP-40, 20 mM Tris (pH 8.0), 137 mM NaCl, 10 % glycerol, 2 mM EDTA, 1 mM sodium orthovanadate, proteas inhibitor cocktail (Sigma)
Substrate solution	Tetramethylbenzidine (GE Healthcare)
Stop solution	2 N H <sub>2</sub> SO <sub>4</sub>

**Table 20: Materials and buffers used for the phospho-VEGFR-2 ELISA by R&D Systems.**

### 6.9.5 Surface plasmon resonance (SPR) biosensor binding studies

SPR-based biosensor analysis represents a common method for the determination of binding affinities for proteins and was employed in this work to investigate the binding of VEGFR-2 to VEGFmut and FLV in collaboration with Prof. Dr. Stefan Höning, Institut für Biochemie I, Uniklinikum Köln. All experiments were run on a BIAcore 3000 using a CM5 sensor surface (Table 18). First, protein A was covalently coupled to the surface by using EDC/NHS as activating reagents and with HBS-N as the running buffer. The degree of coupling was set to approximately 1200 resonance units (RU). Non-specific binding was blocked by inactivation of remaining reactive groups with ethanolamine. Subsequently, VEGFR-2 fused to the Fc fragment of IgG (VEGFR-2 Fc, R&D Systems) was immobilized on the protein A surface to a density of ~ 650 RU. The following binding experiments with VEGFmut and FLV as analytes in TBS were performed at a flow rate of 50 µL/min and with concentrations ranging from 20 to 160 nM. Between different experimental cycles, the bound proteins were stripped from the sensor surface with 10 mM glycine, 200 mM NaCl, pH 1.8. The rate constants for the interaction were determined with the evaluation software supplied by the manufacturer.

Materials and reagents used for SPR studies			
Biacore 300 sensor	GE Healthcare	Protein A	GE Healthcare
Biacore sensor chip CM5	GE Healthcare	VEGFR-2 Fc chimera	R&D Systems
Priming buffer: HBS-N buffer	GE Healthcare	Stripping buffer	10 mM glycine, 200 mM NaCl pH 1.8.
EDC/NHS	GE Healthcare		

**Table 18: Materials and reagents used for Biacore binding studies.**

## 6.10 Fibrin gel formulation

Fibrin gels used in this study were well defined, as protein preparations of high purity were used. For the treatment of skin wounds, stiff fibrin gels were formulated characterized by a high fibrinogen concentration and a high degree of crosslinking in order to prolong their residency within the wound. Fibrin gels were formed in TBS at the final concentrations given in Table 21.

Component	Final concentration	Buffers required	
Fibrinogen	10 mg/mL	TBS	
Thrombin	2 U/mL	135 mM	NaCl
Factor XIII	10 U/mL	18 mM	Tris-HCl, pH 7.4
Aprotinin	17 µg/mL		
CaCl <sub>2</sub>	2.5 mM	TBS CaCl <sub>2</sub> (40x)	
VEGF isoforms	20 µg/mL	100 mM	CaCl <sub>2</sub> in TBS

Table 21: Composition of fibrin gels.

### 6.10.1 Protein stock preparation

0.25 g of human fibrinogen, depleted of plasminogen, von Willebrand factor and fibronectin (Enzyme Research Laboratories, Swansea, UK) was resuspended in 7 ml of sterile Millipore water, pre-warmed to 37°C, and dissolved for one hour at 37°C with repeated shaking. The protein solution was then filtered twice and dialyzed against TBS. The osmolarity was confirmed to be between 290 and 315 mosm/L, and the concentration of the protein solution was determined by NanoDrop measurement and normalized by dividing by the extinction coefficient.

Thrombin from human plasma (Sigma) was resuspended in sterile water at a final concentration of 200 U/mL.

Human Factor XIII was either a gift from Baxter (Deerfield, USA) or obtained as Fibrogamin by CSL Behring (King of Prussia, USA), and a stock of 200 U/mL was prepared in sterile water.

Aprotinin (Roche) was prepared at a stock concentration of 17 mg/mL in sterile water.

All protein solutions (Table 22) were aliquoted and stored at -80°C until use.

Protein	Supplier	Order number	Stock concentration
Human fibrinogen, plasminogen, vWF and fibronectin depleted	Enzyme Research Laboratories	FIB3	variable, 20-30 mg/mL
Thrombin from human plasma	Sigma	T4393	200 U/mL
Fibrogamin (factor XIII)	CSL Behring	1250 E FXIII	200 U/mL
Aprotinin	Roche	236624	17 mg/mL

Table 22: Protein stock solutions for the preparation of fibrin gels.



### **6.10.2 Functionalization of fibrin matrices: incorporation and release of VEGF proteins**

Retention and release recombinant of VEGF proteins in fibrin matrices was tested in order to confirm covalent binding of TG-tagged proteins to fibrin. 50  $\mu$ l fibrin gels, functionalized with 2  $\mu$ g of recombinant protein from *E. coli* or 0.2  $\mu$ g from HEK293-EBNA cells, were formulated at a final concentration of 10 mg/mL fibrinogen, 2 U/mL thrombin, 2 or 10 U/mL factor XIII and 2.5 mM CaCl<sub>2</sub> in TBS. After formation, fibrin gels were washed at 37°C in 10 mL TBS with 0.1% BSA. Aliquots were taken from the wash buffer at various time points, and the VEGF concentration in the wash buffer was determined by ELISA using the VEGF ELISA development kit by Peprotech. 100 % release was defined as 2  $\mu$ g, or 0.2  $\mu$ g, of each construct in 10 mL wash buffer, and the amount of protein released from the fibrin gels was expressed relative to this value.

In some experiments, the washed fibrin gels were digested with 0.02 U of plasmin in 20  $\mu$ L TBS at 37°C until degradation was complete. 20  $\mu$ L aliquots of this solution were then subjected to non-reducing SDS-PAGE and western blot analysis.

### **6.11 Wounding of db/db mice**

The performed animal investigation was approved by Landesamt für Natur, Umwelt und Verbraucherschutz NRW. For wounding experiments, male BKS.Cg-m +/+ Lepr<sup>db</sup>/J (db/db) mice 12-14 weeks of age were used (Charles River Laboratories, Wilmington, USA). This mouse strain is considered a representative animal model for type-2 diabetes and is characterized by impaired wound closure and reduced angiogenesis during skin regeneration. Diabetes was confirmed by determination of blood glucose levels prior to experiments. The blood glucose level in these mice was above 300 mg/dL whereas in wildtype mice it is 100 mg/dL.

Under Ketanest/Rompun anesthesia, the back of the mice was shaved, and washed with ethanol. On the back of the mice, four full thickness punch biopsy wounds with a diameter of 6 mm were created, removing the epidermis, the dermis and the underlying fat tissue. 80  $\mu$ L fibrin gels at a final concentration of 10 mg/mL fibrinogen, 2 U/mL thrombin, 10 U/mL factor XIII, 17  $\mu$ g/mL aprotinin, 2.5 mM CaCl<sub>2</sub>, and 20  $\mu$ g/mL of either VEGFmut, TG-VEGFmut or TG-FLV proteins were formed directly in the wound site. A control was a fibrin gel without growth factors. After polymerization of the gel, the gel was covered with a piece of Adaptic (Johnson + Johnson wound management, Norderstedt, Germany), and a semipermeable hydrofilm (Hartmann,

Heidenheim, Germany) was placed on the wound side in order to keep the gel moist. The hydrofilm was fixed to the skin. For recovery from anesthesia, mice were placed on a heating plate until fully awake. Following surgery, the mice were kept in individual cages lined with tissues and received Tramal (Grünenthal, Aachen, Germany) as analgesia via the drinking water. Materials needed for the surgery are summarized in Table 23.

<b>Anesthetic</b>		<b>Surgery tools</b>	
0.1%	Rompun (Bayer, Leverkusen, Germany)	6 mm biopsy punches	Stiefel (NC, USA)
10 mg/mL	Ketavet (Pfizer, Berlin, Germany)	Scissors	Fine Science Tools (Heidelberg, Germany)
0.9 %	NaCl	Tweezers	Fine Science Tools
<b>Animal care</b>		<b>Wound dressing</b>	
Bepanthen eye cream	Bayer	Adaptic	Johnson & Johnson
Tramal, 40 mg/kg bw	Grünenthal (Aachen, Germany)	Hydrofilm	Hartmann
GlycoMen GlycO'	Menarini (Florence, Italy)		
GlycoMen Sensor	Menarini (Florence, Italy)		
Heating plate			

**Table 23: Materials required for the punch biopsy wounding of mice.**

### 6.11.1 Tissue harvest

Mice were sacrificed by carbon dioxide asphyxiation on day 10 or 14/15 post wounding. The wound tissue was harvested, and either paraffin sections or cryosections were prepared.

For paraffin sections, wounds were fixed in formalin, embedded in paraffin and cut into 6  $\mu\text{m}$  thick sections. Sections were stained with hematoxylin and eosin (H&E) or Masson's Trichrome (TM) stain. H&E is commonly used in histology for overview sections. Eosin stains eosinophilic structures like cytoplasm and protein pink, and erythrocytes red. Hematoxylin stains basophilic structures such as nucleic acids blue to purple. The TM stain was developed to distinguish cells, in particular erythrocytes, from connective tissues. Keratin and muscle fibers stain red, collagen stains green, cytoplasm stains pink, and nuclei can be identified by their black shading. Sectioning and staining was performed according to established standard protocols at the histology core facility of the dermatology compartment of the University Hospital of Cologne.

For cryosections, wounds were embedded in OCT compound (TissueTek) and frozen. 10  $\mu\text{m}$  thick sections were fixed in cold acetone and used for immunohistochemistry.

### 6.11.2 Staining for CD31 and desmin

Wound sections were blocked in 10% normal goat serum and probed with antibodies directed against desmin (Dako Glostrup, Denmark, 1:100 in 1% BSA), a marker for pericytes, and CD31 (BD Pharmingen, 1:1000 in 1% BSA), a marker for endothelial cells (Table 24). Primary antibodies were detected with Alexa Flour<sup>®</sup> 488 or 594 coupled secondary antibodies (Invitrogen, 1:500 in 1% BSA), and nuclei of cells were stained with DAPI (1 µg/mL).

Antibodies used for Immunofluorescence						
Primary antibodies				Secondary antibodies		
Antigen	Host species	Supplier	Dilution		Supplier	Dilution
CD31	Rat	BD Pharmingen	1:1000	Goat α Mouse IgG, Alexa Flour <sup>®</sup> 488	Invitrogen	1:500
Desmin	Mouse	Dako	1:100	Goat α Rat Alexa Flour <sup>®</sup> 594	Invitrogen	1:500

**Table 24: Antibodies used for immunohistochemistry on wound cryosections.**

#### 6.11.2.1 Quantification of wound angiogenesis on CD31 and desmin stained sections

For the quantification of the CD31 and desmin positive areas as well as of classical wound parameters (distance between epidermal tips, amount of granulation tissue, distance between the ends of panniculus carnosus), serial images of the entire wound area were taken using a Nikon eclipse E800 fluorescence microscope, and assembled in Adobe Photoshop CS5 (Adobe, Dublin, Ireland). Using the image analysis program ImageJ (Wayne Rasband, National Institute of Mental Health, Bethesda, USA), the channels were split, regions exhibiting a positive signal were selected manually via the thresholding tool, and the area was determined. The desmin and CD31-positive areas were analyzed in relation to the overall area of granulation tissue. Measurements were performed several times. Pictures shown were optimized in Adobe Photoshop CS5 (Dublin, Ireland) by background reduction

#### 6.11.2.2 Statistical analysis of CD31 and desmin stained section

Data were obtained from a total of 11 mice, sacrificed at day 10 (n=7) and 14 (n=4) post injury. Data analysis was carried out using the GraphPadPrism 5 software package (La Jolla USA). Statistical significance was tested by paired t-tests and accepted for  $p < 0.05$ .

## 7 References

- Abramsson A, Kurup S, Busse M, Yamada S, Lindblom P, Schallmeiner E, Stenzel D, Sauvaget D, Ledin J, Ringvall M et al. . 2007. Defective N-sulfation of heparan sulfate proteoglycans limits PDGF-BB binding and pericyte recruitment in vascular development. *Genes Dev* 21(3):316-331.
- Akiri G, Nahari D, Finkelstein Y, Le SY, Elroy-Stein O, and Levi BZ. 1998. Regulation of vascular endothelial growth factor (VEGF) expression is mediated by internal initiation of translation and alternative initiation of transcription. *Oncogene* 17(2):227-236.
- Anitua E, Andia I, Ardanza B, Nurden P, and Nurden AT. 2004. Autologous platelets as a source of proteins for healing and tissue regeneration. *Thromb Haemost* 91(1):4-15.
- Aota S, Nomizu M, and Yamada KM. 1994. The short amino acid sequence Pro-His-Ser-Arg-Asn in human fibronectin enhances cell-adhesive function. *J Biol Chem* 269(40):24756-24761.
- Armulik A, Abramsson A, and Betsholtz C. 2005. Endothelial/pericyte interactions. *Circ Res* 97(6):512-523.
- Asahara T, Chen D, Takahashi T, Fujikawa K, Kearney M, Magner M, Yancopoulos GD, and Isner JM. 1998. Tie2 receptor ligands, angiopoietin-1 and angiopoietin-2, modulate VEGF-induced postnatal neovascularization. *Circ Res* 83(3):233-240.
- Ashikari-Hada S, Habuchi H, Kariya Y, and Kimata K. 2005. Heparin regulates vascular endothelial growth factor165-dependent mitogenic activity, tube formation, and its receptor phosphorylation of human endothelial cells. Comparison of the effects of heparin and modified heparins. *J Biol Chem* 280(36):31508-31515.
- Backer MV, and Backer JM. 2001. Functionally active VEGF fusion proteins. *Protein Expr Purif* 23(1):1-7.
- Bader BL, Rayburn H, Crowley D, and Hynes RO. 1998. Extensive vasculogenesis, angiogenesis, and organogenesis precede lethality in mice lacking all alpha v integrins. *Cell* 95(4):507-519.
- Bahary N, Leibel RL, Joseph L, and Friedman JM. 1990. Molecular mapping of the mouse db mutation. *Proc Natl Acad Sci U S A* 87(21):8642-8646.
- Barleon B, Sozzani S, Zhou D, Weich HA, Mantovani A, and Marme D. 1996. Migration of human monocytes in response to vascular endothelial growth factor (VEGF) is mediated via the VEGF receptor flt-1. *Blood* 87(8):3336-3343.
- Bates DO, and Curry FE. 1996. Vascular endothelial growth factor increases hydraulic conductivity of isolated perfused microvessels. *Am J Physiol* 271(6 Pt 2):H2520-2528.
- Bates DO, and Jones RO. 2003. The role of vascular endothelial growth factor in wound healing. *Int J Low Extrem Wounds* 2(2):107-120.
- Bentley K, Gerhardt H, and Bates PA. 2008. Agent-based simulation of notch-mediated tip cell selection in angiogenic sprout initialisation. *J Theor Biol* 250(1):25-36.
- Bernfield M, Gotte M, Park PW, Reizes O, Fitzgerald ML, Lincecum J, and Zako M. 1999. Functions of cell surface heparan sulfate proteoglycans. *Annu Rev Biochem* 68:729-777.
- Blaess S, Kammerer RA, and Hall H. 1998. Structural analysis of the sixth immunoglobulin-like domain of mouse neural cell adhesion molecule L1 and its interactions with alpha(v)beta3, alpha(IIb)beta3, and alpha5beta1 integrins. *J Neurochem* 71(6):2615-2625.
- Borges E, Jan Y, and Ruoslahti E. 2000. Platelet-derived growth factor receptor beta and vascular endothelial growth factor receptor 2 bind to the beta 3 integrin through its extracellular domain. *J Biol Chem* 275(51):39867-39873.

## References

---

- Bottomley MJ, Webb NJ, Watson CJ, Holt PJ, Freemont AJ, and Brenchley PE. 1999. Peripheral blood mononuclear cells from patients with rheumatoid arthritis spontaneously secrete vascular endothelial growth factor (VEGF): specific up-regulation by tumour necrosis factor-alpha (TNF-alpha) in synovial fluid. *Clin Exp Immunol* 117(1):171-176.
- Braiman-Wiksmann L, Solomonik I, Spira R, and Tennenbaum T. 2007. Novel insights into wound healing sequence of events. *Toxicol Pathol* 35(6):767-779.
- Brem H, Kodra A, Golinko MS, Entero H, Stojadinovic O, Wang VM, Sheahan CM, Weinberg AD, Woo SL, Ehrlich HP et al. . 2009. Mechanism of sustained release of vascular endothelial growth factor in accelerating experimental diabetic healing. *J Invest Dermatol* 129(9):2275-2287.
- Brooks PC, Clark RA, and Cheresh DA. 1994a. Requirement of vascular integrin alpha v beta 3 for angiogenesis. *Science* 264(5158):569-571.
- Brooks PC, Montgomery AM, Rosenfeld M, Reisfeld RA, Hu T, Klier G, and Cheresh DA. 1994b. Integrin alpha v beta 3 antagonists promote tumor regression by inducing apoptosis of angiogenic blood vessels. *Cell* 79(7):1157-1164.
- Brown LF, Yeo KT, Berse B, Yeo TK, Senger DR, Dvorak HF, and van de Water L. 1992. Expression of vascular permeability factor (vascular endothelial growth factor) by epidermal keratinocytes during wound healing. *J Exp Med* 176(5):1375-1379.
- Byzova TV, Goldman CK, Pampori N, Thomas KA, Bett A, Shattil SJ, and Plow EF. 2000. A mechanism for modulation of cellular responses to VEGF: activation of the integrins. *Mol Cell* 6(4):851-860.
- Carrio MM, Corchero JL, and Villaverde A. 1998. Dynamics of in vivo protein aggregation: building inclusion bodies in recombinant bacteria. *FEMS Microbiol Lett* 169(1):9-15.
- Cebe Suarez S, Pieren M, Cariolato L, Arn S, Hoffmann U, Bogucki A, Manlius C, Wood J, and Ballmer-Hofer K. 2006. A VEGF-A splice variant defective for heparan sulfate and neuropilin-1 binding shows attenuated signaling through VEGFR-2. *Cell Mol Life Sci* 63(17):2067-2077.
- Cheresh DA. 1987. Human endothelial cells synthesize and express an Arg-Gly-Asp-directed adhesion receptor involved in attachment to fibrinogen and von Willebrand factor. *Proc Natl Acad Sci U S A* 84(18):6471-6475.
- Cheresh DA, and Stupack DG. 2008. Regulation of angiogenesis: apoptotic cues from the ECM. *Oncogene* 27(48):6285-6298.
- Cho CH, Kammerer RA, Lee HJ, Steinmetz MO, Ryu YS, Lee SH, Yasunaga K, Kim KT, Kim I, Choi HH et al. . 2004. COMP-Ang1: a designed angiopoietin-1 variant with nonleaky angiogenic activity. *Proc Natl Acad Sci U S A* 101(15):5547-5552.
- Chraïbi H, Dereure O, Teot L, and Guillot B. 2004. The diagnosis and treatment of carcinomas occurring at the sites of chronic pressure ulcers. *J Wound Care* 13(10):447-448.
- Clark RA. 2003. Fibrin is a many splendored thing. *J Invest Dermatol* 121(5):xxi-xxii.
- Clark RA, Ghosh K, and Tonnesen MG. 2007. Tissue engineering for cutaneous wounds. *J Invest Dermatol* 127(5):1018-1029.
- Cohen SN, Chang AC, and Hsu L. 1972. Nonchromosomal antibiotic resistance in bacteria: genetic transformation of *Escherichia coli* by R-factor DNA. *Proc Natl Acad Sci U S A* 69(8):2110-2114.
- Connolly DT, Heuvelman DM, Nelson R, Olander JV, Eppley BL, Delfino JJ, Siegel NR, Leimgruber RM, and Feder J. 1989. Tumor vascular permeability factor stimulates endothelial cell growth and angiogenesis. *J Clin Invest* 84(5):1470-1478.
- Conolly ME. 1989. Alternative to euthanasia: pain management. *Issues Law Med* 4(4):497-507.
- Crasto CJ, and Feng JA. 2000. LINKER: a program to generate linker sequences for fusion proteins. *Protein Eng* 13(5):309-312.

- Cumberbatch M, Dearman RJ, Griffiths CE, and Kimber I. 2000. Langerhans cell migration. *Clin Exp Dermatol* 25(5):413-418.
- Cunningham SA, Tran TM, Arrate MP, and Brock TA. 1999. Characterization of vascular endothelial cell growth factor interactions with the kinase insert domain-containing receptor tyrosine kinase. A real time kinetic study. *J Biol Chem* 274(26):18421-18427.
- Danen EH, Aota S, van Kraats AA, Yamada KM, Ruiters DJ, and van Muijen GN. 1995. Requirement for the synergy site for cell adhesion to fibronectin depends on the activation state of integrin alpha 5 beta 1. *J Biol Chem* 270(37):21612-21618.
- Datta SR, Dudek H, Tao X, Masters S, Fu H, Gotoh Y, and Greenberg ME. 1997. Akt phosphorylation of BAD couples survival signals to the cell-intrinsic death machinery. *Cell* 91(2):231-241.
- Davanloo P, Rosenberg AH, Dunn JJ, and Studier FW. 1984. Cloning and expression of the gene for bacteriophage T7 RNA polymerase. *Proc Natl Acad Sci U S A* 81(7):2035-2039.
- Davis S, Aldrich TH, Jones PF, Acheson A, Compton DL, Jain V, Ryan TE, Bruno J, Radziejewski C, Maisonpierre PC et al. . 1996. Isolation of angiopoietin-1, a ligand for the TIE2 receptor, by secretion-trap expression cloning. *Cell* 87(7):1161-1169.
- de Vries C, Escobedo JA, Ueno H, Houck K, Ferrara N, and Williams LT. 1992. The fms-like tyrosine kinase, a receptor for vascular endothelial growth factor. *Science* 255(5047):989-991.
- Deroanne CF, Hajitou A, Calberg-Bacq CM, Nusgens BV, and Lapiere CM. 1997. Angiogenesis by fibroblast growth factor 4 is mediated through an autocrine up-regulation of vascular endothelial growth factor expression. *Cancer Res* 57(24):5590-5597.
- DiPietro LA, and Polverini PJ. 1993. Role of the macrophage in the positive and negative regulation of wound neovascularization. *Behring Inst Mitt*(92):238-247.
- Du X, and Ginsberg MH. 1997. Integrin alpha IIb beta 3 and platelet function. *Thromb Haemost* 78(1):96-100.
- Ehrbar M, Djonov VG, Schnell C, Tschanz SA, Martiny-Baron G, Schenk U, Wood J, Burri PH, Hubbell JA, and Zisch AH. 2004. Cell-demanded liberation of VEGF(121) from fibrin implants induces local and controlled blood vessel growth. *Circ Res* 94(8):1124-1132.
- Ehrbar M, Metters A, Zammaretti P, Hubbell JA, and Zisch AH. 2005. Endothelial cell proliferation and progenitor maturation by fibrin-bound VEGF variants with differential susceptibilities to local cellular activity. *J Control Release* 101(1-3):93-109.
- Eliceiri BP, Klemke R, Stromblad S, and Cheresh DA. 1998. Integrin alphavbeta3 requirement for sustained mitogen-activated protein kinase activity during angiogenesis. *J Cell Biol* 140(5):1255-1263.
- Eming SA, Brachvogel B, Odorisio T, and Koch M. 2007a. Regulation of angiogenesis: wound healing as a model. *Prog Histochem Cytochem* 42(3):115-170.
- Eming SA, Kaufmann J, Lohrer R, and Krieg T. 2007b. [Chronic wounds. Novel approaches in research and therapy]. *Hautarzt* 58(11):939-944.
- Eming SA, Krieg T, and Davidson JM. 2007c. Inflammation in wound repair: molecular and cellular mechanisms. *J Invest Dermatol* 127(3):514-525.
- Fernandez ML, Broadbent JA, Shooter GK, Malda J, and Upton Z. 2008. Development of an enhanced proteomic method to detect prognostic and diagnostic markers of healing in chronic wound fluid. *Br J Dermatol* 158(2):281-290.
- Ferrara N. 2004. Vascular endothelial growth factor: basic science and clinical progress. *Endocr Rev* 25(4):581-611.
- Ferrara N, and Henzel WJ. 1989. Pituitary follicular cells secrete a novel heparin-binding growth factor specific for vascular endothelial cells. *Biochem Biophys Res Commun* 161(2):851-858.

## References

---

- Fiebich BL, Jager B, Schollmann C, Weindel K, Wilting J, Kochs G, Marme D, Hug H, and Weich HA. 1993. Synthesis and assembly of functionally active human vascular endothelial growth factor homodimers in insect cells. *Eur J Biochem* 211(1-2):19-26.
- Finkenzeller G, Sparacio A, Technau A, Marme D, and Siemeister G. 1997. Sp1 recognition sites in the proximal promoter of the human vascular endothelial growth factor gene are essential for platelet-derived growth factor-induced gene expression. *Oncogene* 15(6):669-676.
- Fleury ME, Boardman KC, and Swartz MA. 2006. Autologous morphogen gradients by subtle interstitial flow and matrix interactions. *Biophys J* 91(1):113-121.
- Folkman J. 2006. Angiogenesis. *Annu Rev Med* 57:1-18.
- Fong GH, Zhang L, Bryce DM, and Peng J. 1999. Increased hemangioblast commitment, not vascular disorganization, is the primary defect in flt-1 knock-out mice. *Development* 126(13):3015-3025.
- Frank S, Hubner G, Breier G, Longaker MT, Greenhalgh DG, and Werner S. 1995. Regulation of vascular endothelial growth factor expression in cultured keratinocytes. Implications for normal and impaired wound healing. *J Biol Chem* 270(21):12607-12613.
- Frappier L, and O'Donnell M. 1992. EBNA1 distorts oriP, the Epstein-Barr virus latent replication origin. *J Virol* 66(3):1786-1790.
- Galiano RD, Tepper OM, Pelo CR, Bhatt KA, Callaghan M, Bastidas N, Bunting S, Steinmetz HG, and Gurtner GC. 2004. Topical vascular endothelial growth factor accelerates diabetic wound healing through increased angiogenesis and by mobilizing and recruiting bone marrow-derived cells. *Am J Pathol* 164(6):1935-1947.
- Gamble JR, Drew J, Trezise L, Underwood A, Parsons M, Kasminkas L, Rudge J, Yancopoulos G, and Vadas MA. 2000. Angiopoietin-1 is an antipermeability and anti-inflammatory agent in vitro and targets cell junctions. *Circ Res* 87(7):603-607.
- Garlick JA, and Taichman LB. 1994. Fate of human keratinocytes during reepithelialization in an organotypic culture model. *Lab Invest* 70(6):916-924.
- Gavard J, Patel V, and Gutkind JS. 2008. Angiopoietin-1 prevents VEGF-induced endothelial permeability by sequestering Src through mDia. *Dev Cell* 14(1):25-36.
- Geer DJ, Swartz DD, and Andreadis ST. 2002. Fibrin promotes migration in a three-dimensional in vitro model of wound regeneration. *Tissue Eng* 8(5):787-798.
- Gerhardt H, Golding M, Fruttiger M, Ruhrberg C, Lundkvist A, Abramsson A, Jeltsch M, Mitchell C, Alitalo K, Shima D et al. . 2003. VEGF guides angiogenic sprouting utilizing endothelial tip cell filopodia. *J Cell Biol* 161(6):1163-1177.
- Gipson IK, Spurr-Michaud SJ, and Tisdale AS. 1988. Hemidesmosomes and anchoring fibril collagen appear synchronously during development and wound healing. *Dev Biol* 126(2):253-262.
- Gitay-Goren H, Soker S, Vlodaysky I, and Neufeld G. 1992. The binding of vascular endothelial growth factor to its receptors is dependent on cell surface-associated heparin-like molecules. *J Biol Chem* 267(9):6093-6098.
- Gluzman-Poltorak Z, Cohen T, Herzog Y, and Neufeld G. 2000. Neuropilin-2 is a receptor for the vascular endothelial growth factor (VEGF) forms VEGF-145 and VEGF-165 [corrected]. *J Biol Chem* 275(24):18040-18045.
- Goad DL, Rubin J, Wang H, Tashjian AH, Jr., and Patterson C. 1996. Enhanced expression of vascular endothelial growth factor in human SaOS-2 osteoblast-like cells and murine osteoblasts induced by insulin-like growth factor I. *Endocrinology* 137(6):2262-2268.
- Gorbet MB, and Sefton MV. 2005. Endotoxin: the uninvited guest. *Biomaterials* 26(34):6811-6817.

- Gorodetsky R, Vexler A, An J, Mou X, and Marx G. 1998. Haptotactic and growth stimulatory effects of fibrin(ogen) and thrombin on cultured fibroblasts. *J Lab Clin Med* 131(3):269-280.
- Gospodarowicz D, Abraham JA, and Schilling J. 1989. Isolation and characterization of a vascular endothelial cell mitogen produced by pituitary-derived folliculo stellate cells. *Proc Natl Acad Sci U S A* 86(19):7311-7315.
- Grant RP, Spitzfaden C, Altroff H, Campbell ID, and Mardon HJ. 1997. Structural requirements for biological activity of the ninth and tenth FIII domains of human fibronectin. *J Biol Chem* 272(10):6159-6166.
- Grondahl-Hansen J, Lund LR, Ralfkiaer E, Ottevanger V, and Dano K. 1988. Urokinase- and tissue-type plasminogen activators in keratinocytes during wound reepithelialization in vivo. *J Invest Dermatol* 90(6):790-795.
- Grunewald FS, Prota AE, Giese A, and Ballmer-Hofer K. 2010. Structure-function analysis of VEGF receptor activation and the role of coreceptors in angiogenic signaling. *Biochim Biophys Acta* 1804(3):567-580.
- Hall H, Djonov V, Ehrbar M, Hoehli M, and Hubbell JA. 2004. Heterophilic interactions between cell adhesion molecule L1 and alphavbeta3-integrin induce HUVEC process extension in vitro and angiogenesis in vivo. *Angiogenesis* 7(3):213-223.
- Hall H, and Hubbell JA. 2004. Matrix-bound sixth Ig-like domain of cell adhesion molecule L1 acts as an angiogenic factor by ligating alphavbeta3-integrin and activating VEGF-R2. *Microvasc Res* 68(3):169-178.
- Hellstrom M, Kalen M, Lindahl P, Abramsson A, and Betsholtz C. 1999. Role of PDGF-B and PDGFR-beta in recruitment of vascular smooth muscle cells and pericytes during embryonic blood vessel formation in the mouse. *Development* 126(14):3047-3055.
- Hellstrom M, Phng LK, Hofmann JJ, Wallgard E, Coultas L, Lindblom P, Alva J, Nilsson AK, Karlsson L, Gaiano N et al. . 2007. Dll4 signalling through Notch1 regulates formation of tip cells during angiogenesis. *Nature* 445(7129):776-780.
- Helm CL, Fleury ME, Zisch AH, Boschetti F, and Swartz MA. 2005. Synergy between interstitial flow and VEGF directs capillary morphogenesis in vitro through a gradient amplification mechanism. *Proc Natl Acad Sci U S A* 102(44):15779-15784.
- Henschen A, Lottspeich F, Kehl M, and Southan C. 1983. Covalent structure of fibrinogen. *Ann N Y Acad Sci* 408:28-43.
- Hinz B, Phan SH, Thannickal VJ, Galli A, Bochaton-Piallat ML, and Gabbiani G. 2007. The myofibroblast: one function, multiple origins. *Am J Pathol* 170(6):1807-1816.
- Hiratsuka S, Minowa O, Kuno J, Noda T, and Shibuya M. 1998. Flt-1 lacking the tyrosine kinase domain is sufficient for normal development and angiogenesis in mice. *Proc Natl Acad Sci U S A* 95(16):9349-9354.
- Hoch RV, and Soriano P. 2003. Roles of PDGF in animal development. *Development* 130(20):4769-4784.
- Hodivala-Dilke KM, McHugh KP, Tsakiris DA, Rayburn H, Crowley D, Ullman-Cullere M, Ross FP, Collier BS, Teitelbaum S, and Hynes RO. 1999. Beta3-integrin-deficient mice are a model for Glanzmann thrombasthenia showing placental defects and reduced survival. *J Clin Invest* 103(2):229-238.
- Holmqvist K, Cross MJ, Rolny C, Hagerkvist R, Rahimi N, Matsumoto T, Claesson-Welsh L, and Welsh M. 2004. The adaptor protein shb binds to tyrosine 1175 in vascular endothelial growth factor (VEGF) receptor-2 and regulates VEGF-dependent cellular migration. *J Biol Chem* 279(21):22267-22275.



## References

---

- Horowitz JR, Rivard A, van der Zee R, Hariawala M, Sheriff DD, Esakof DD, Chaudhry GM, Symes JF, and Isner JM. 1997. Vascular endothelial growth factor/vascular permeability factor produces nitric oxide-dependent hypotension. Evidence for a maintenance role in quiescent adult endothelium. *Arterioscler Thromb Vasc Biol* 17(11):2793-2800.
- Houck KA, Ferrara N, Winer J, Cachianes G, Li B, and Leung DW. 1991. The vascular endothelial growth factor family: identification of a fourth molecular species and characterization of alternative splicing of RNA. *Mol Endocrinol* 5(12):1806-1814.
- Houck KA, Leung DW, Rowland AM, Winer J, and Ferrara N. 1992. Dual regulation of vascular endothelial growth factor bioavailability by genetic and proteolytic mechanisms. *J Biol Chem* 267(36):26031-26037.
- Howdieshell TR, Callaway D, Webb WL, Gaines MD, Procter CD, Jr., Sathyanarayana, Pollock JS, Brock TL, and McNeil PL. 2001. Antibody neutralization of vascular endothelial growth factor inhibits wound granulation tissue formation. *J Surg Res* 96(2):173-182.
- Hubner G, Brauchle M, Smola H, Madlener M, Fassler R, and Werner S. 1996. Differential regulation of pro-inflammatory cytokines during wound healing in normal and glucocorticoid-treated mice. *Cytokine* 8(7):548-556.
- Huston JS, Levinson D, Mudgett-Hunter M, Tai MS, Novotny J, Margolies MN, Ridge RJ, Bruccoleri RE, Haber E, Crea R et al. . 1988. Protein engineering of antibody binding sites: recovery of specific activity in an anti-digoxin single-chain Fv analogue produced in *Escherichia coli*. *Proc Natl Acad Sci U S A* 85(16):5879-5883.
- Huston JS, Mudgett-Hunter M, Tai MS, McCartney J, Warren F, Haber E, and Oppermann H. 1991. Protein engineering of single-chain Fv analogs and fusion proteins. *Methods Enzymol* 203:46-88.
- Hutchings H, Ortega N, and Plouet J. 2003. Extracellular matrix-bound vascular endothelial growth factor promotes endothelial cell adhesion, migration, and survival through integrin ligation. *Faseb J* 17(11):1520-1522.
- Ishikawa T, Eguchi M, Wada M, Iwami Y, Tono K, Iwaguro H, Masuda H, Tamaki T, and Asahara T. 2006. Establishment of a functionally active collagen-binding vascular endothelial growth factor fusion protein in situ. *Arterioscler Thromb Vasc Biol* 26(9):1998-2004.
- Ivan M, Kondo K, Yang H, Kim W, Valiando J, Ohh M, Salic A, Asara JM, Lane WS, and Kaelin WG, Jr. 2001. HIF $\alpha$  targeted for VHL-mediated destruction by proline hydroxylation: implications for O<sub>2</sub> sensing. *Science* 292(5516):464-468.
- Jain RK. 2003. Molecular regulation of vessel maturation. *Nat Med* 9(6):685-693.
- Jakobsson L, Kreuger J, Holmborn K, Lundin L, Eriksson I, Kjellen L, and Claesson-Welsh L. 2006. Heparan sulfate in trans potentiates VEGFR-mediated angiogenesis. *Dev Cell* 10(5):625-634.
- Jameson JM, Sharp LL, Witherden DA, and Havran WL. 2004. Regulation of skin cell homeostasis by gamma delta T cells. *Front Biosci* 9:2640-2651.
- Jang JH, and Chung CP. 2004. Engineering and expression of a recombinant fusion protein possessing fibroblast growth factor-2 and fibronectin fragment. *Biotechnol Lett* 26(24):1837-1840.
- Jeon E, Kim HW, and Jang JH. 2009. Protein engineering of a fibroblast growth factor-1 fusion protein with cell adhesive activity. *Acta Biochim Biophys Sin (Shanghai)* 41(10):852-857.
- Joukov V, Sorsa T, Kumar V, Jeltsch M, Claesson-Welsh L, Cao Y, Saksela O, Kalkkinen N, and Alitalo K. 1997. Proteolytic processing regulates receptor specificity and activity of VEGF-C. *Embo J* 16(13):3898-3911.

- Keck PJ, Hauser SD, Krivi G, Sanzo K, Warren T, Feder J, and Connolly DT. 1989. Vascular permeability factor, an endothelial cell mitogen related to PDGF. *Science* 246(4935):1309-1312.
- Keyt BA, Berleau LT, Nguyen HV, Chen H, Heinsohn H, Vandlen R, and Ferrara N. 1996. The carboxyl-terminal domain (111-165) of vascular endothelial growth factor is critical for its mitogenic potency. *J Biol Chem* 271(13):7788-7795.
- Kietzmann T, Roth U, and Jungermann K. 1999. Induction of the plasminogen activator inhibitor-1 gene expression by mild hypoxia via a hypoxia response element binding the hypoxia-inducible factor-1 in rat hepatocytes. *Blood* 94(12):4177-4185.
- Kishimoto J, Ehama R, Ge Y, Kobayashi T, Nishiyama T, Detmar M, and Burgeson RE. 2000. In vivo detection of human vascular endothelial growth factor promoter activity in transgenic mouse skin. *Am J Pathol* 157(1):103-110.
- Kitajima T, Terai H, and Ito Y. 2007. A fusion protein of hepatocyte growth factor for immobilization to collagen. *Biomaterials* 28(11):1989-1997.
- Kobayashi M, Nishita M, Mishima T, Ohashi K, and Mizuno K. 2006. MAPKAPK-2-mediated LIM-kinase activation is critical for VEGF-induced actin remodeling and cell migration. *Embo J* 25(4):713-726.
- Koolwijk P, van Erck MG, de Vree WJ, Vermeer MA, Weich HA, Hanemaaijer R, and van Hinsbergh VW. 1996. Cooperative effect of TNFalpha, bFGF, and VEGF on the formation of tubular structures of human microvascular endothelial cells in a fibrin matrix. Role of urokinase activity. *J Cell Biol* 132(6):1177-1188.
- Koster MI. 2009. Making an epidermis. *Ann N Y Acad Sci* 1170:7-10.
- Ku DD, Zaleski JK, Liu S, and Brock TA. 1993. Vascular endothelial growth factor induces EDRF-dependent relaxation in coronary arteries. *Am J Physiol* 265(2 Pt 2):H586-592.
- Laemmli UK. 1970. Cleavage of structural proteins during the assembly of the head of bacteriophage T4. *Nature* 227(5259):680-685.
- Lamallice L, Houle F, Jourdan G, and Huot J. 2004. Phosphorylation of tyrosine 1214 on VEGFR2 is required for VEGF-induced activation of Cdc42 upstream of SAPK2/p38. *Oncogene* 23(2):434-445.
- Lamallice L, Le Boeuf F, and Huot J. 2007. Endothelial cell migration during angiogenesis. *Circ Res* 100(6):782-794.
- Landry J, and Huot J. 1995. Modulation of actin dynamics during stress and physiological stimulation by a signaling pathway involving p38 MAP kinase and heat-shock protein 27. *Biochem Cell Biol* 73(9-10):703-707.
- Lauer G, Sollberg S, Cole M, Flamme I, Sturzebecher J, Mann K, Krieg T, and Eming SA. 2000. Expression and proteolysis of vascular endothelial growth factor is increased in chronic wounds. *J Invest Dermatol* 115(1):12-18.
- Lauer G, Sollberg S, Cole M, Krieg T, and Eming SA. 2002. Generation of a novel proteolysis resistant vascular endothelial growth factor(165) variant by a site-directed mutation at the plasmin sensitive cleavage site. *Febs Letters* 531(2):309-313.
- Laurens N, Koolwijk P, and de Maat MP. 2006. Fibrin structure and wound healing. *J Thromb Haemost* 4(5):932-939.
- Le Boeuf F, Houle F, Sussman M, and Huot J. 2006. Phosphorylation of focal adhesion kinase (FAK) on Ser732 is induced by rho-dependent kinase and is essential for proline-rich tyrosine kinase-2-mediated phosphorylation of FAK on Tyr407 in response to vascular endothelial growth factor. *Mol Biol Cell* 17(8):3508-3520.
- Lee TH, Seng S, Li H, Kennel SJ, Avraham HK, and Avraham S. 2006. Integrin regulation by vascular endothelial growth factor in human brain microvascular endothelial cells: role of alpha6beta1 integrin in angiogenesis. *J Biol Chem* 281(52):40450-40460.

## References

---

- Leung DW, Cachianes G, Kuang WJ, Goeddel DV, and Ferrara N. 1989. Vascular endothelial growth factor is a secreted angiogenic mitogen. *Science* 246(4935):1306-1309.
- Levy NS, Goldberg MA, and Levy AP. 1997. Sequencing of the human vascular endothelial growth factor (VEGF) 3' untranslated region (UTR): conservation of five hypoxia-inducible RNA-protein binding sites. *Biochim Biophys Acta* 1352(2):167-173.
- Li J, Perrella MA, Tsai JC, Yet SF, Hsieh CM, Yoshizumi M, Patterson C, Endege WO, Zhou F, and Lee ME. 1995. Induction of vascular endothelial growth factor gene expression by interleukin-1 beta in rat aortic smooth muscle cells. *J Biol Chem* 270(1):308-312.
- Li W, Fan J, and Woodley DT. 2001. Nck/Dock: an adapter between cell surface receptors and the actin cytoskeleton. *Oncogene* 20(44):6403-6417.
- Lin H, Chen B, Sun W, Zhao W, Zhao Y, and Dai J. 2006. The effect of collagen-targeting platelet-derived growth factor on cellularization and vascularization of collagen scaffolds. *Biomaterials* 27(33):5708-5714.
- Liu ZJ, Shirakawa T, Li Y, Soma A, Oka M, Dotto GP, Fairman RM, Velazquez OC, and Herlyn M. 2003. Regulation of Notch1 and Dll4 by vascular endothelial growth factor in arterial endothelial cells: implications for modulating arteriogenesis and angiogenesis. *Mol Cell Biol* 23(1):14-25.
- Lohela M, Bry M, Tammela T, and Alitalo K. 2009. VEGFs and receptors involved in angiogenesis versus lymphangiogenesis. *Curr Opin Cell Biol* 21(2):154-165.
- Mahabeleshwar GH, Chen J, Feng W, Somanath PR, Razorenova OV, and Byzova TV. 2008. Integrin affinity modulation in angiogenesis. *Cell Cycle* 7(3):335-347.
- Mahabeleshwar GH, Feng W, Phillips DR, and Byzova TV. 2006. Integrin signaling is critical for pathological angiogenesis. *J Exp Med* 203(11):2495-2507.
- Mahabeleshwar GH, Feng W, Reddy K, Plow EF, and Byzova TV. 2007. Mechanisms of integrin-vascular endothelial growth factor receptor cross-activation in angiogenesis. *Circ Res* 101(6):570-580.
- Makogonenko E, Tsurupa G, Ingham K, and Medved L. 2002. Interaction of fibrin(ogen) with fibronectin: further characterization and localization of the fibronectin-binding site. *Biochemistry* 41(25):7907-7913.
- Martin P. 1997. Wound healing--aiming for perfect skin regeneration. *Science* 276(5309):75-81.
- Martino MM, and Hubbell JA. 2010. The 12th-14th type III repeats of fibronectin function as a highly promiscuous growth factor-binding domain. *FASEB J*.
- Masson-Gadais B, Houle F, Laferriere J, and Huot J. 2003. Integrin alphavbeta3, requirement for VEGFR2-mediated activation of SAPK2/p38 and for Hsp90-dependent phosphorylation of focal adhesion kinase in endothelial cells activated by VEGF. *Cell Stress Chaperones* 8(1):37-52.
- Matoltsy AG, and Viziám CB. 1970. Further observations on epithelialization of small wounds: an autoradiographic study of incorporation and distribution of 3H-thymidine in the epithelium covering skin wounds. *J Invest Dermatol* 55(1):20-25.
- McGrath JA, Eady RAJ, and Pope FM. 2008. *Anatomy and Organization of Human Skin*: Blackwell Publishing, Inc. 45-128 p.
- Menke NB, Ward KR, Witten TM, Bonchev DG, and Diegelmann RF. 2007. Impaired wound healing. *Clin Dermatol* 25(1):19-25.
- Michaels Jt, Dobryansky M, Galiano RD, Bhatt KA, Ashinoff R, Ceradini DJ, and Gurtner GC. 2005. Topical vascular endothelial growth factor reverses delayed wound healing secondary to angiogenesis inhibitor administration. *Wound Repair Regen* 13(5):506-512.
- Moffatt BA, and Studier FW. 1987. T7 lysozyme inhibits transcription by T7 RNA polymerase. *Cell* 49(2):221-227.

- Mole DR, Pugh CW, Ratcliffe PJ, and Maxwell PH. 2002. Regulation of the HIF pathway: enzymatic hydroxylation of a conserved prolyl residue in hypoxia-inducible factor alpha subunits governs capture by the pVHL E3 ubiquitin ligase complex. *Adv Enzyme Regul* 42:333-347.
- Mosesson MW, Siebenlist KR, and Meh DA. 2001. The structure and biological features of fibrinogen and fibrin. *Ann N Y Acad Sci* 936:11-30.
- Murakami M, and Simons M. 2009. Regulation of vascular integrity. *J Mol Med* 87(6):571-582.
- Namiki A, Brogi E, Kearney M, Kim EA, Wu T, Couffinhal T, Varticovski L, and Isner JM. 1995. Hypoxia induces vascular endothelial growth factor in cultured human endothelial cells. *J Biol Chem* 270(52):31189-31195.
- Neufeld G, Cohen T, Gengrinovitch S, and Poltorak Z. 1999. Vascular endothelial growth factor (VEGF) and its receptors. *Faseb J* 13(1):9-22.
- Nguyen BP, Gil SG, and Carter WG. 2000. Deposition of laminin 5 by keratinocytes regulates integrin adhesion and signaling. *J Biol Chem* 275(41):31896-31907.
- Noli C, and Miolo A. 2001. The mast cell in wound healing. *Vet Dermatol* 12(6):303-313.
- Nwomeh BC, Liang HX, Diegelmann RF, Cohen IK, and Yager DR. 1998a. Dynamics of the matrix metalloproteinases MMP-1 and MMP-8 in acute open human dermal wounds. *Wound Repair Regen* 6(2):127-134.
- Nwomeh BC, Yager DR, and Cohen IK. 1998b. Physiology of the chronic wound. *Clin Plast Surg* 25(3):341-356.
- Odrliin TM, Shainoff JR, Lawrence SO, and Simpson-Haidaris PJ. 1996. Thrombin cleavage enhances exposure of a heparin binding domain in the N-terminus of the fibrin beta chain. *Blood* 88(6):2050-2061.
- Olsson AK, Dimberg A, Kreuger J, and Claesson-Welsh L. 2006. VEGF receptor signalling - in control of vascular function. *Nat Rev Mol Cell Biol* 7(5):359-371.
- Ozawa CR, Banfi A, Glazer NL, Thurston G, Springer ML, Kraft PE, McDonald DM, and Blau HM. 2004. Microenvironmental VEGF concentration, not total dose, determines a threshold between normal and aberrant angiogenesis. *J Clin Invest* 113(4):516-527.
- Pan Q, Chathery Y, Wu Y, Rathore N, Tong RK, Peale F, Bagri A, Tessier-Lavigne M, Koch AW, and Watts RJ. 2007. Neuropilin-1 binds to VEGF121 and regulates endothelial cell migration and sprouting. *J Biol Chem* 282(33):24049-24056.
- Pang Y, Wang X, Ucuzian AA, Brey EM, Burgess WH, Jones KJ, Alexander TD, and Greisler HP. 2010. Local delivery of a collagen-binding FGF-1 chimera to smooth muscle cells in collagen scaffolds for vascular tissue engineering. *Biomaterials* 31(5):878-885.
- Pankov R, and Yamada KM. 2002. Fibronectin at a glance. *J Cell Sci* 115(Pt 20):3861-3863.
- Park JE, Keller GA, and Ferrara N. 1993. The vascular endothelial growth factor (VEGF) isoforms: differential deposition into the subepithelial extracellular matrix and bioactivity of extracellular matrix-bound VEGF. *Mol Biol Cell* 4(12):1317-1326.
- Parsons JT. 2003. Focal adhesion kinase: the first ten years. *J Cell Sci* 116(Pt 8):1409-1416.
- Pilcher BK, Wang M, Qin XJ, Parks WC, Senior RM, and Welgus HG. 1999. Role of matrix metalloproteinases and their inhibition in cutaneous wound healing and allergic contact hypersensitivity. *Ann N Y Acad Sci* 878:12-24.
- Potter MD, Barbero S, and Cheresh DA. 2005. Tyrosine phosphorylation of VE-cadherin prevents binding of p120- and beta-catenin and maintains the cellular mesenchymal state. *J Biol Chem* 280(36):31906-31912.
- Preissner KT, and Jenne D. 1991. Vitronectin: a new molecular connection in haemostasis. *Thromb Haemost* 66(2):189-194.
- Proksch E, Brandner JM, and Jensen JM. 2008. The skin: an indispensable barrier. *Exp Dermatol* 17(12):1063-1072.

## References

---

- Pytela R, Pierschbacher MD, and Ruoslahti E. 1985. A 125/115-kDa cell surface receptor specific for vitronectin interacts with the arginine-glycine-aspartic acid adhesion sequence derived from fibronectin. *Proc Natl Acad Sci U S A* 82(17):5766-5770.
- Qi JH, Ebrahem Q, Moore N, Murphy G, Claesson-Welsh L, Bond M, Baker A, and Anand-Apte B. 2003. A novel function for tissue inhibitor of metalloproteinases-3 (TIMP3): inhibition of angiogenesis by blockage of VEGF binding to VEGF receptor-2. *Nat Med* 9(4):407-415.
- Rajkumar VS, Shiwen X, Bostrom M, Leoni P, Muddle J, Ivarsson M, Gerdin B, Denton CP, Bou-Gharios G, Black CM et al. . 2006. Platelet-derived growth factor-beta receptor activation is essential for fibroblast and pericyte recruitment during cutaneous wound healing. *Am J Pathol* 169(6):2254-2265.
- Raut S, and Gaffney PJ. 1996. Interaction of heparin with fibrinogen using surface plasmon resonance technology: investigation of heparin binding site on fibrinogen. *Thromb Res* 81(4):503-509.
- Reynolds AR, Hart IR, Watson AR, Welti JC, Silva RG, Robinson SD, Da Violante G, Gourlaouen M, Salih M, Jones MC et al. . 2009. Stimulation of tumor growth and angiogenesis by low concentrations of RGD-mimetic integrin inhibitors. *Nat Med* 15(4):392-400.
- Reynolds AR, Reynolds LE, Nagel TE, Lively JC, Robinson SD, Hicklin DJ, Bodary SC, and Hodivala-Dilke KM. 2004. Elevated Flk1 (vascular endothelial growth factor receptor 2) signaling mediates enhanced angiogenesis in beta3-integrin-deficient mice. *Cancer Res* 64(23):8643-8650.
- Rolny C, Spillmann D, Lindahl U, and Claesson-Welsh L. 2002. Heparin amplifies platelet-derived growth factor (PDGF)- BB-induced PDGF alpha -receptor but not PDGF beta -receptor tyrosine phosphorylation in heparan sulfate-deficient cells. Effects on signal transduction and biological responses. *J Biol Chem* 277(22):19315-19321.
- Romano Di Peppe S, Mangoni A, Zambruno G, Spinetti G, Melillo G, Napolitano M, and Capogrossi MC. 2002. Adenovirus-mediated VEGF(165) gene transfer enhances wound healing by promoting angiogenesis in CD1 diabetic mice. *Gene Ther* 9(19):1271-1277.
- Roth D, Piekarek M, Paulsson M, Christ H, Bloch W, Krieg T, Davidson JM, and Eming SA. 2006. Plasmin modulates vascular endothelial growth factor-A-mediated angiogenesis during wound repair. *Am J Pathol* 168(2):670-684.
- Ruhrberg C, Gerhardt H, Golding M, Watson R, Ioannidou S, Fujisawa H, Betsholtz C, and Shima DT. 2002. Spatially restricted patterning cues provided by heparin-binding VEGF-A control blood vessel branching morphogenesis. *Genes Dev* 16(20):2684-2698.
- Ryuto M, Ono M, Izumi H, Yoshida S, Weich HA, Kohno K, and Kuwano M. 1996. Induction of vascular endothelial growth factor by tumor necrosis factor alpha in human glioma cells. Possible roles of SP-1. *J Biol Chem* 271(45):28220-28228.
- Sahni A, and Francis CW. 2000. Vascular endothelial growth factor binds to fibrinogen and fibrin and stimulates endothelial cell proliferation. *Blood* 96(12):3772-3778.
- Sahni A, Odrliin T, and Francis CW. 1998. Binding of basic fibroblast growth factor to fibrinogen and fibrin. *J Biol Chem* 273(13):7554-7559.
- Sakiyama-Elbert SE, and Hubbell JA. 2000. Controlled release of nerve growth factor from a heparin-containing fibrin-based cell ingrowth matrix. *J Control Release* 69(1):149-158.
- Sakiyama-Elbert SE, Panitch A, and Hubbell JA. 2001. Development of growth factor fusion proteins for cell-triggered drug delivery. *Faseb J* 15(7):1300-1302.
- Sambrook J. 2001. *Molecular cloning : a laboratory manual* / Joseph Sambrook, David W. Russell. Cold Spring Harbor, N.Y. :: Cold Spring Harbor Laboratory.

- Saunders WB, Bohnsack BL, Faske JB, Anthis NJ, Bayless KJ, Hirschi KK, and Davis GE. 2006. Coregulation of vascular tube stabilization by endothelial cell TIMP-2 and pericyte TIMP-3. *J Cell Biol* 175(1):179-191.
- Scaffidi AK, Petrovic N, Moodley YP, Fogel-Petrovic M, Kroeger KM, Seeber RM, Eidne KA, Thompson PJ, and Knight DA. 2004.  $\alpha(v)\beta(3)$  Integrin interacts with the transforming growth factor beta (TGFbeta) type II receptor to potentiate the proliferative effects of TGFbeta1 in living human lung fibroblasts. *J Biol Chem* 279(36):37726-37733.
- Schense JC, and Hubbell JA. 1999. Cross-linking exogenous bifunctional peptides into fibrin gels with factor XIIIa. *Bioconjug Chem* 10(1):75-81.
- Schmoekel HG, Weber FE, Schense JC, Gratz KW, Schawalder P, and Hubbell JA. 2005. Bone repair with a form of BMP-2 engineered for incorporation into fibrin cell ingrowth matrices. *Biotechnol Bioeng* 89(3):253-262.
- Schneller M, Vuori K, and Ruoslahti E. 1997.  $\alpha v \beta 3$  integrin associates with activated insulin and PDGFbeta receptors and potentiates the biological activity of PDGF. *Embo J* 16(18):5600-5607.
- Schwarz Q, and Ruhrberg C. 2010. Neuropilin, you gotta let me know: should I stay or should I go? *Cell Adh Migr* 4(1):61-66.
- Senger DR, Claffey KP, Benes JE, Perruzzi CA, Sergiou AP, and Detmar M. 1997. Angiogenesis promoted by vascular endothelial growth factor: regulation through  $\alpha 1 \beta 1$  and  $\alpha 2 \beta 1$  integrins. *Proc Natl Acad Sci U S A* 94(25):13612-13617.
- Senger DR, Galli SJ, Dvorak AM, Perruzzi CA, Harvey VS, and Dvorak HF. 1983. Tumor cells secrete a vascular permeability factor that promotes accumulation of ascites fluid. *Science* 219(4587):983-985.
- Senger DR, Perruzzi CA, Streit M, Koteliansky VE, de Fougères AR, and Detmar M. 2002. The  $\alpha(1)\beta(1)$  and  $\alpha(2)\beta(1)$  integrins provide critical support for vascular endothelial growth factor signaling, endothelial cell migration, and tumor angiogenesis. *Am J Pathol* 160(1):195-204.
- Shaw TJ, and Martin P. 2009. Wound repair at a glance. *J Cell Sci* 122(Pt 18):3209-3213.
- Shibuya M, Yamaguchi S, Yamane A, Ikeda T, Tojo A, Matsushima H, and Sato M. 1990. Nucleotide sequence and expression of a novel human receptor-type tyrosine kinase gene (flt) closely related to the fms family. *Oncogene* 5(4):519-524.
- Smack DP, Korge BP, and James WD. 1994. Keratin and keratinization. *J Am Acad Dermatol* 30(1):85-102.
- Soker S, Miao HQ, Nomi M, Takashima S, and Klagsbrun M. 2002. VEGF165 mediates formation of complexes containing VEGFR-2 and neuropilin-1 that enhance VEGF165-receptor binding. *J Cell Biochem* 85(2):357-368.
- Soker S, Takashima S, Miao HQ, Neufeld G, and Klagsbrun M. 1998. Neuropilin-1 is expressed by endothelial and tumor cells as an isoform-specific receptor for vascular endothelial growth factor. *Cell* 92(6):735-745.
- Soldi R, Mitola S, Strasly M, Defilippi P, Tarone G, and Bussolino F. 1999. Role of  $\alpha v \beta 3$  integrin in the activation of vascular endothelial growth factor receptor-2. *Embo J* 18(4):882-892.
- Somanath PR, Malinin NL, and Byzova TV. 2009. Cooperation between integrin  $\alpha v \beta 3$  and VEGFR2 in angiogenesis. *Angiogenesis* 12(2):177-185.
- Stalmans I, Ng YS, Rohan R, Fruttiger M, Bouche A, Yuce A, Fujisawa H, Hermans B, Shani M, Jansen S et al. . 2002. Arteriolar and venular patterning in retinas of mice selectively expressing VEGF isoforms. *J Clin Invest* 109(3):327-336.
- Stratman AN, Malotte KM, Mahan RD, Davis MJ, and Davis GE. 2009. Pericyte recruitment during vasculogenic tube assembly stimulates endothelial basement membrane matrix formation. *Blood* 114(24):5091-5101.

## References

---

- Stromblad S, Becker JC, Yebra M, Brooks PC, and Cheresh DA. 1996. Suppression of p53 activity and p21WAF1/CIP1 expression by vascular cell integrin alphaVbeta3 during angiogenesis. *J Clin Invest* 98(2):426-433.
- Studier FW, and Moffatt BA. 1986. Use of bacteriophage T7 RNA polymerase to direct selective high-level expression of cloned genes. *J Mol Biol* 189(1):113-130.
- Stupack DG, and Cheresh DA. 2002. ECM remodeling regulates angiogenesis: endothelial integrins look for new ligands. *Sci STKE* 2002(119):pe7.
- Suri C, Jones PF, Patan S, Bartunkova S, Maisonpierre PC, Davis S, Sato TN, and Yancopoulos GD. 1996. Requisite role of angiopoietin-1, a ligand for the TIE2 receptor, during embryonic angiogenesis. *Cell* 87(7):1171-1180.
- Takahashi T, Ueno H, and Shibuya M. 1999. VEGF activates protein kinase C-dependent, but Ras-independent Raf-MEK-MAP kinase pathway for DNA synthesis in primary endothelial cells. *Oncogene* 18(13):2221-2230.
- Takahashi T, Yamaguchi S, Chida K, and Shibuya M. 2001. A single autophosphorylation site on KDR/Flk-1 is essential for VEGF-A-dependent activation of PLC-gamma and DNA synthesis in vascular endothelial cells. *Embo J* 20(11):2768-2778.
- Tonnesen MG, Feng X, and Clark RA. 2000. Angiogenesis in wound healing. *J Investig Dermatol Symp Proc* 5(1):40-46.
- Trautmann A, Toksoy A, Engelhardt E, Brocker EB, and Gillitzer R. 2000. Mast cell involvement in normal human skin wound healing: expression of monocyte chemoattractant protein-1 is correlated with recruitment of mast cells which synthesize interleukin-4 in vivo. *J Pathol* 190(1):100-106.
- Tredget EE, and Ding J. 2009. Wound healing: from embryos to adults and back again. *Lancet* 373(9671):1226-1228.
- Trentin D, Hall H, Wechsler S, and Hubbell JA. 2006. Peptide-matrix-mediated gene transfer of an oxygen-insensitive hypoxia-inducible factor-1alpha variant for local induction of angiogenesis. *Proc Natl Acad Sci U S A* 103(8):2506-2511.
- Waltenberger J, Claesson-Welsh L, Siegbahn A, Shibuya M, and Heldin CH. 1994. Different signal transduction properties of KDR and Flt1, two receptors for vascular endothelial growth factor. *J Biol Chem* 269(43):26988-26995.
- Wang L, Zeng H, Wang P, Soker S, and Mukhopadhyay D. 2003. Neuropilin-1-mediated vascular permeability factor/vascular endothelial growth factor-dependent endothelial cell migration. *J Biol Chem* 278(49):48848-48860.
- Weisel JW. 2004. The mechanical properties of fibrin for basic scientists and clinicians. *Biophys Chem* 112(2-3):267-276.
- Weller K, Foitzik K, Paus R, Syska W, and Maurer M. 2006. Mast cells are required for normal healing of skin wounds in mice. *Faseb J* 20(13):2366-2368.
- Werner S, Krieg T, and Smola H. 2007. Keratinocyte-fibroblast interactions in wound healing. *J Invest Dermatol* 127(5):998-1008.
- Whitaker GB, Limberg BJ, and Rosenbaum JS. 2001. Vascular endothelial growth factor receptor-2 and neuropilin-1 form a receptor complex that is responsible for the differential signaling potency of VEGF(165) and VEGF(121). *J Biol Chem* 276(27):25520-25531.
- Wierzbicka-Patynowski I, and Schwarzbauer JE. 2003. The ins and outs of fibronectin matrix assembly. *J Cell Sci* 116(Pt 16):3269-3276.
- Wiesmann C, Fuh G, Christinger HW, Eigenbrot C, Wells JA, and de Vos AM. 1997. Crystal structure at 1.7 A resolution of VEGF in complex with domain 2 of the Flt-1 receptor. *Cell* 91(5):695-704.

- Wijelath ES, Murray J, Rahman S, Patel Y, Ishida A, Strand K, Aziz S, Cardona C, Hammond WP, Savidge GF et al. . 2002. Novel vascular endothelial growth factor binding domains of fibronectin enhance vascular endothelial growth factor biological activity. *Circ Res* 91(1):25-31.
- Wijelath ES, Rahman S, Namekata M, Murray J, Nishimura T, Mostafavi-Pour Z, Patel Y, Suda Y, Humphries MJ, and Sobel M. 2006. Heparin-II domain of fibronectin is a vascular endothelial growth factor-binding domain: enhancement of VEGF biological activity by a singular growth factor/matrix protein synergism. *Circ Res* 99(8):853-860.
- Williams CK, Li JL, Murga M, Harris AL, and Tosato G. 2006. Up-regulation of the Notch ligand Delta-like 4 inhibits VEGF-induced endothelial cell function. *Blood* 107(3):931-939.
- Wong C, and Jin ZG. 2005. Protein kinase C-dependent protein kinase D activation modulates ERK signal pathway and endothelial cell proliferation by vascular endothelial growth factor. *J Biol Chem* 280(39):33262-33269.
- Woolard J, Wang WY, Bevan HS, Qiu Y, Morbidelli L, Pritchard-Jones RO, Cui TG, Sugiono M, Waite E, Perrin R et al. . 2004. VEGF165b, an inhibitory vascular endothelial growth factor splice variant: mechanism of action, in vivo effect on angiogenesis and endogenous protein expression. *Cancer Res* 64(21):7822-7835.
- Yan X, Chen B, Lin Y, Li Y, Xiao Z, Hou X, Tan Q, and Dai J. 2010. Acceleration of diabetic wound healing by collagen-binding vascular endothelial growth factor in diabetic rat model. *Diabetes Res Clin Pract* 90(1):66-72.
- Yana I, Sagara H, Takaki S, Takatsu K, Nakamura K, Nakao K, Katsuki M, Taniguchi S, Aoki T, Sato H et al. . 2007. Crosstalk between neovessels and mural cells directs the site-specific expression of MT1-MMP to endothelial tip cells. *J Cell Sci* 120(Pt 9):1607-1614.
- Yancopoulos GD, Davis S, Gale NW, Rudge JS, Wiegand SJ, and Holash J. 2000. Vascular-specific growth factors and blood vessel formation. *Nature* 407(6801):242-248.
- Yayon A, Klagsbrun M, Esko JD, Leder P, and Ornitz DM. 1991. Cell surface, heparin-like molecules are required for binding of basic fibroblast growth factor to its high affinity receptor. *Cell* 64(4):841-848.
- Zachary I. 2005. Signal transduction in angiogenesis. *EXS*(94):267-300.
- Zeng H, Dvorak HF, and Mukhopadhyay D. 2001. Vascular permeability factor (VPF)/vascular endothelial growth factor (VEGF) peceptor-1 down-modulates VPF/VEGF receptor-2-mediated endothelial cell proliferation, but not migration, through phosphatidylinositol 3-kinase-dependent pathways. *J Biol Chem* 276(29):26969-26979.
- Zhang Y, Furumura M, and Morita E. 2008. Distinct signaling pathways confer different vascular responses to VEGF 121 and VEGF 165. *Growth Factors* 26(3):125-131.
- Zheng Y, Watanabe M, Kuraishi T, Hattori S, Kai C, and Shibuya M. 2007. Chimeric VEGF-ENZ7/PlGF specifically binding to VEGFR-2 accelerates skin wound healing via enhancement of neovascularization. *Arterioscler Thromb Vasc Biol* 27(3):503-511.
- Zisch AH, Lutolf MP, and Hubbell JA. 2003. Biopolymeric delivery matrices for angiogenic growth factors. *Cardiovasc Pathol* 12(6):295-310.
- Zisch AH, Schenk U, Schense JC, Sakiyama-Elbert SE, and Hubbell JA. 2001. Covalently conjugated VEGF--fibrin matrices for endothelialization. *J Control Release* 72(1-3):101-113.



## Abbreviations

%	Percentage
°C	Degree Celsius
Ang	Angiopoietin
APS	Ammonium persulfate
BAD	Bcl-2-associated death promoter
BCA	Bicinchoninic acid
Bcl-2	B-cell lymphoma-2
bFGF	Basic fibroblast growth factor
BSA	Bovine serum albumin
C-terminus	Carboxyl-terminus
CAM	Chorioallantoic membrane
CD31	Cluster of differentiation 31
Cdc42	Cell division control protein 42
Cdk	Cyclin-dependent kinase
d	Dermis
DAPI	4',6-diamidino-2-phenylindole
DMEM	Dulbecco's Modified Eagle's Medium
DMSO	Dimethyl sulfoxide
DNA	Deoxyribonucleic acid
dNTP	Deoxyribonucleoside triphosphate
e	Epidermis
E. coli	Escherichia coli
ECL	Enhanced chemiluminescence
EDC/NHS	1-Ethyl-3-[3-dimethylaminopropyl]carbodiimide Hydrochloride/ N-Hydroxysuccinimide
EDTA	Ethylenediaminetetraacetic acid
ELISA	Enzyme-linked immuno sorbent assay
Erk	Extracellular signal regulated kinase
F	Fibrin
FAK	Focal adhesion kinase
FCS	Fetal calf serum
FGF	Fibroblast growth factor
FLV	Fibronectin type III domain 10 linker vascular endothelial growth factor-A mutant Lys 110/Pro111
FNIII10	Fibronectin type III domain 10
FPLC	Fast protein liquid chromatography
g	Granulation tissue
g	Gram
GST	Glutathione-S-transferase
GTP	Guanosine triphosphat
H&E	Heamatoxylin & eosin
HB-EGF	Heparin-binding epidermal growth factor
HEK	Human embryonic kidney
HGF	Hepatocyte growth factor
HIF	Hypoxia-inducible factor-1
HRP	Horse radish peroxidase
HSP	Heat shock protein
HSPG	Heparan sulfate proteoglycans
HUVEC	Human Umbilical Vein Endothelial Cells
Ig	Immunoglobulin
IgG	Immunoglobulin G
IPTG	Isopropyl beta-D-1 thiogalactopyranosidase
ka	Association rate constant
kb	Kilo base pair
kd	Dissociation rate constant
KD	Equilibrium dissociation constant
kDa	Kilo Dalton

KGF	Keratinocyte growth factor
L	Liter
LB	Lysogeny broth
LC-MS/MS	Liquid chromatography tandem mass spectrometry
LPS	Lipopolysaccharides
M	Molar
m	milli-
m	Meter
MAPK	Mitogen activated protein kinase
MAPKAP K2	Mitogen-activated protein kinase activated protein kinase 2
MEK	Mitogen-activated protein kinase/extracellular signal-regulated kinase kinase
MKK3/6	Mitogen-activated protein kinase kinase 3
MMP	Matrix-metalloproteases
mRNA	Messenger Ribonucleic acid
n	nano-
N-terminal	Amino-terminal
N-WASP	Neuronal Wiskott-Aldrich symptome protein
Nrp	Neuropilin
PAE	Porcine aortic endothelial
PAK	p21 activated kinase
PBS	Phosphate buffered saline
pc	Panniculus carnosus
PCR	Polymerase chain reaction
PDGF	Platelet-derived growth factor
PDGF	Platelet-derived growth factor
PDMS	Polydimethylsiloxane
PDMS	Polydimethylsiloxane
PE	Polyethylene
PFA	Paraformaldehyde
PH	Pleckstrin homology
pH	Potential of hydrogen
PHD	Prolyl-4-hydroxylase
PI3K	Phosphoinositide 3-kinase
PKB	Protein kinase B
PKC	Protein kinase C
PKD	Protein kinase D
PL	Plasmin sensitive site, LIKMKP
PLC	Phospholipase C
PMF	Peptide mass finger printing
PMSF	Phenylmethylsulfonyl fluoride
PVDF	Polyvinylidene fluoride
RGD	Arginine-Glycine-Aspartic aci
ROCK	Rho-associated coiled-coil-forming protein kinase
ROCK	Rho-associated coiled-coil-forming protein kinase
rpm	Revolutions per minute
RU	Resonance unit
SAPK2/p38	Stress activated protein kinase 2 /p38
sc	Subcutaneous fat tissue
SDS-PAGE	Sodium dodecylsulfate polyacrylamide gel electrophoresis
SH2	Src homology 2
Shb	Src homology 2 domain containing adaptor protein B
SOC	Super optimal broth with catabolite repression
SPR	Surface plasmon resonance
TAE	Tris-acetate-EDTA
TBS	Tris-buffered saline
TBST	TBS containing 0.1 % Tween-20
TEMED	N, N, N, N,-tetramethylethylenediamine
TG	Factor XIIIa substrate sequence of $\alpha$ 2 plasmin inhibitor, NQEQVSPL
TGF	Transforming growth factor
Tie	Tyrosine kinase with immunoglobulin-like and EGF-like domains

## Abbreviations

---

TIMP	Tissue inhibitor of metalloproteinase
Tris	Tris(hydroxymethyl)aminomethane
U	Units
UV	Ultra violet
VE	Vascular endothelial
VEGF	Vascular endothelial growth factor
VEGFmut	Vascular endothelial growth factor-A mutant Lys110/Pro111
VEGFR	Vascular endothelial growth factor receptor
VPF	Vascular permeability factor
w/v	Weight per volume
YT	Yeast extract and tryptone
μ	mico-

## **Danksagungen**

Ganz besonders möchte ich mich an dieser Stelle bei Frau Professor Dr. med. Sabine Eming für die stets sehr engagierte Betreuung meiner Doktorarbeit bedanken, sowie für das spannende, interdisziplinäre Thema, dessen Bearbeitung mir viel Freude bereitet hat. Sehr dankbar bin ich ihr für die außergewöhnliche Möglichkeit, einen Teil meiner Promotion in unserem Kollaborationslabor in Lausanne zu bearbeiten; dieser lange Auslandsaufenthalt war eine ganz besondere Erfahrung für mich, die mich beruflich und privat stark geprägt hat.

Herrn Professor Dr. med. Thomas Krieg danke ich für die Bereitstellung meines Arbeitsplatzes an der Klinik und Poliklinik für Dermatologie und Venerologie der Universitätsklinik zu Köln.

Herrn Professor Dr. Jeffrey Hubbell möchte ich sehr für die Aufnahme in seinem Labor, die Unterstützung meiner Arbeit und viele konstruktive Diskussionen während der Zeit in Lausanne danken.

Herrn Professor Dr. Matthias Hammerschmidt danke ich sehr für die Übernahme des Erstgutachtens dieser Arbeit. Bei Herrn Professor Dr. Paulsson bedanke ich mich für die Übernahme des Zweitgutachtens, und besonders für die vielen Diskussionen über proteinbiochemische Fragen, für die er sich immer viel Zeit genommen hat.

Herrn Professor Dr. Andreas Zisch danke ich herzlich für sein reges Interesse an meiner Arbeit und für seine Unterstützung mit wertvollen Ratschlägen zur Proteinaufreinigung. Auch während meines einwöchigen Arbeitsaufenthalt in seinem Labor habe ich sehr viel gelernt.

Besonders bedanke ich mich auch bei Herrn Dr. Martin Ehrbar für viele lebhafte und hilfreiche Diskussionen bezüglich der Fibrinengele.

Herrn Professor Dr. Stefan Höning bin ich sehr dankbar für die Durchführung und Auswertung der SPR-Messungen und die intensive Diskussion der Ergebnisse.

Bei Herrn Professor Dr. Manuel Koch bedanke ich mich vielmals für die konstruktive Auseinandersetzung mit meiner Arbeit.

Bei Herrn Dr. Burkhard Fugmann, Frau Dr. Gabriela Bald und Herrn Dr. Felix Oehme danke ich sehr für die Durchführung der Endotoxintests und für konstruktive Diskussionen über Endotoxine.

Für lebhafte und kritische Diskussionen, wertvolle Denkanstöße und die Unterstützung beim Design von Experimenten bedanke ich mich vielmals bei Herrn Dr. Mikael Martino, Frau Dr. Beate Eckes, Frau Dr. Sara Wickström, Frau Dr. Katrin Blumbach und Frau Jessica Morgner. Wertvolle Unterstützung meiner Arbeit erhielt ich ferner von Frau Kristen Lorentz, Frau Dr. Eleonora Simeoni, Herrn Professor Dr. Hilual Lashuel, Frau Dr. Jacqueline Shields, Frau Dr. Mayumi Mochizuki, Herrn PD Dr. Martin Hellmich und Frau Dr. Astrid Schauss. Besonders herzlich bedanke ich mich auch bei Frau Dr. Jennifer Patterson für das Gegenlesen meiner Arbeit, für die kritische Diskussion der Ergebnisse, methodische Ratschläge und ihre allgemein positiv-rationale Grundhaltung.

Besonders möchte ich mich bei meinen Kollegen im LMRP in Lausanne und in der Dermatologie in Köln bedanken, die mich mit ihrem kompetenten und fundierten Fachwissen, aber auch in persönlicher, sozialer und freundschaftlicher Hinsicht außerordentlich unterstützt haben und dadurch entscheidend zum Gelingen dieser Arbeit beigetragen haben. Herzlicher und besonderer Dank gebührt vor allem meiner Arbeitsgruppe. Ich danke Daniel Hoffmann, Johanna Knipper, Michael Piekarek, Rajeev Ranjan, Sebastian Willenborg, und Tina Lucas (in alphabetischer Reihenfolge) für ihre ständige fachliche und persönliche Unterstützung, für das warme Arbeitsklima und den sozialen Rückhalt.

Einen großen Beitrag zum Gelingen dieser Arbeit hat zweifellos meine Familie durch ihren bedingungslosen Rückhalt, ihre ständige Zuversicht und Ermutigung geleistet.

## **Erklärung**

Ich versichere, dass ich die von mir vorgelegte Dissertation selbstständig angefertigt, die benutzten Quellen und Hilfsmittel vollständig angegeben und die Stellen der Arbeit – einschließlich Tabellen, Karten und Abbildungen –, die anderen Werken im Wortlaut oder dem Sinn nach entnommen sind, in jedem Einzelfall als Entlehnung kenntlich gemacht habe; dass diese Dissertation noch keiner anderen Fakultät oder Universität zur Prüfung vorgelegen hat, dass sie – abgesehen von den unten angegebenen Teilpublikationen – noch nicht veröffentlicht worden ist sowie, dass ich eine solche Veröffentlichung vor Abschluss des Promotionsverfahrens nicht vornehmen werde.

Die Bestimmungen dieser Promotionsordnung sind mir bekannt. Die von mir vorgelegte Dissertation ist von Frau Professor Dr. med. Sabine Eming betreut worden.

Ich versichere, dass ich alle Angaben wahrheitsgemäß nach bestem Wissen und Gewissen gemacht habe und verpflichte mich, jedmögliche, die obigen Angaben betreffenden Veränderungen, dem Dekanat unverzüglich mitzuteilen.

## Curriculum Vitae

### Stephanie Traub, Dipl.-Biol.

date of birth: 9.10.1981, place of birth: Göppingen

### Education

November 2006  
- present

#### PhD-studies

at University of Cologne, Germany, department of life science  
Since June 2009: Department of dermatology, University hospital of Cologne, Germany, Prof. Dr. med. Sabine Eming  
November 2006-June 2009: guest in the Laboratory for Regenerative Medicine & Pharmacobiology, École Polytechnique Fédérale de Lausanne, Switzerland, Prof. Dr. Jeffrey Hubbell

*PhD-thesis:* Interplay between vascular endothelial growth factor-A and extracellular matrix in angiogenesis: molecular and cellular mechanisms  
Supervisor: Prof. Dr. med. Sabine Eming

October 2001-  
August 2006

#### Studies in biology

at Johann-Wolfgang-Goethe-University, Frankfurt, Germany

Main subjects:

- cell and developmental biology
- toxicology
- human biology

*Diploma thesis:* Novel interaction partners of reggie-proteins  
Supervisor: Prof. Dr. Ritva Tikkanen

May 2001

**School leaving exam** at Albert-Einstein-Schule Maintal, Germany

### Posters

- Traub S., Hoffmann D., Martino M., Lorentz K., Bonvin C., Ziogas A., Ehrbar M., Zisch A., Swartz M., Hubbell J., Eming S.: VEGF-isoforms for tissue regeneration.  
(EU project meeting Angioscaff, Zürich, December 2009)
- Traub S., Hoffmann D., Martino M., Koch M., Hubbell J., Eming S.: VEGF-isoforms for tissue regeneration.  
(EU project meeting Angioscaff, Barcelona, December 2010)

### Oral presentations

- VEGF-isoforms for tissue regeneration.  
(EU project meeting Angioscaff, Zürich, December 2009)
- VEGF-isoforms for tissue regeneration.  
(EU project meeting Angioscaff, Barcelona, December 2010)

**Publications**

Traub S., Lucas T., Hoffmann D., Krieg T., Eming S. Design of a novel Protease-resisten vascular endothelial growth factor-A Protein for angiogenic therapy. Yearbook of the American Wound Healing Society 2010; Advances in wound care: Vol 1, chapter 58

Martino M.M., Tortelli F., Mochizuki M., Traub S., Ben-David D., Kuhn G. A., Müller R., Livne E., Eming S. A., Hubbell J. A.: Engineering the growth factor microenvironment with fibronectin domains to promote skin and bone healing (submitted)

Tomasovic A., Traub S., Tikkanen R.: Interaction with reggie-2/ flotillin-1 regulates Tyr phosphorylation of Fibroblast Growth Factor Receptor Substrate 2 but not its nuclear localization (in preparation)

Mai 2011